# ANNULAR COLLOID THRUSTER FOR THREE-AXIS STABILIZED MILITARY SATELLITES

Marshall N. Huberman

TRW Systems Group

Prepared for:

Air Force Rocket Propulsion Laboratory

June 1973

AFRPL-TR-73-39

AD 767601

# ANNULAR COLLOID THRUSTER FOR THREE-AXIS STABILIZED MILITARY SATELLITES

PREPARED BY:
M. HUBERMAN

JUNE 1973



AFRPL-TR-73-39



APPROVED FOR PUBLIC RELEASE
DISTRIBUTION UNLIMITED

AIR FORCE ROCKET PROPULSION LABORATORY
DIRECTOR OF SCIENCE AND TECHNOLOGY
AIR FORCE SYSTEMS COMMAND
EDWARDS AIR FORCE BASE, CALIFORNIA

UNCLASSIFIED

Security Classification

**DOCUMENT CONTROL DATA - R & D**

*(Security classification of title, body of abstract and indexing annotation must be entered when the overall report is classified)*

| | |
|---|---|
| 1. ORIGINATING ACTIVITY (Corporate author)<br>TRW Systems<br>One Space Park<br>Redondo Beach, California | 2a. REPORT SECURITY CLASSIFICATION<br>UNCLASSIFIED<br>2b. GROUP<br>N/A |

3. REPORT TITLE

Annular Colloid Thruster for Three-Axis Stabilized Military Satellites

4. DESCRIPTIVE NOTES (Type of report and inclusive dates)
Technical Report, 15 November 1971 to April 1973

5. AUTHOR(S) (First name, middle initial, last name)

Marshall N. Huberman

| | | |
|---|---|---|
| 6. REPORT DATE<br>June 1973 | 7a. TOTAL NO. OF PAGES<br>~~133~~ 134 | 7b. NO. OF REFS<br>7 |
| 8a. CONTRACT OR GRANT NO<br>F04611-72-C-0018<br>b. PROJECT NO<br>c.<br>d. | 9a. ORIGINATOR'S REPORT NUMBER(S)<br>AFRPL-TR-73-39<br>9b. OTHER REPORT NO(S) (Any other numbers that may be assigned this report) | |

10. DISTRIBUTION STATEMENT
Approved for public release - distribution unlimited.

| | |
|---|---|
| 11. SUPPLEMENTARY NOTES | 12. SPONSORING MILITARY ACTIVITY<br>Air Force Rocket Propulsion Laboratory<br>Director of Science and Technology<br>Air Force Systems Command<br>Edwards Air Force Base, California |

13. ABSTRACT

This report describes a program to increase the performance capability of high thrust density colloid thrusters. Single emitter sources have been developed which produce greater than 25 µlbs thrust at 75 percent efficiency and 1300 seconds specific impulse as measured by time-of-flight techniques. Multi-source modules were built and successfully tested in the 100 µlb range for periods of the order of 100 hours. The ability to maintain constant performance within ±3 percent was also demonstrated. Beam probe measurements indicated that 90 percent of the propellant exhaust was contained within a 15° half angle. Lithium iodide and potassium iodide doped glycerol solutions were briefly looked at as candidate propellants with no performance improvements observed. Also the ability of Shell ASA-3 antistatic additive to induce electrical conductivity in a low vapor pressure pump oil (Santovac 5) was investigated with negative results. New evaporation rate measurements made with pure glycerol showed that the sodium iodide/glycerol evaporation rate was 40 percent below that of pure glycerol. Furthermore the measured results showed that the evaporated mass loss at typical operating temperatures would be of the order of one percent of the nominal thruster operating mass flow.

Details of illustrations in this document may be better studied on microfiche.

DD FORM 1 NOV 1473



UNCLASSIFIED

Security Classification

UNCLASSIFIED
Security Classification

| 14 KEY WORDS | LINK A | | LINK B | | LINK C | |
|---|---|---|---|---|---|---|
| | ROLE | WT | ROLE | WT | ROLE | WT |
| Electric Propulsion | | | | | | |
| Colloid Propulsion | | | | | | |
| Microthruster Technology | | | | | | |



UNCLASSIFIED
Security Classification

## NOTICE

When Government drawings, specifications, or other data are used for any purpose other than in connection with a definitely related Government procurement operation, the United States Government thereby incurs no responsibility nor any obligation whatsoever; and the fact that the government may have formulated, furnished, or in any way supplied the said drawings, specifications, or other data, is not to be regarded by implication or otherwise as in any manner licensing the holder or any other person or corporation, or conveying any rights or permission to manufacture, use, or sell any patented invention that may in any way be related thereto.

Copies of this report should not be returned unless return is required by security considerations, contractual obligations, or notice on a specific document.

ib

## FOREWORD

This document was prepared by TRW Systems, Redondo Beach, California, under United States Air Force Contract No. FO4611-72-C-0018. This work was sponsored and directed by the Air Force Rocket Propulsion Laboratory (AFRPL), Air Force Flight Test Center, Edwards Air Force Base. Captain S. G. Rosen provided program management and technical guidance for AFRPL.

This report describes the work performed from 15 November 1971, to 1 April 1973, by the Electric Propulsion Department, Applied Technology Division, TRW Systems. Dr. M. N. Huberman was Program Manager.

A. S. Seaton and N. E. Law provided invaluable technical support throughout the program. Managerial and technical advice was provided by Ernest Cohen, Manager of the Electric Propulsion Department.

This report was submitted by the author in June 1973.

This Technical Report has been reviewed and is approved.

WALTER A. DETJEN, Chief
Engine Development Branch

## ABSTRACT

This report describes a program to increase the performance capability of high thrust density colloid thrusters. Single emitter sources have been developed which produce greater than 25 μlbs thrust at 75 percent efficiency and 1300 seconds specific impulse as measured by time-of-flight techniques. Multi-source modules were also built and successfully tested in the 100 μlb range for periods of the order of 100 hours. The ability to maintain constant performance within ±3 percent was also demonstrated. Beam probe measurements indicated that 90 percent of the propellant exhaust was contained within a 15° half angle. Lithium iodide and potassium iodide doped glycerol solutions were briefly looked at as candidate propellants with no performance improvements observed. Also the ability of Shell ASA-3 antistatic additive to induce electrical conductivity in a low vapor pressure pump oil (Santovac 5) was investigated with negative results. New evaporation rate measurements made with pure glycerol showed that the sodium iodide/glycerol evaporation rate was 40 percent below that of pure glycerol. Furthermore the measured results showed that the evaporated mass loss at typical operating temperatures would be of the order of one percent of the nominal thruster operating mass flow.

CONTENTS

## ILLUSTRATIONS

ILLUSTRATIONS (Continued)

## ILLUSTRATIONS (Continued)

ILLUSTRATIONS (Continued)

## TABLES

# 1. INTRODUCTION AND SUMMARY

The main purpose of this program was to continue the development of high thrust colloid sources for military satellite propulsion applications. Particular emphasis was placed on improving thruster efficiency and demonstrating reliable performance up to the 100 μlb range*. The major conclusions of the program were that large diameter tubular sources can produce more than ten times the thrust of a needle and can provide long term stable operation at 75 percent efficiency and 1300 seconds specific impulse.

There are several reasons for developing high thrust sources. The main advantage derives from their ability to produce more than ten times greater thrust per unit than can be attained with the conventional needles used in the Colloid ADP thruster. Since only 1/10 as many emitters are required for a given thrust level, this will result in increased reliability, smaller thruster size and weight, decreased mechanical complexity, and reduced manufacturing and testing costs. The reliability benefits can be envisioned in several ways. For example, if we assume that a single high thrust source has the same failure rate as a single needle, then the failure probability for a complete thruster will be decreased by a factor of ten; i.e., an additional 9 will be added

---

* Unless otherwise stated, all results presented in this report are based on time-of-flight measurements. These measurements are used to calculate thrust, specific impulse, charge-to-mass ratios, mass flow, and thruster efficiency. The efficiency in this case is defined as $T^2/2\dot{M}P$, where T and $\dot{M}$ are, respectively, the thrust and mass flow resulting from the time-of-flight calculations, and P is the product of the applied needle voltage times the current supplied to the thruster. The time-of-flight calculations neglect the effects of beam spread, an approximate 400-volt loss in the spraying process and the presence of neutral particles in the beam.

The time-of-flight performance results are usually given as a function of propellant feed pressure which is a well defined and easily controlled parameter. Propellant mass flow, as calculated from time-of-flight measurements, is also stated for many of the runs. When one approximate mass flow is stated for several measurements at different voltage settings, the quoted mass flow should be considered a rough value given for reference purposes only and which can vary by as much as ±20 percent or more from the specific time-of-flight value for each individual setting. The specific time-of-flight values for each point can be obtained from the ratio of thrust to specific impulse.

to the thruster reliability number. Another way of looking at the reliability implication is to note that for a given total reliability goal, decreasing the number of individual sources by a factor of ten will allow the system to tolerate a factor of ten higher single element failure rate. The easing of this constraint can significantly reduce flight system development and test costs, especially for thrusters operating in the one-to-ten millipound range.

The work described here has advanced high thrust source technology to the point where steady reliable performance has been demonstrated at greater than 25 μlbs per unit, 75% efficiency and 1300 seconds specific impulse for periods on the order of 100 hours. This was achieved after performing an extensive test program on a wide variety of thruster configurations. The most significant findings were the importance of orienting the emitter vertically in order to equalize gravitational effects around the emitter rim, the enlarging of the extractor aperture to 1/2 inch, and the development of a special emitter forming tool. It was then possible to achieve the performance levels quoted above.

Electrostatic x-y vectoring capability was also demonstrated for a single source equipped with a three electrode deflector system. The maximum vectoring angle varied from 5.8° to 17° depending on the orientation of the vectoring direction relative to the deflector electrode symmetry axis.

After completing the single emitter experiments, multi-source modules were built to operate in the 100 μlb range. A four-source module was subjected to extensive performance testing in addition to long-term runs of 100 hours and 360 hours. Long-term steady performance was demonstrated at several levels up to 123 μlbs at 75% time-of-flight efficiency and 1325 seconds specific impulse. The ability to neutralize the beam without interfering with thruster performance was also demonstrated. Beam probe measurements showed that 90% of the beam was contained within a 15° half angle. The thruster's ability to provide constant performance to within $\pm$3% was also demonstrated. During short term testing at high feed pressures, the four-source thruster produced 301 μlbs at 70% efficiency and 1029 seconds specific impulse.

New evaporation rate measurements were made with pure glycerol and sodium iodide/glycerol. The measurements showed that the sodium iodide/glycerol evaporation rate was 40% below that of pure glycerol. Furthermore the measured results showed that the evaporated mass loss at typical operating temperatures would be of the order of 1% of the nominal thruster operating mass flow.

In order to improve the reliability of time-of-flight measurements a registered grid time-of-flight collector was built and installed in the 24" diffusion pump test facility. Lithium iodide and potassium iodide doped glycerol solutions were briefly looked at as candidate propellants with no performance improvements observed. Also the ability of Shell ASA-3 anti-static additive to induce electrical conductivity in a low vapor pressure pump oil (Santovac 5) was investigated with negative results.

## 2. GENERAL APPROACH

The basic thruster configuration is as shown in Figure 1. The main features of the emitter are a flow impedance tube for mass flow control, the emitter tip which is designed to provide the proper emission characteristics and an external shank to provide good mechanical and thermal coupling to the module base. The emitter is positioned within three deflector electrodes which, in turn, are centered in an extractor aperture that has been 1/2" in diameter on our most recent thrusters. As their name implies, the deflector electrodes can be used to vector the colloid beam. They also allow the extraction field strength to be modified independently of the total emitter accelerating voltage. Another function of the deflector electrodes is to modify the field in front of the thruster in such a way as to make it difficult for returning ions to strike the extractor in the region immediately adjacent to the extractor aperture, where they could create secondary electrons which have a high probability of bombarding the emitter tip. Furthermore, the deflector electrodes also provide line-of-sight mechanical shielding between the emitter and extractor.

Initially, a major program goal was to increase the thruster specific impulse to 2000 seconds at 65% efficiency, and 25 μlb thrust for a single source, but later in the program the goal was changed in order to emphasize improvements in efficiency instead of specific impulse. The goals then became 80% efficiency at 1500 seconds for a single source and 75% efficiency for a 100 μlb multi-source module. In all cases a thrust of 25 μlb per source was required and the main problem to be overcome was that of improving a given performance parameter without degrading other thruster performance parameters or operational stability.

The interrelationship between the performance parameters can best be seen from the fact that the specific impulse is proportional to the square root of the product of the net accelerating voltage, the average charge-to-mass ratio, and the specific charge distribution efficiency. The first two variables can be increased by raising the total source voltage while holding all other control parameters constant, since this increases the extraction field strength and the average charge-to-mass ratio. However, raising the

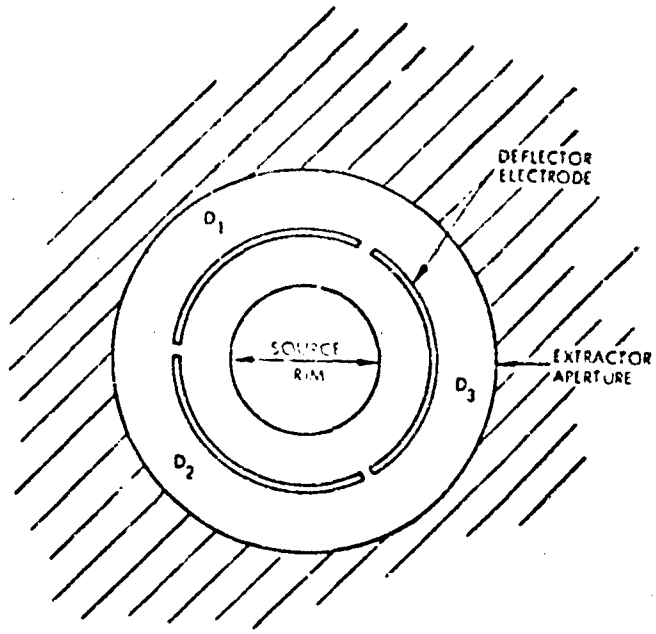


1-a. Electrode Geometry

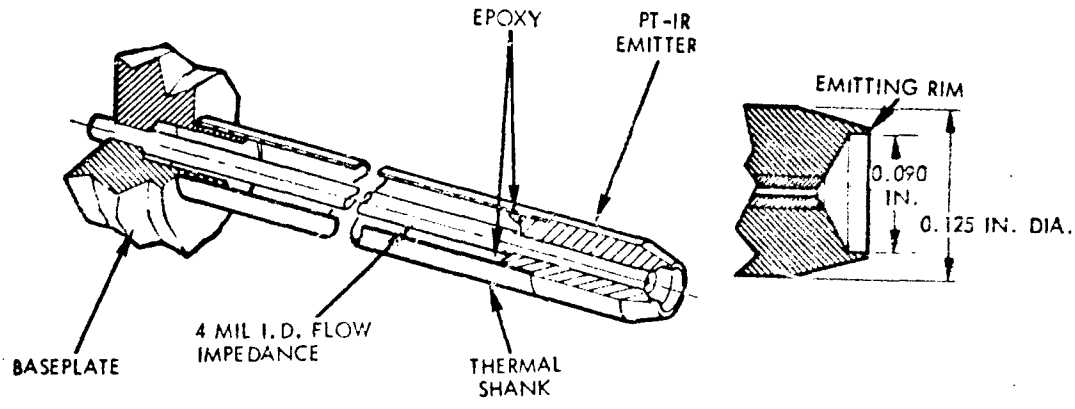


1-b. Emitter Schematic

Figure 1. High Thrust Source Configuration

voltage in this manner can increase the ion content in the thruster exhaust, thus lowering the beam efficiency. Similarly, past observations have often indicated that higher efficiencies can be achieved at lower charge-to-mass ratios. For a given accelerating voltage this would result in lower specific impulse. For these reasons it is necessary to decouple the total thruster voltage from the extraction field strength so that these quantities can be adjusted independently in order to insure that the thruster performance is fully optimized.

The deflector electrodes satisfy the above requirement by allowing the extraction field to be modified so as to require a higher total accelerating voltage for a given field strength and charge-to-mass ratio. Thus, a major experimental approach was to work at higher deflector voltages in order to obtain lower charge-to-mass ratio and higher efficiency while maintaining high specific impulse.

In addition to the previous considerations which would apply to any specific thruster geometrical configuration, variations in geometry were also investigated as a means of improving performance. There are several ways in which the thruster geometry impacts on performance. For example, the emitter rim thickness is one of the factors determine the field strength and uniformity in the vicinity of the e gion. Similarly, the deflector to emitter spacing, the extractor aperture diameter, and the relative heights of the deflector, emitter and extractor all influence the trajectories of returning secondary particles, the probability of electron emission from thruster surfaces, beam focusing, collision probabilities and energies within the thruster exhaust, and field strength and uniformity at the emitter tip. Furthermore, the emitter tip interior geometry and surface condition affect the propellant depth and surface configuration in the vicinity of the emission region. All the foregoing effects are interrelated and no adequate theoretical treatment exists. For this reason variations in these parameters were experimentally investigated to determine if performance improvements could be attained relative to the base-line design. The major finding was that widening the extractor aperture extended the range of stable high voltage performance, thus allowing lower charge-to-mass operation.

Changing to a vertical thruster orientation in order to eliminate meniscus non-uniformities due to the gravitational effects within the emitter also produced a major performance gain. Another significant improvement was the development of an emitter forming tool which provided two major advantages: (1) emitter-to-emitter mechanical reproducibility, and (2) complete rim uniformity around the entire emitter perimeter. The latter feature is particularly crucial for the following reason. There is an optimum combination of field strength, field direction and mass flow for achieving stable high performance operation. Variations in the detailed emitter rim geometry around the perimeter will cause corresponding variations in the above parameters, resulting in off-optimum local operating conditions. The rim forming tool that was developed provided a simple solution to this problem.

## 3. SINGLE SOURCE WORK

The single source work consisted of horizontally and vertically oriented testing (test facilities are described in Appendix A). This was due to the realization, approximately mid-way through the program, that a major key to raising efficiency was to orient the thruster vertically so that the thruster exhaust was emitted vertically downward. The latter orientation greatly improved performance by virtue of symmetrizing gravitational effects and insuring that the meniscus shape and emission were uniform all around the rim. The vertical work was begun after an extensive series of horizontal runs with various emitter configurations were unable to produce the desired performance improvements. The main problem encountered with the earlier horizontal work was that whenever voltages were raised to the point where high efficiencies and specific impulses could be attained, the thruster would tend to be unstable. This was apparently due to overfeeding at the bottom of the rim. Thruster beam profiles tended to be skewed toward the bottom of the tank and microscopic visual observations of the emitter tip showed a tendency to spill out at the bottom. When arcing occurred it tended to do so at the bottom of the rim. A review of work prior to the present program also indicated a tendency for the thruster to operate at higher efficiencies when oriented vertically, but no great significance was attached to the fact at that time since the main purpose of those vertical orientation tests was to determine if thruster orientation had any major influence on estimated life time at the operating voltages then being employed[1].

### 3.1 Horizontal Testing

Table I summarizes the best performance points attained with various geometries during the horizontal test program. Impressive performance was attained with several thruster configurations; however, these points were obtained under conditions where the propellant meniscus within the emitter was unstable; i.e., visual observations indicated rippling and

## TABLE I. HORIZONTAL TEST PROGRAM PERFORMANCE SUMMARY

| | $V_S$ kv | $V_D$ kv | $I_{sp}$ sec | THRUST µlb | EFFICIENCY % |
|---|---|---|---|---|---|
| Basic Geometry | | | | | |
| 1/4 inch extractor | 17.7 | 15.5 | 1648 | 22.5 | 73.7 |
| 3/8 inch extractor | 21.2 | 19.4 | 1484 | 50.6 | 83.0 |
| 1/2 inch extractor | 25.0 | 25.0 | 2500 | 28.0 | 83.0 |
| Deep Well Emitters | | | | | |
| Basic | 19.2 | 16.2 | 900 | 22.0 | 88.0 |
| 0.010 ledge | Same as above beam spread too wide to get good time of flight | | | | |
| 0.023 ledge | same as above | | | | |
| 0.045 ledge | same as above | | | | |
| Totally flat top | Less than 10 microamperes | | | | |
| Deflector Electrode Position (Normal 0.160 inch diameter) | | | | | |
| 0.190 inch diameter | 20.4 | 18.9 | 1500 | 19.0 | 70.0 |
| 0.006 inch forward (0.160 inch diameter) | 15.9 | 9.2 | 1500 | 18.0 | 75.0 |
| 0.005 inch behind (0.160 inch diameter) | 18.8 | 12.4 | 1750 | 23.0 | 73.0 |
| Center Plug | Wide beam spread - tendency to run from bottom | | | | |
| Double Rim | Wide beam spread - no collector current | | | | |
| Rim Thickness (Normally 0.001 Radius) | | | | | |
| 0.0005 | 18.2 | 17.0 | 1470 | 28.0 | 65.0 |
| 0.002 | 15.0 | 7.0 | 1100 | 30.0 | 80.0 |
| Bias Plates | | | | | |
| Single bias plate | 16.9 | 15.0 | 1238 | 22.0 | 83.8 |
| Double bias plate | 16.5 | 10.5 | 1525 | 27.1 | 70.0 |
| Propellants | | | | | |
| Lithium Iodide | 14.7 | 7.0 | 1240 | 30.5 | 74.0 |
| Potassium Iodide | 20.0 | 12.0 | 1546 | 27.7 | 70.8 |
| Surface Modifications | | | | | |
| Sandblast - to top of rim | 22.0 | 19.0 | 1219 | 42.0 | 68.0 |
| Sandblast to outside | Beam spread too wide | | | | |

bubbling at the propellant surface. During the course of these experiments, many different emitter configurations were tried. The following pages describe these experiments in greater detail.

RUN 7112-01: CONVENTIONAL THRUSTER

This run was performed with a 1/4" extractor aperture thruster from a previous program. Time-of-flight performance parameters were first measured for 5" Hg feed pressure ($P_F$), 14.45 kv source voltage ($V_S$), 7.2 kv deflector voltage ($V_D$) and -1 kv extractor voltage ($V_X$). The thruster operated very smoothly and quietly at 64 μamps, 1881 seconds, 16,710 coulombs/kilogram (c/kg), 70.4 percent efficiency, 15.9 μlbs thrust and 3.83 μgms/sec mass flow. The feed pressure was then increased to 7.15" Hg in order to increase mass flow and thrust. This produced 73.2 percent efficiency, 4.89 μgm/sec, 1846 seconds, 19.9 μlbs and 15,340 c/kg.

In order to explore higher voltage operation, the source voltage was raised to 16.8 kv and the deflectors to 12.8 kv; and time-of-flight performance was measured for various feed pressures. The results are tabulated in Table II. Time-of-flights taken at the higher pressures were repeated in order to evaluate the performance variability when the thruster was pushed this hard. The variability was of the order of ±10 percent from the average.

We then examined the effect of going to a higher source voltage. At $V_S$=17.7 kv, $V_D$=15.5 kv, $P_F$=9.3" Hg, the time-of-flight parameters were 73.7 percent, 6.20 μgm/sec, 1,648 seconds, 61 μamps, 22.5 μlbs and 10,000 c/kg. However, there were slow, large amplitude variations in the source current. Typically, the current would slowly decrease to approximately 30 μamps, and then, a few minutes later, would rise back to the order of 60 μamps. By visually observing the fluid within the emitter tip, the current variations could be correlated with a partial emptying of the emitter tip, followed by a gradual refilling until the fluid bulged out to a shape where the field strength was sufficient to reshape the meniscus surface and then draw out propellant at a faster rate than it was being supplied.

TABLE II. PERFORMANCE SUMMARY FOR PREVIOUS PROGRAM'S THRUSTER

RUN 7112-31

$V_s$=16.8 kv nominal, $V_d$=12.8 kv, $V_x$= -1 kv

| $P_F$ "Hg | $I_N$ μA | η % | $\dot{M}$ μg/sec | $I_{sp}$ sec | T μlbs | q/m c/kg |
|---|---|---|---|---|---|---|
| 5 | 53 | 71.9 | 3.53 | 1943 | 15.1 | 15,030 |
| 6 | 62 | 71.7 | 4.41 | 1878 | 19.2 | 14,070 |
| 7 | 66 | 70.8 | 6.10 | 1637 | 22.0 | 10,830 |
| 7 | 66 | 71.6 | 3.97 | 2039 | 17.9 | 16,620 |
| 7 | 68 | 70.3 | 4.87 | 1825 | 19.6 | 13,550 |
| 7 | 65 | 72.9 | 5.41 | 1762 | 21.0 | 12,190 |
| 8 | 60 | 71.2 | 4.74 | 1796 | 18.6 | 12,670 |
| 8 | 64 | 71.3 | 5.33 | 1735 | 20.4 | 12,000 |
| 8 | 68 | 71.9 | 5.47 | 1769 | 21.3 | 12,440 |
| 9 | 64 | 72.2 | 7.47 | 1475 | 24.3 | 8,570 |
| 9 | 68 | 72.6 | 7.97 | 1474 | 25.9 | 8,530 |
| 9 | 70 | 71.7 | 8.21 | 1461 | 26.5 | 8,520 |

## RUN 7112-02: 3/8" EXTRACTOR APERTURE

This was the same thruster as before except that the extractor aperture was enlarged to 3/8" diameter. The main features of this run were that (1) it was possible to operate at higher source voltages with no extractor field emission problems and, (2) the higher voltages increased the source current cycling and rippling observed on the previous run.

Early in the run, it was possible to obtain performance which met the final program goals. However, due to rippling, there was a cycling of the needle current between 60 and 70 μamps. Table III shows the time-of-flight results for this part of the run.

In Table III, repetition of the time-of-flight measurements at a given operating point is for the purpose of illustrating variability due to rippling at the thruster tip. Later in the experiment, when the thruster was operating at 8.5" Hg feed pressure, 21 kv source voltage and 20.7 kv deflector voltage, the current cycling increased to where the current was varying between 38 and 80 μamps with a 2.5-minute period. We found that by increasing the feed pressure to 12.5" Hg, we could decrease the period of oscillation to one minute and the amplitude to a variation between 68 and 88 μamps. Since higher pressures seemed to smooth operation, the feed pressure was then raised to 20.3" Hg to evaluate high mass flow performance. Table IV shows some of the high pressure data.

In Table IV, two time-of-flight measurements, taken five minutes apart, are shown for each deflector voltage setting in order to get a feeling for the data reproducibility. Thrusts up to 50 μlbs were attained at high efficiencies and specific impulses approaching 1500 seconds. The high efficiency may have been due to spraying taking place from the central region of the meniscus where the surface electric field is more uniformly distributed rather than at the thruster rim.

## RUN 7112-03: DEFLECTORS PLACED .006" FORWARD OF THE EMITTER

In addition to the new deflector position, the emitter surface conditioning treatment was modified for this run. On all previous runs on this program it was standard procedure to coat the inside of the emitter tip with a thin layer of sodium iodide immediately after the emitter was

TABLE III

RUN 7112-02 - TIME-OF-FLIGHT RESULTS
DURING INITIAL PERFORMANCE SCAN

| $P_F$ "Hg | $V_s$ kv | $I_S$ μA | $V_d$ kv | η % | $\dot{M}$ μg/sec | $I_{sp}$ secs | T μlbs | q/m c/kg |
|---|---|---|---|---|---|---|---|---|
| 6.2 | 15.5 | 60 | 9.0 | 71.7 | 4.25 | 1806 | 16.9 | 14,120 |
| 7.0 | 16.2 | 72 | 9.0 | 71.6 | 4.90 | 1880 | 20.3 | 14,690 |
| 8.2 | 17.5 | 66 | 13.0 | 72.0 | 6.69 | 1584 | 24.1 | 19,580 |
| 8.45 | 18.0 | 63 | 13.6 | 72.1 | 6.31 | 1642 | 22.8 | 9,990 |
| 8.45 | 18.0 | 70 | 12.2 | 73.3 | 6.49 | 1721 | 24.6 | 10,780 |
| 8.45 | 20.0 | 69 | 16.2 | 73.2 | 6.02 | 1868 | 24.8 | 11,460 |
| 8.45 | 20.0 | 68 | 16.2 | 73.7 | 5.65 | 1921 | 23.9 | 12,030 |
| 8.45 | 21.3 | 58 | 20.7 | 76.9 | 5.09 | 1970 | 22.1 | 11,390 |
| 8.45 | 21.3 | 62 | 20.7 | 76.4 | 6.54 | 1787 | 25.8 | 9,480 |
| 8.45 | 21.3 | 67 | 20.7 | 76.0 | 6.55 | 1851 | 26.7 | 10,230 |
| 8.45 | 21.3 | 66 | 20.7 | 75.8 | 8.89 | 1575 | 30.9 | 7,420 |
| 8.45 | 21.3 | 62 | 20.7 | 76.6 | 5.49 | 1952 | 23.6 | 11,290 |
| 8.45 | 21.3 | 60 | 20.7 | 76.5 | 4.21 | 2192 | 20.3 | 14,250 |
| 8.45 | 21.3 | 60 | 20.7 | 75.4 | 5.87 | 1844 | 23.9 | 10,220 |

TABLE IV

RUN 7112-02 - HIGH MASS FLOW DATA AT
20.3"HG FEED PRESSURE, $V_X$ = -3KV

| $V_s$ kv | $I_N$ μA | $V_d$ kv | n % | $\dot{M}$ μg/sec | $I_{sp}$ sec | T μlbs | q/m c/kg |
|---|---|---|---|---|---|---|---|
| 21.3 | 64 | 20.6 | 75.5 | 17.2 | 1115 | 42.4 | 3,710 |
| 21.3 | 62 | 20.6 | 74.7 | 17.5 | 1082 | 41.8 | 3,540 |
| 21.3 | 76 | 20.7 | 78.4 | 14.4 | 1353 | 43.0 | 5,280 |
| 21.3 | 75 | 20.2 | 79.0 | 16.9 | 1245 | 46.5 | 4,430 |
| 21.2 | 84 | 19.8 | 83.1 | 14.9 | 1440 | 47.1 | 5,660 |
| 21.2 | 84 | 19.8 | 82.0 | 15.9 | 1383 | 48.4 | 5,290 |
| 21.2 | 93 | 19.4 | 83.0 | 15.5 | 1484 | 50.6 | 6,020 |
| 21.2 | 92 | 19.4 | 81.6 | 14.9 | 1491 | 49.0 | 6,180 |

cleaned. The purpose of the sodium iodide was to provide a glycerol soluble protective surface coating to prevent oil contamination of the emitter tip interior surfaces, since good wetting by the propellants is essential to good operation.

The salting was omitted on this run in order to further verify that it would be harder to start the thruster without this preliminary treatment. The test results strongly confirmed that it was now much more difficult to get the entire emitter interior wet at start-up. During operation, the current cycling was relatively extreme. At higher voltages, the emitter would appear to completely empty out during the low part of the cycle. Although the severity of the problem was no doubt related to the emitter not having been salted, the results also indicated that moving the deflectors forward has no beneficial effect.

RUN 7112-04: DEFLECTOR ELECTRODES 0.005" BEHIND EMITTER

The thruster once again appeared insensitive to a variation in relative deflector location. Typical performance parameters were of the order of 1750 seconds Isp, 73 percent efficiency, 23 μlbs thrust and 11,000 c/kg at

18.8 kv source voltage, 12.4 kv deflector voltage, 67 μamps source current. Any attempts to achieve higher charge-to-mass ratios or source voltages led to excessive ripple instability.

In order to more closely simulate a flight quality thruster this run used a braze joint between the impedance and emitter tip instead of the usual epoxy joing technique. A nickel-chromium brazing element was used and no difficulties were encountered.

RUN 7201-01: DEEP WELL EMITTER

The emitter well in the original thruster design was not deep enough to allow a full hemispherical meniscus. This means there is a possibility that if the well is made deep enough to accomodate a full hemisphere, the resultant lowering of the surface in the center would decrease the surface electric field and reduce emission from the emitter interior. However, the net effects on performance were not easy to envision theoretically and therefore had to be determined experimentally.

The emitter for this run was designed to have sufficient depth to accommodate a fully concave meniscus. Figure 2 is a schematic of the design. It can be seen that the wall height in this design is 0.035" as opposed to the 0.015" value used on other designs to date.

Visual observation of the thruster during operation appeared to indicate that emission from the interior was considerably reduced. No traces of the usual interior rippling were observed. However, the total emission current, the average charge-to-mass ratio and the specific impulse were all much lower than is usually obtained with a single rim source. Efficiency, however, was extremely high, usually above 85 percent.

Our first interpretation of the results was that the emission was all taking place from near the rim since the fluid was so quiet within the emitter interior region. In retrospect, however, it is also possible that the emission was taking place from the interior region, but the lower surface field strength and emission current density contributed to a smoother performance. This would be more in agreement with previous hypotheses that higher efficiencies arise from emission away from the rim. Attempts to raise the charge-to-mass ratio by increasing the emitter field strength were not successful due to the onset of instabilities. These instabilities were

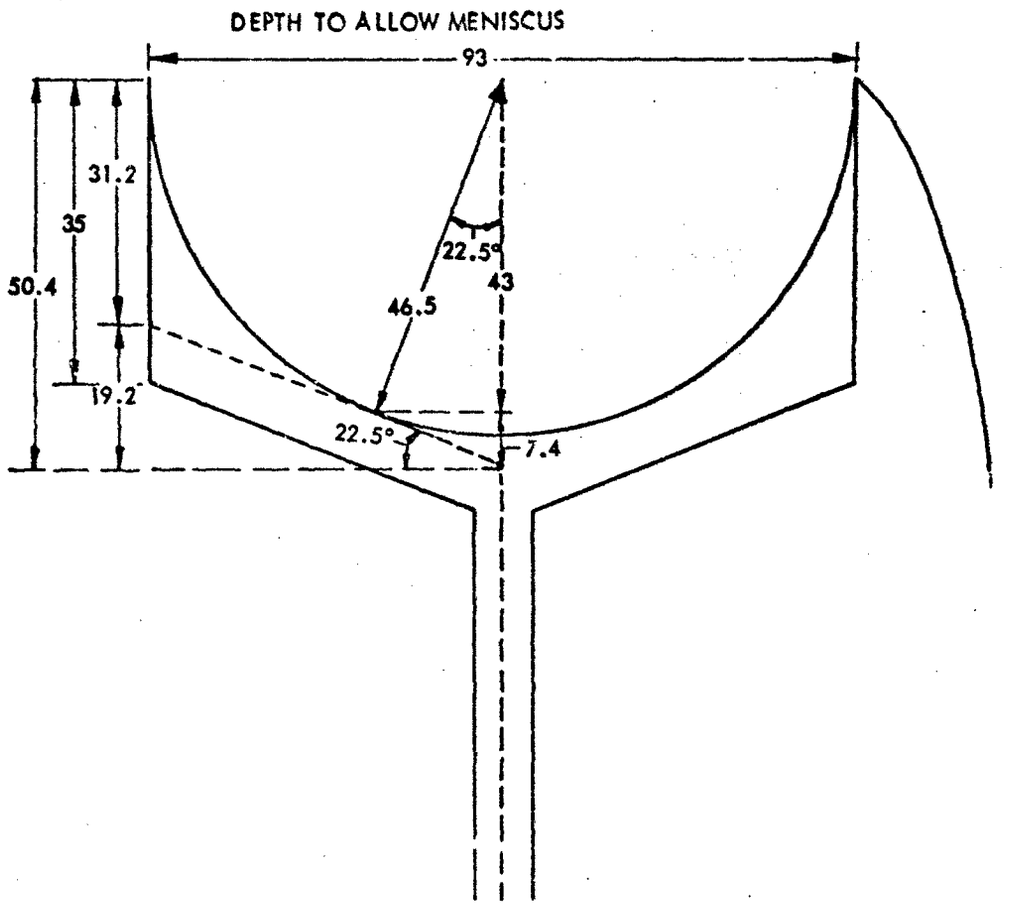


Figure 2. Deep Well Emitter Design - This allows room for formation of a complete, concave, hemispherical meniscus.

usually in the form of a tendency for propellant to surge out at the bottom of the well. This indicated that gravitational effects were coming into play, and that the large interior volume made it easier for the fluid to accumulate towards the bottom in horizontal operation.

Table V lists approximate average performance parameters when the thruster was operating smoothly. The first three lines in the table show the effect of varying the deflector voltage while holding the source voltage constant. The other operating points were meant to show the effect of simultaneously raising the source and deflector voltages in order to maintain stable operation at the higher source voltages. These points were characterized by a wide variation in time-of-flight mass flows even though the feed pressure was held constant. Possibly this was due to the tendency for the meniscus to spill towards the bottom at times.

RUN 7201-02: REPEAT OF 7201-01 DESIGN

The gravity effect on the previous run (7201-01) could possibly have been due to inadequate wetting of the emitter interior. It was therefore decided to test this design one more time after carefully cleaning and

TABLE V

RUN 7201-1 - AVERAGE PERFORMANCE PARAMETERS
AT 10" $H_g$ FEED PRESSURE, -2 KV EXTRACTOR VOLTAGE

| $V_N$ KV | $I_N$ μA | $V_D$ KV | η % | $\dot{M}$ μG/SEC | $I_{SP}$ SEC | T μLBS | Q/M C/KG |
|---|---|---|---|---|---|---|---|
| 16.2 | 28 | 11.2 | 84 | 11.0 | 800 | 25 | 2500 |
| ↓ | 31 | 10.2 | 88 | 8.4 | 1050 | 19 | 3700 |
| ↓ | 36 | 9.2 | 86 | 8.7 | 1100 | 20 | 4500 |
| 17.2 | 30 | 12.2 | 87 | 9.7 | 1000 | 20 | 3000 |
| 18.2 | 30 | 14.2 | 85 | 15.0 | 800 | 25 | 2000 |
| 19.2 | 28 | 16.2 | 88 | 10.0 | 900 | 22 | 2700 |

salting the emitter interior all the way out to the rim. The behavior was similar to the previous run, indicating that low q/m performance is indeed a characteristic of this design configuration. The inability to obtain consistent time-of-flight mass flow values was also repeated during this run, thus indicating that this phenomenon was also a characteristic of this emitter geometry during horizontal operation.

RUN 7201-03: HALF-INCH EXTRACTOR APERTURE

A previous run (Run 7112-02) had shown that higher source voltages could be attained by increasing the extractor aperture to 3/8". The purpose of this new run was to determine if further increasing the aperture to 1/2" diameter would additionally benefit performance. This indeed turned out to be the case in that it was now possible to operate at identical source and deflector voltages (25 kv). In addition to producing a high specific impulse, this mode of operation allowed for the future possibility (for non-vectoring thrusters) of converting the deflector electrodes into a continuous shield electrode mounted directly on the emitter shank, thus simplifying module fabrication. At 25 kv on both the deflectors and source, and 9 inches Hg feed pressure, we were able to get 83 percent efficiency 5 μlbs thrust, 2500 seconds specific impulse, 28 μlbs thrust, 15,000 c/kg. At 20 kv on the deflectors and source, it was possible to get 75 percent efficiency, 5 μg/sec mass flow, 1700 seconds specific impulse, 19 μlbs thrust and 9000 c/kg.

While the 25 kv data were extremely encouraging in regard to the performance levels, there was still a tendency to oscillate and therefore the major task remaining was still to attain greater operational stability.

RUNS 7201-04 AND 7201-05: DEEP WELL EMITTER WITH EMISSION LEDGE

The emitter design for this test is shown in Figure 3. It was similar to the deep well design of Figure 2 except that it provided a 30° bevel inner edge at the emitter rim. The intention here was to see if the fluid would anchor at the ledge and thus have a stable emission region, i.e., from the flat portion of the bevel. The performance was essentially the same as on Run 7201-01. By this we mean that whenever voltage was increased to raise the q/m, we would get unstable operation with a tendency to spill towards the bottom. For Run 7201-05, extra

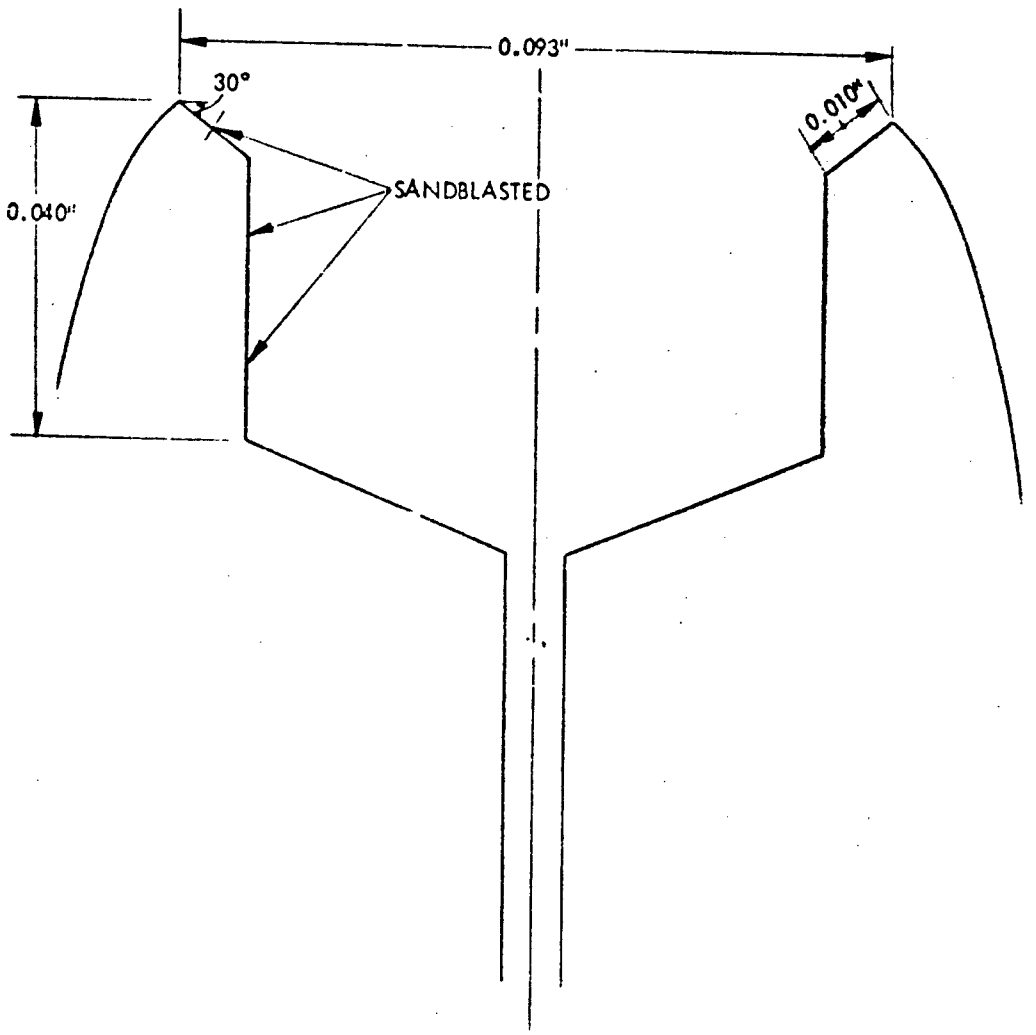


Figure 3. Deep Well Emitter With 0.010" Beveled Emission Edges

precautions were taken to guarantee rim cleanliness in order to ensure that the inability to anchor firmly was indeed due to the inherent thruster design rather than lack of experimental precautions. The operational results were essentially the same as in the previous run.

RUNS 7201-06, 7201-07, AND 7201-08: 0.190" I.D. DEFLECTOR ELECTRODE DIAMETER

The primary purpose of these runs was to determine if increasing the spacing between the thruster and deflectors improved performance. This was accomplished by increasing the inner deflector diameter to 0.190" instead of the usual 0.160". In order to simplify fabrication, the deflector electrode consisted of a complete circular cross section instead of being segmented into three parts. The extractor aperture was 3/8". Also, in addition to the usual thermistor inserted in the module base, a thermocouple was spot-welded to the emitter exterior approximately 1/32" below the tip in order to verify that the tip temperature was not significantly different from the base temperature. The first two runs were terminated prematurely. On the first run, electrostatic forces pulled the 0.002" thermocouple leads over to the extractor. On the second run, one of the thermocouple leads broke after several time-of-flight pulses. At this point, 0.010" thermocouple wires were introduced to eliminate these problems. The best performance was attained at 20.4 kv needle voltage, 18.9 kv deflector voltage and -2 kv extractor voltage. At 8.4" Hg feed pressure, the thruster produced 26 μamps beam current, 70 percent efficiency, 4.5 μg/sec mass flow, 1500 seconds specific impulse, 15 μlbs thrust and 8,000 c/kg. At 12.3" Hg, the thruster produced 37 μamps, 73 percent efficiency, 6.5 μg/sec, 1300 seconds, 19 μlbs and 5500 c/kg. Attempts to further raise the charge-to-mass ratio by adjusting voltages led to decreased stability and it was judged that the increased deflector diameter produced no improvements in this regard.

The thermocouple provided interesting information. During normal operation, the thruster temperature agreed with module temperature. However, illuminating the thruster with an outside spotlight raised the thruster tip temperature to approximately 1/2°C higher than the module. The thruster was then deliberately operated in a highly unstable mode to determine the effect on tip temperature. The reason for doing this

is that in the past it has been observed that under conditions of extremely high instability and back bombardment, the fluid at the tip, as observed visually, appears to have a considerably lower viscosity than normal, which could be indicative of increased tip temperature. In order to achieve operation in this mode the deflector electrode was electrically coupled to the -2 kv extractor while holding the emitter at 15 kv. This mode of operation is equivalent to operating with a 0.190-inch extractor aperture and no deflector electrodes. Using this technique it was possible to raise the emitter current to 150 μamps with the deflector current meter past its 25 μamps full scale. In this mode the tip temperature rose to 88°C with only a very minor (<1°C) main module temperature perturbation. The observations in general showed that the visual viscosity observations could be correlated with emitter temperature variations, and also that the thruster could be cooled back to its original operating temperature (25°C) by reducing the emitter voltage to 11 kv. The current and temperature would then steadily decrease back to normal operation within approximately 10 minutes.

With the electrodes wired up this way, the thruster could operate stably at emitter voltages below 14 kv (while still holding the deflectors and extractor at -2 kv). At 12.2" Hg feed pressure, 13 kv emitter voltage, the thruster produced 55 percent efficiency, 10 μg/sec, 1000 seconds specific impulse, 23 μlbs thrust and 8,000 c/Kg.

RUN 7201-09: DEEP WELL EMITTER WITH 0.023" EMISSION LEDGE

The emitter for this run was a deep well design similar to that shown in Figure 3 except that the beveled portion near the rim was now 0.023" wide and cut at a 41° angle relative to the emitter axis. The purpose of the larger ledge was to produce a greater emitting region from which to obtain a stable, high emission current. Previous problems with deep well emitters were once again encountered. The fluid tended to spill towards the bottom and produce electrical discharges.

RUN 7202-02: SMALL CENTER PLUG

The thruster for this run had a small center plug, as shown in Figure 4, to discourage emission from the center of the emitter. It was also hoped that the plug, by providing additional wetting surface, would

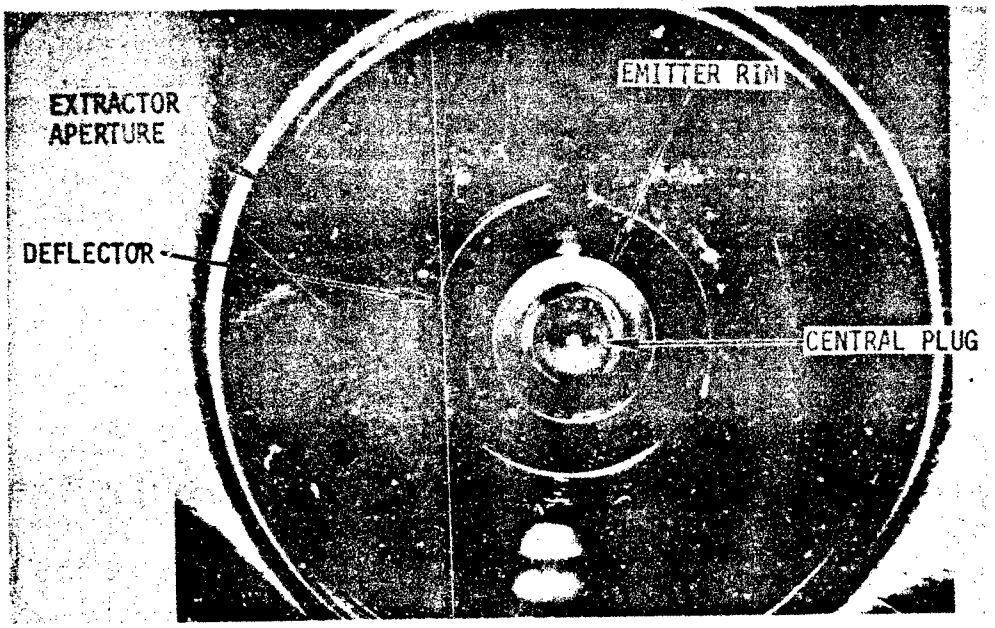


Figure 4. Small Central Plug Emitter, Design 7202-02

eliminate the tendency to spill towards the bottom which had existed with the previous deep well design. Figure 5 is a schematic of the design. The operation was characterized by low charge-to-mass ratio, high beam spread and a tendency for propellant to run out at the bottom.

RUN 7202-05: DOUBLE RIMMED EMITTER

This run used a center plug which completely filled the emitter well except for a small slit around the perimeter. Figure 6 is a photograph of this emitter. Figure 7 is a schematic of the design. The performance was characterized by low beam currents and extremely high beam spread. As a result, the collector current was too low to perform time-of-flight measurements. The emission was visually observed to be predominantly in a 45° half angle cone with a large fraction of the beam being collected by the vacuum tank liner. The neutralizer was turned on to see if the beam spread was due to space charge, since in this case neutralization would narrow the beam. However, no such effect was observed. Thus the spread was due to the emission pattern at the emitting surface. Since the current was very stable and smooth for this thruster, it would be

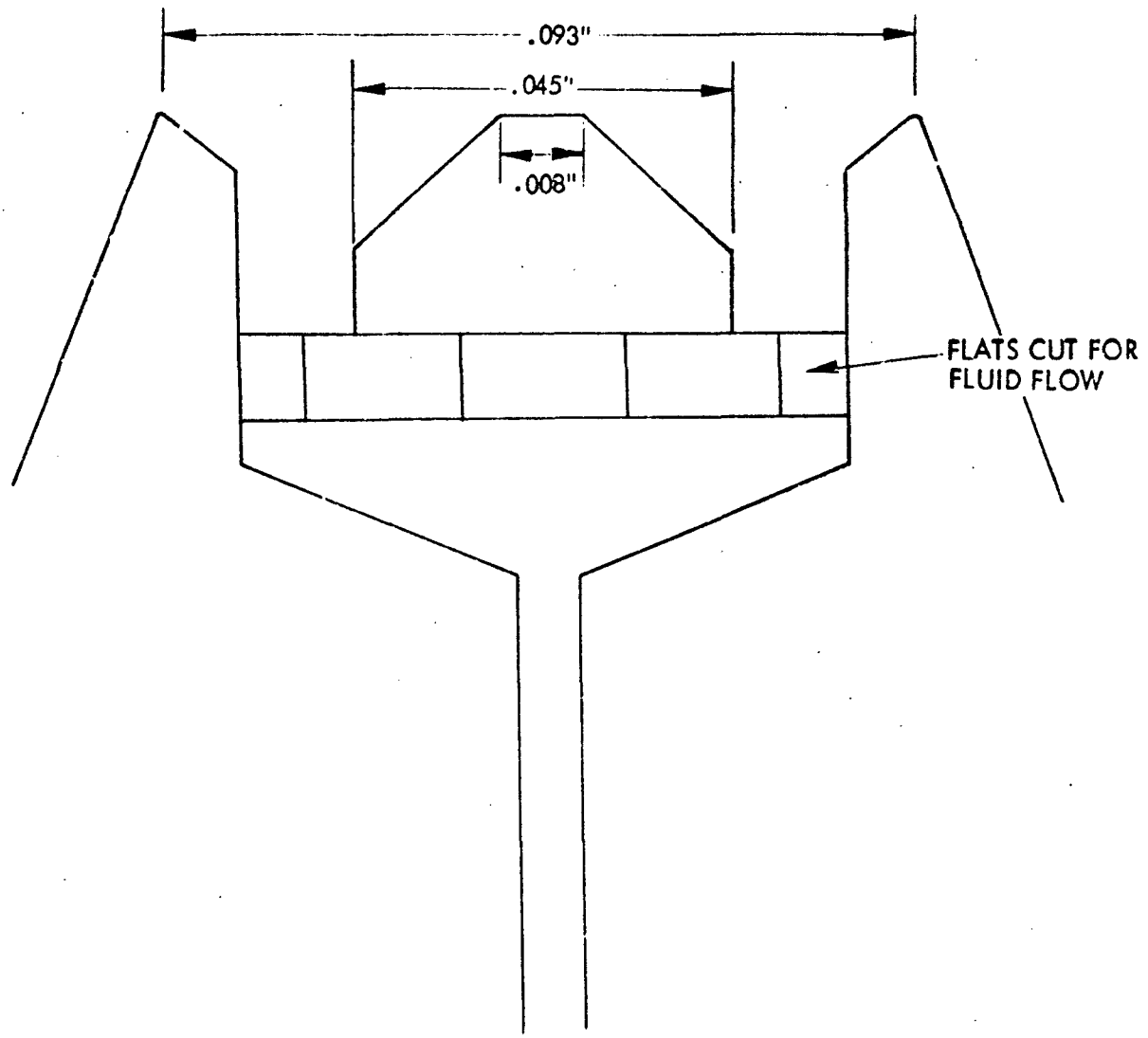


Figure 5 - Small Central Plug Emitter Schematic,
Design 7202-02

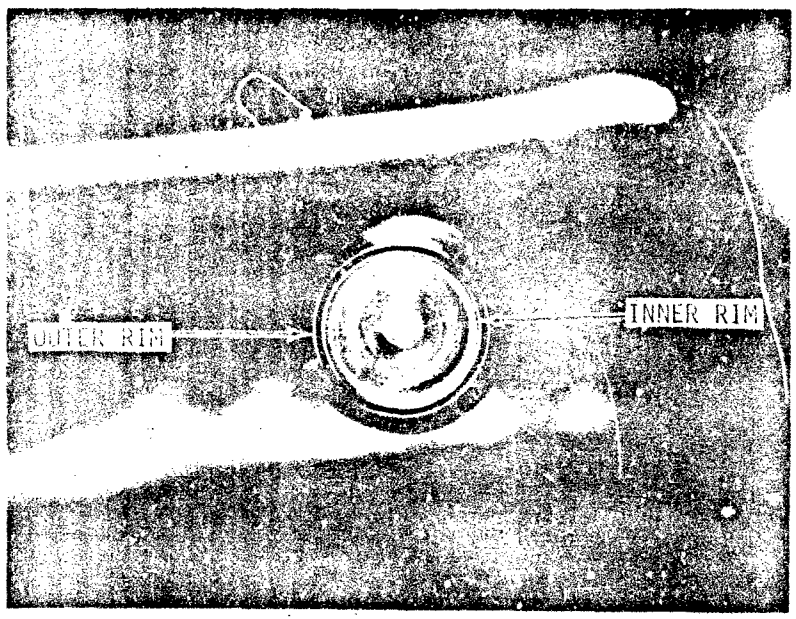


Figure 6. Double Rimmed Small Source, Design 7202-05

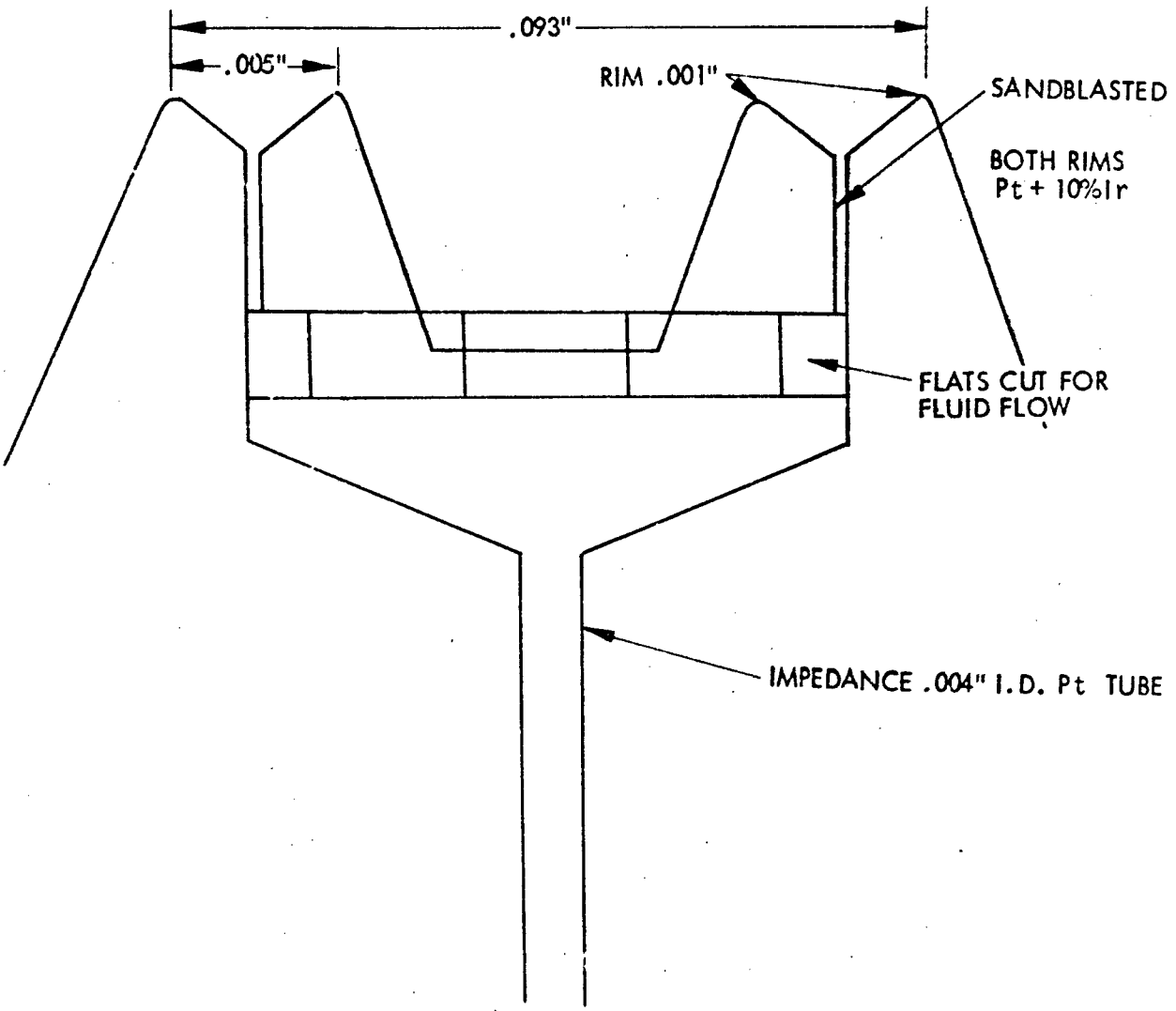


Figure 7. Double Rimmed Emitter Schematic, Design 7202-05

tempting to experiment with configurational variations which would alter the emission and field geometries. However, no such experiments are planned at this time. We did, however, make two more runs (7205-08) with the same configuration to verify that the wide beam spread was a reproducible property of this geometry, which did turn out to be the case. The latter of these two runs (7205-08) was performed with an unsalted needle to determine if reduced wetting would decrease the beam spread. No significant effect was observed.

RUN 7202-12: THIN RIM EMITTER

This was a conventional source except that it included a thin, 0.0005" radius rim. Specific impulses as high as 2000 seconds could be attained, but only at low efficiency (~ 60%). A tight well collimated beam profile was obtained as shown in Figure 8. The main conclusion drawn from this test is that going to a narrower rim diameter does not significantly affect performance except that it does lower efficiency.

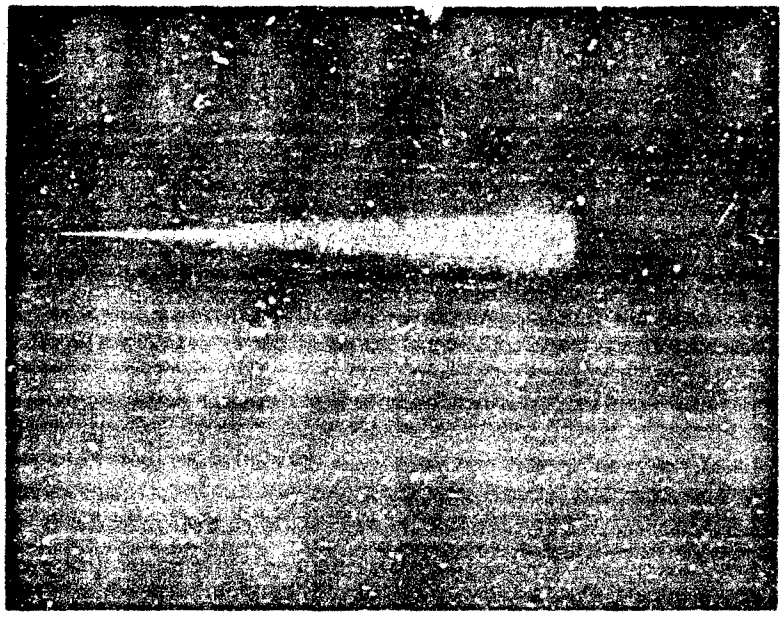

Figure 8. Visual Beam Profile Run 7201-12 (Photographed with Polaroid 3000 film, f4 aperture, 45 second exposure at background pressure of approximately $2 \times 10^{-5}$ torr)

RUN 7202-03: EXTRA BIAS PLATE

This run used a conventional source in a 3/8" extractor hole with an additional bias plate placed in front of the extractor as shown in Figure 9. The bias plate contained a 3/8" aperture which was positioned 0.175" in front of the extractor. Unfortunately, this blocked a direct view of the emitter tip while it was operating. It was possible to get high efficiency (75-80 percent), low $I_{sp}$ (1100-1300 seconds) operation. Attempts to raise the $I_{sp}$ would cause sparking behind the bias plate. The fact that the bias plate blocked a direct view of the emitter prevented a determination of the point of origin of these sparks. For this reason a new thruster was built with a slotted bias plate which allowed a direct view of the thruster. This is discussed in the following run.

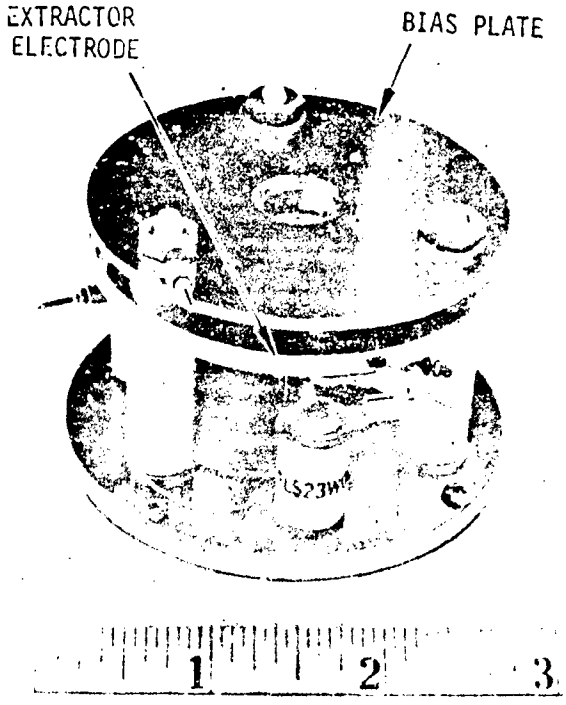


Figure 9. Conventional Thruster with Added Bias Plate Design 7202-03

## RUN 7203-03: 1" APERTURE SLOTTED BIAS PLATE

In this run the bias plate had a 1" hole in it and was placed 1/4" in front of the extractor. A 1/4" slot was machined in the bias plate to allow an unobstructed view of the thruster from the view port. The thruster current was strongly dependent on the bias plate voltage in the neighborhood of zero volts bias. Figure 10 is a plot of this behavior. The data showed a minimum beam current (18 μamps) between -25 and -50 volts. These data were taken at 18" feed pressure, 14.7 kv needle voltage, 8 kv deflector voltage, -3 kv extractor bias, 67% efficiency, 1000 seconds specific impulse and 14 μlbs thrust. At approximately -140 volts bias, the needle current leveled at 65 μamps and stayed relatively constant up to -3 kv. When the plate was driven positive, the current increased again up to approximately 60 μamps at 100 volts, at which point the fluid became highly unstable and rippled violently.

The observed behavior can be explained on the basis of two separate mechanisms coming into play for the two different bias polarities. For the negative bias, it is convenient to discuss the variation as the negative bias decreases below the -140 volts transition point. At this point, since the bias plate is highly positive relative to the negative extractor, it begins to cancel the negative extractor field, thus decreasing the extraction field strength and also to some extent possibly allowing the plasma potential to become more positive in front of the emitter, thus increasing space charge effects. Both of these effects would then cause the emitter current to decrease. During this range of operation, the plate's negative bias is still sufficient to provide a negative barrier in front of the thruster which prevents electrons from the rest of the chamber from bombarding the thruster. When the bias voltage is brought still closer to zero, the barrier begins to disappear, allowing electrons to penetrate the bias plate aperture. These electrons can reduce the space charge immediately in front of the emitter and also penetrate far enough to bombard the emitter. This condition is further enhanced as the bias is driven positive until at 100 volts the thruster becomes unstable, due to bombardment.

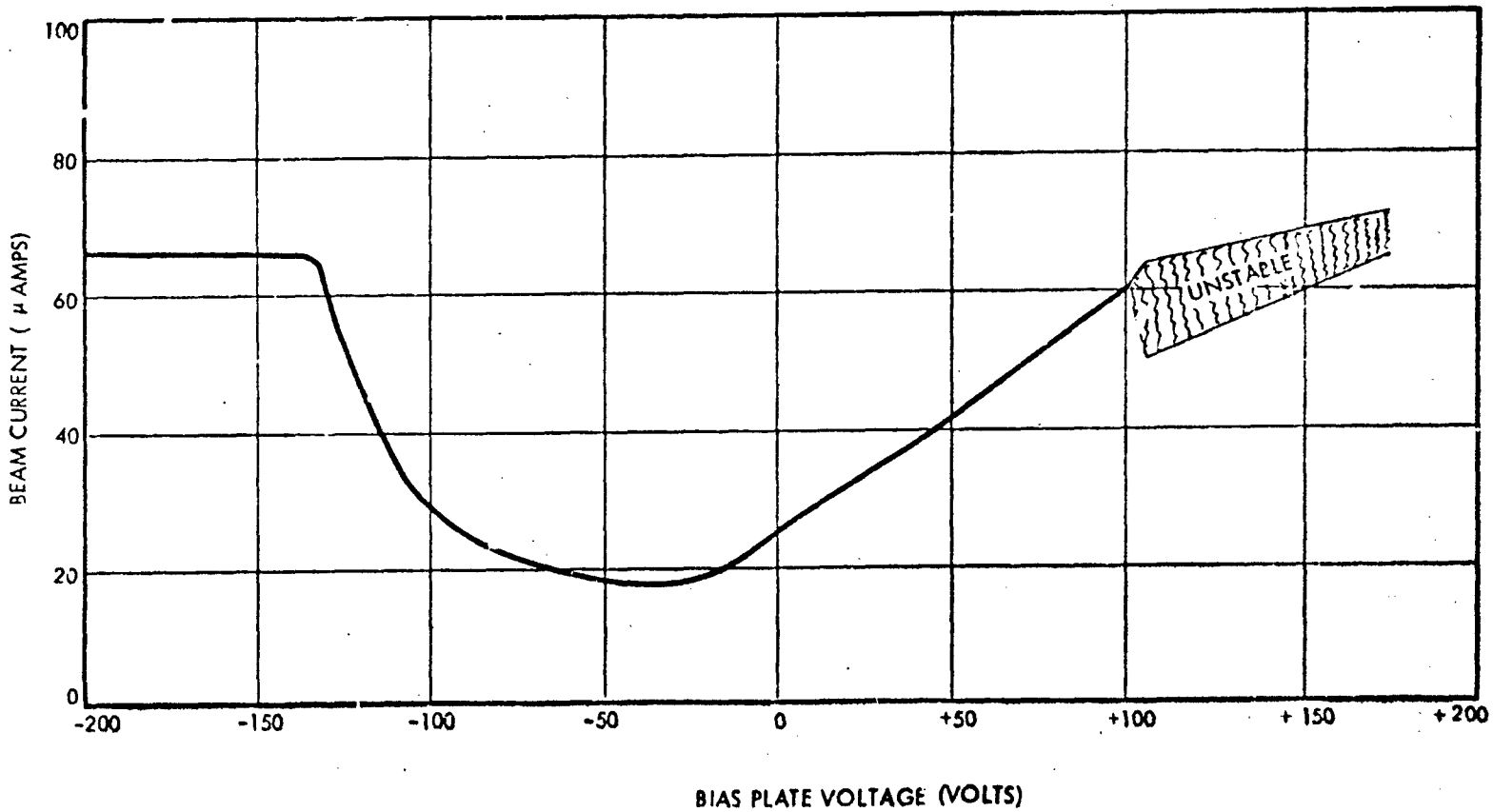


Figure 10. Run 7203-03, Thruster Current versus Bias Plate Voltage

Even with the plate bias at -3 kv, attempts to drive the thruster harder by varying other voltages led to instability and rippling. This is of special interest in this case because we can be confident that the bias voltage was more than adequate to keep electrons out under normal conditions. This leads to the conclusion that some other phenomenon is occurring. Two strong possibilities are: (1) higher performance levels result in an increased plasma and/or positive space charge density which can shield out the negative bias plate and extractor potentials and (2) higher specific impulse and higher current densities increase both the frequency and the violence of collisions within the thruster exhaust. The fact that the beam space charge can shield out negative biases has been observed in past experiments which have demonstrated that a neutralizer, although nominally immersed in the negative field near the extractor will satisfactorily emit electrons because of the ability of the thruster exhaust to shield out the negative bias.

RUN 7204-05: DOUBLE BIAS PLATE

The above considerations suggested another course of action which was later investigated. That is, if the high voltage and high field performance limitation is due to collisions within the exhaust, the violence of these collisions might be reduced by providing a longer acceleration distance so that the droplets do not achieve their full velocity until they are further from the thruster than is possible with the present geometry. At this more remote location the particle density will be lower, thus reducing the collision probability. Furthermore, the emitter will then present a relatively smaller target for the back-scattered collision products.

The purpose of this run was to see if we could achieve greater thruster stability by delaying the final droplet acceleration until the droplets were outside the immediate vicinity of the emitter surface. This was accomplished by placing two bias plates out in front of the extractor as shown in Figure 11. Slots were cut out of the plates in order to allow an unobstructed line of sight which would permit visual observation of the thruster during operation.

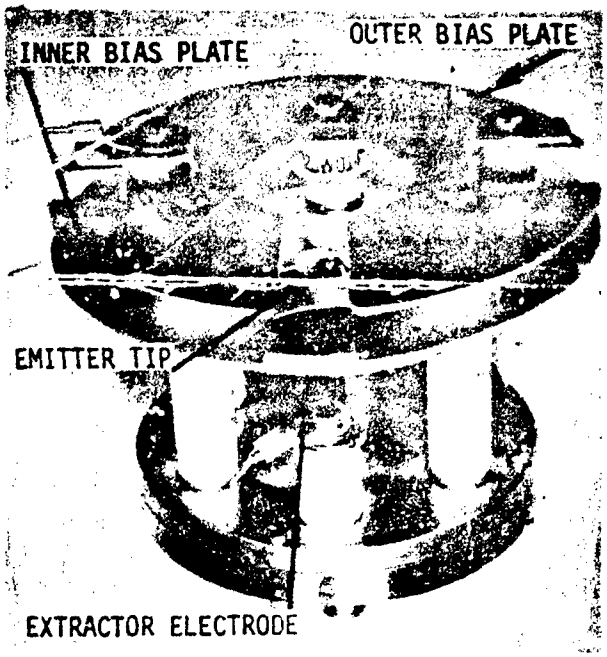


Figure 11. Double Bias Plate Module (Key slots in bias plates are to allow unobstructed visual path to emitter tip.)

The idea behind this arrangement was to bias the outermost plate negatively to provide an electron barrier while maintaining the innermost bias plate highly positive in order to provide a positive potential drift region prior to final acceleration. With this arrangement, it was possible to go as high as 10 kv bias on either plate, the limitation at this point being due to the external circuitry.

The overall results tended to confirm our previous theories. That is, there were unstable operating modes that could subsequently be stabilized by driving the innermost plate more positive. It was also found that the outer plate had to be held negative to maintain stability in this mode. Otherwise, electrons could be pulled into the positive potential region and subsequently bombard the emitter. Also, the higher the positive voltage on the inner plate, the higher the negative voltage required on the outer plate. Usually, the negative bias would have to be approximately 10 percent of the positive voltage. Going to too high a

negative voltage ( ~-5 kv) on the outer plate would also create instabilities, apparently due to secondary electron production at the negative electrode. The performance at a given set of deflector, emitter and extractor voltages was relatively independent of bias plate settings. In spite of the aforementioned stabilizing influences, it was still not possible to stably exceed 21 kv emitter voltage, even after the bias plate circuitry had been modified to permit biases up to 13 kv. For this reason, our main conclusion is that these experiments qualitatively verified the collision aspect of the voltage effect on stability but the results were not great enough to significantly affect overall performance potential.

RUN 7203-06: THICK-RIMMED (0.002" DIAMETER) EMITTER

This test, which was performed with a 3/8" diameter extractor aperture, was for the purpose of determining if a thicker rim would lead to improved efficiency. The efficiency was high, usually around 80 percent, with low $I_{sp}$ (800-1200 seconds). The thruster operated smoothly up to 30 μlbs.

However, although the efficiency was high, the concurrent $I_{sp}$ reduction was deemed too great to justify further work with thick rimmed emitters.

RUN 7206-01: ELECTROPOLISHED EMITTERS

The purpose of this run was to evaluate the influence of electropolishing on thruster performance. Mechanically finished emitters have small spiral machining grooves that can be seen under high magnification. Since the propellant has to flow across these grooves to wet out to the rim, there is a possibility that the grooves could impede the wetting process. Actually, these grooves exist in all machined emitters. However, it seemed appropriate at this time, with the extremely good mechanical finish that could be attained with the emitter forming tool, to see if this could be further improved upon by electropolishing away the residual grooves. The surface area within the emitter below the electropolished rim region was sandblasted in the usual manner. After final cleaning, the emitter was given the usual surface salting treatment.

The thruster performance differed markedly from that of previous emitters. Visually, it appeared that the emitter interior was well wetted right out to the rim. However, the current was very low, of the order of 20 μamps, consisting of mostly ions for the various voltage combinations that were tried. Emission and rippling at the center would become increasingly unstable as further attempts were made to increase either voltage or feed pressure. In view of the apparently anomalous behavior, the run was terminated to allow a detailed inspection of the emitter interior and the thruster module to determine if there was some constructional fault which was responsible for the behavior. However, apart from the fact that the emitter well was a little shallow (0.0135" instead of 0.015"), nothing unusual was found and a decision was made to repeat the test to determine if the behavior was reproducible.

RUN 7202-02: ELECTROPOLISHED EMITTER

The emitter from the previous run was carefully cleaned and reinstalled to determine if its performance would repeat that of the earlier test. The performance characteristics of the previous test were once again observed, confirming that this thruster would operate only in a low current mode. At this time, a decision was made to deepen the well of this emitter to make sure that the performance problems were not related to the well depth.

RUN 7206-06: ELECTROPOLISHED DEEP WELL EMITTER

This was an electropolished emitter with a deeper well (0.015") than the previous tests of this configuration. This resulted in higher stable mode currents than the previous runs (up to 36 μamps) but still at efficiencies lower than 70 percent. The overall results of these tests indicated that electropolishing does not produce high efficiency operation, and for this reason they were discontinued.

RUN 7206-04: EXTENDED SANDBLASTING

In order to cover the two extremes of surface finish; in addition to the electropolished runs, a thruster was fabricated which went to the other extreme; sandblasting out to the outer rim to provide a completely roughened emission area. During operation the thruster had

a wide beam spread which confirmed the validity of sandblasting only out to the inner rim. The beam spread was due to the fluid wetting and flowing very well over all sandblasted surfaces, which in this case included the outer regions. Emission originating at the outer surfaces had a large radial velocity component due to the radial electrostatic field in these regions. Also, the emission was now occurring over regions of greatly varying field strengths, thus producing a large spread in charge-to-mass ratios. When the beam was widely spread, there was a high ion content in the center of the beam and relatively low charge-to-mass ratios on the outside. This was not surprising since the outer surfaces of the emitter, where the wide angle emission originated, were closer to the highly positive deflector electrodes, and hence had a lower surface field strength, thus resulting in lower charge-to-mass ratios.

### 3.1.1 Tool Made Emitters

Several runs were made to fully characterize the performance characteristics of tool-made emitters of the type which had given the best performance to date. Three identical emitters (hereafter designated as TM1, TM2 and TM3) were made using a specially shaped lathe tool which guaranteed emitter-to-emitter rim reproducibility and rim uniformity around the diameter of each emitter. This technique had several advantages. It eliminated q/m variations around the rim due to geometric variations. The increased q/m uniformity increased efficiency and also reduced the number of collisions within the beam, thus increasing beam stability. Furthermore, since increasing the efficiency for a given average charge-to-mass ratio also allowed a lower accelerating voltage for a given specific impulse, rim uniformity also increased thruster stability by lowering the required accelerating voltage. Operational stability was also increased by the elimination of localized regions of excessively high field strength. The remaining runs on the program were made with tool-formed emitters. The tool is described in greater detail in Appendix B.

#### RUN 7207-06: 1/2-INCH EXTRACTOR (EMITTER TM1)

This was the first run to map the full performance range of a tool-made thruster, using a 1/2" diameter extractor. Stable performance could be obtained over the full range of source voltages from 16 to 22 kv. However, the range of permissible deflector voltages decreased as we went up in the source voltage. Thus, at 22 kv source voltage, the

difference between source and deflector voltages could not exceed 4 kv. The performance was mapped at 25°C at 2" feed pressure increments from 3.5 to 9.5" Hg. The results are shown on Figures 12 through 15. Well collimated, stable beams with thrusts from less than 20 to greater than 50 μlbs could be attained. Specific impulses and efficiencies, however, were on the low side, rarely exceeding 1200 seconds or 65 percent. This was the result of a long, low amplitude tail on the time-of-flight curves. It is believed that this was due to overfeeding at the bottom of the emitter due to gravity effects. During the performance mapping of a 3/8" diameter extractor aperture on a later test, a vertical beam probe showed that the beam was being emitted preferentially a few degrees downward, which indicated that there was a gravity effect.

RUN 7208-01: 3/8" EXTRACTOR

The performance was similar to that obtained with the 1/2" extractor aperture. Stable performance could be obtained over the full range of source voltages; however, as in the previous case, the range of allowable deflector voltages narrowed as the source voltage was increased to 22 kv. Thrusts up to the order of 50 μlbs could be obtained, but the specific impulse rarely exceeded 1200 seconds and the efficiency was usually in the low 60's. There were a few high specific impulse points at low feed pressure (3.5" Hg) but these were at low thrust and low efficiency. Figures 16 through 19 show the performance that was obtained.

The beam profile was scanned vertically with a vertical time-of-flight probe. Two interesting facts were observed. As can be seen from Figure 20, the beam profile was skewed downward. Secondly, the probe time-of-flight consistently gave higher specific impulses than were observed with the total beam collector. This could mean that there was a large slow velocity beam component directed in some off-axis direction which missed the probe and which was causing a long total current time-of-flight tail, thus implying low total efficiency and specific impulse. These observations were in agreement with our suspicions that the thruster's horizontal orientation was causing propellant to overfeed at the bottom of the emitter rim thus causing vertical asymmetry in the beam profile and low efficiency. The obvious cure for

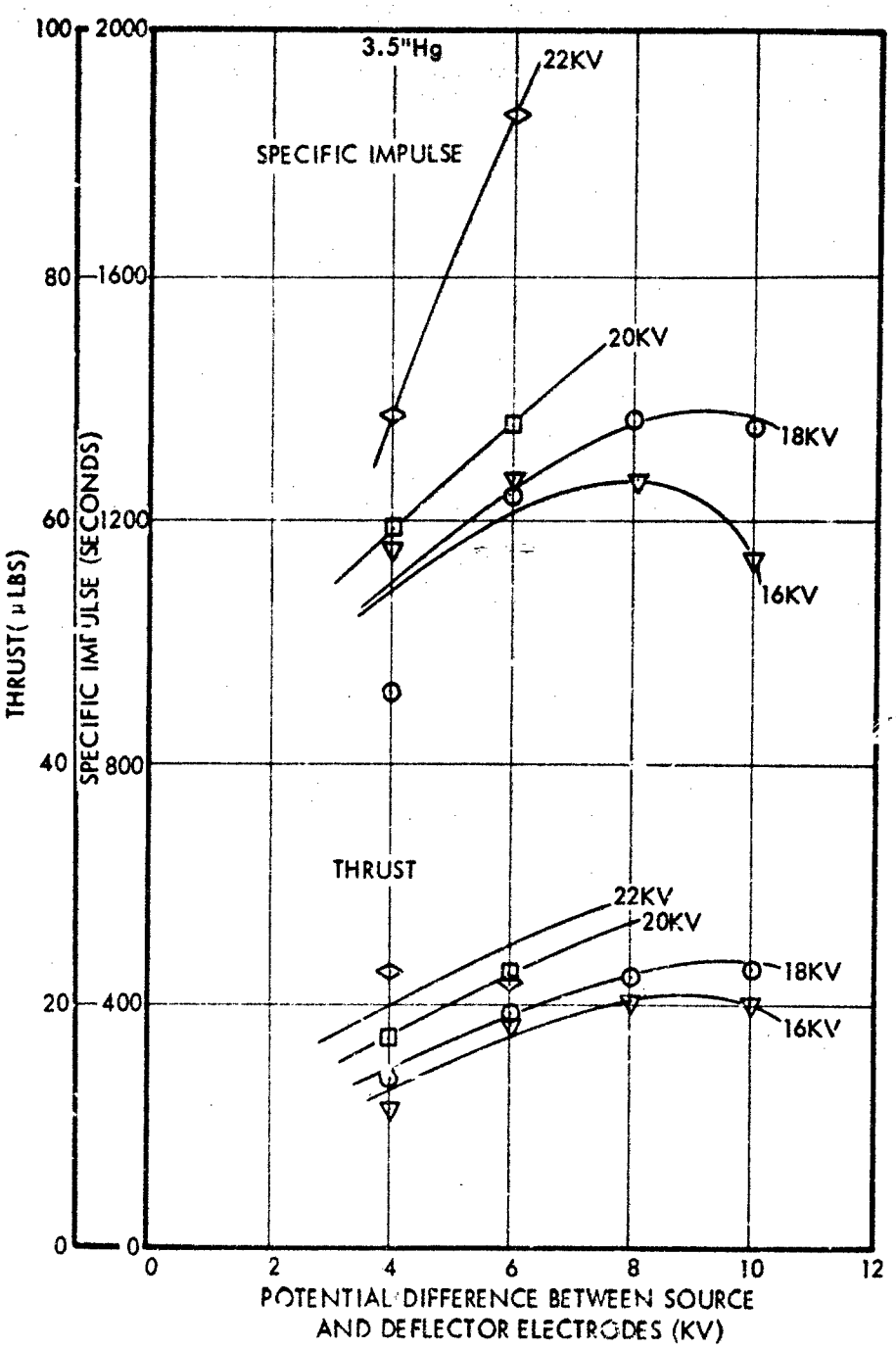


Figure 12. Run 7207-06. Thrust and Specific Impulse as a Function of Source to Deflector Voltage Difference at 3.5" Hg Feed Pressure (∿ 7 μg/sec mass flow)

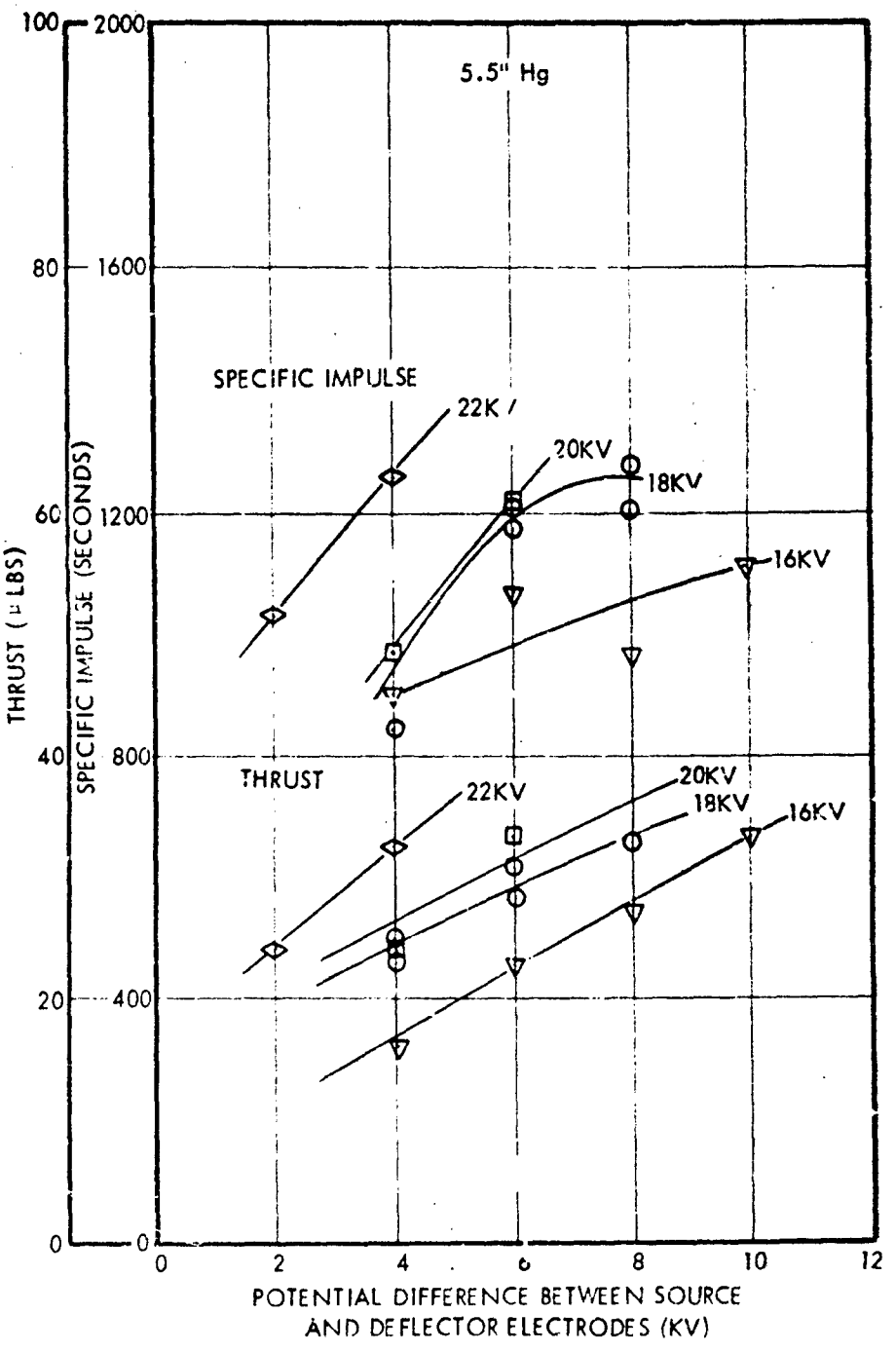


Figure 13. Run 7207-06. Thrust and Specific Impulse as a Function of Source to Deflector Voltage Difference at 5.5" Hg Feed Pressure (∿ 11 μg/sec mass flow)

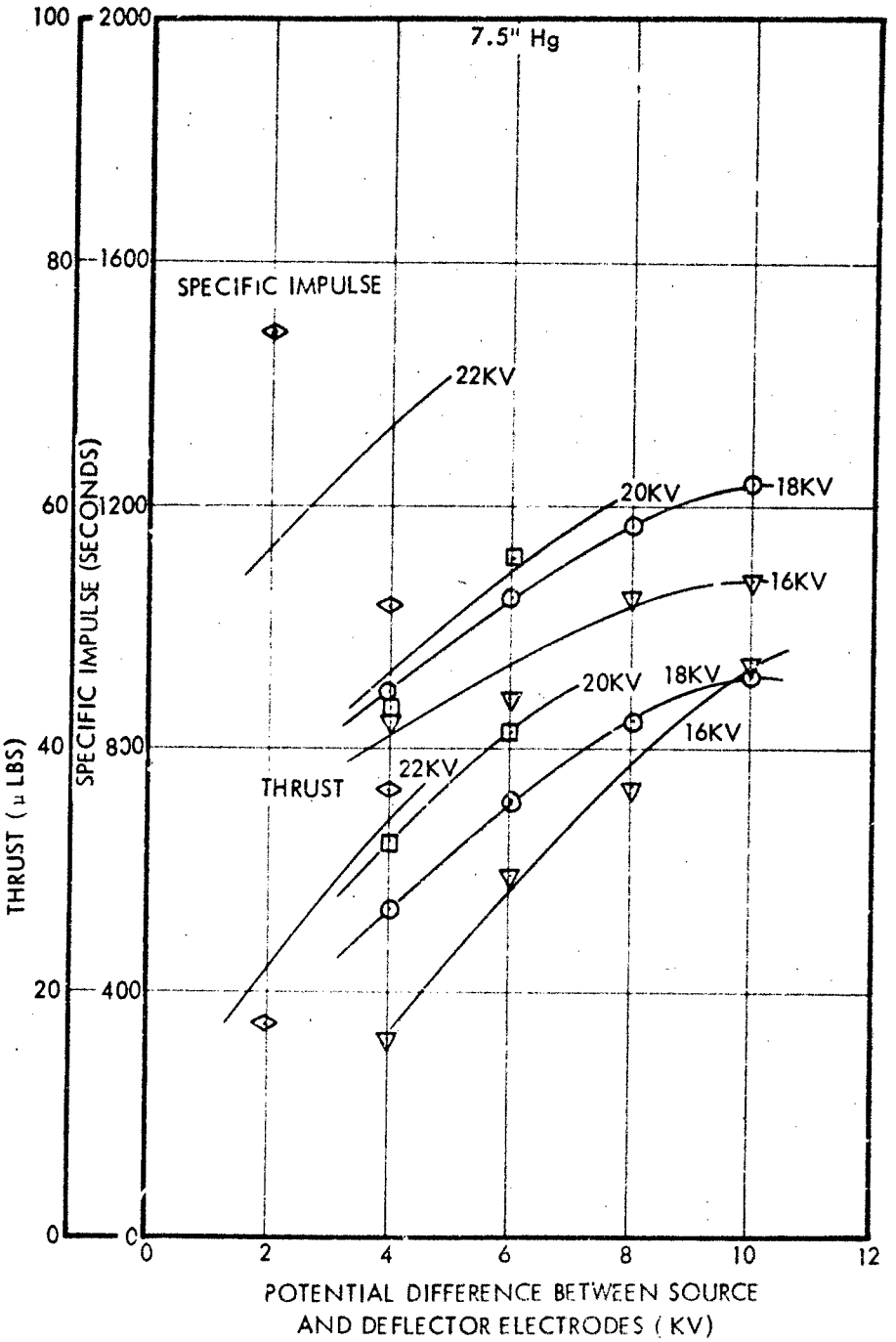


Figure 14. Run 7207-06. Thrust and Specific Impulse as a Function of Source to Deflector Voltage Difference at 7.5" Hg Feed Pressure (~ 16 μg/sec mass flow)

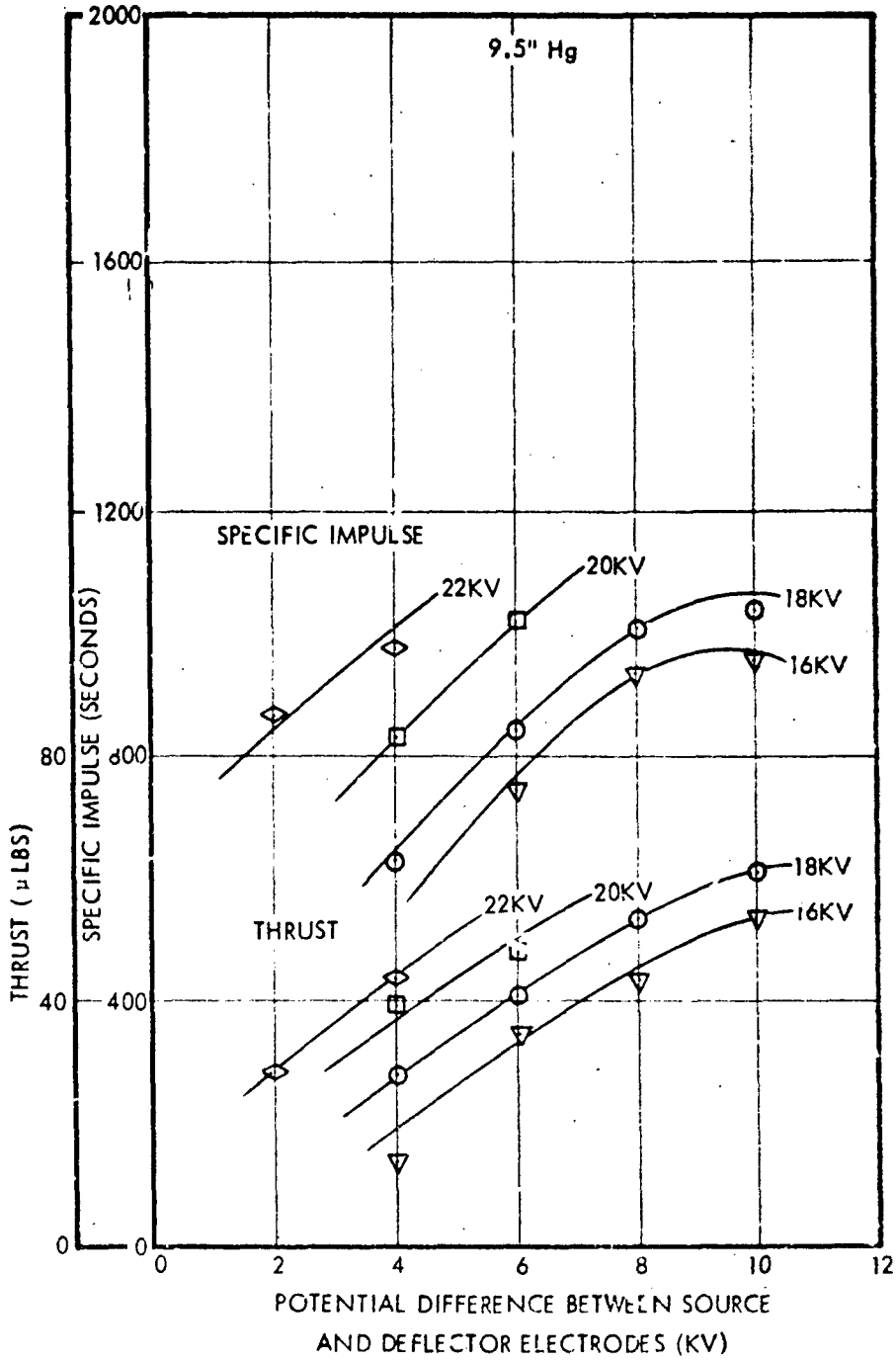


Figure 15. Run 7207-06. Thrust and Specific Impulse as a Function of Source to Deflector Voltage Difference at 9.5" Hg Feed Pressure (∿ 22 μg/sec mass flow)

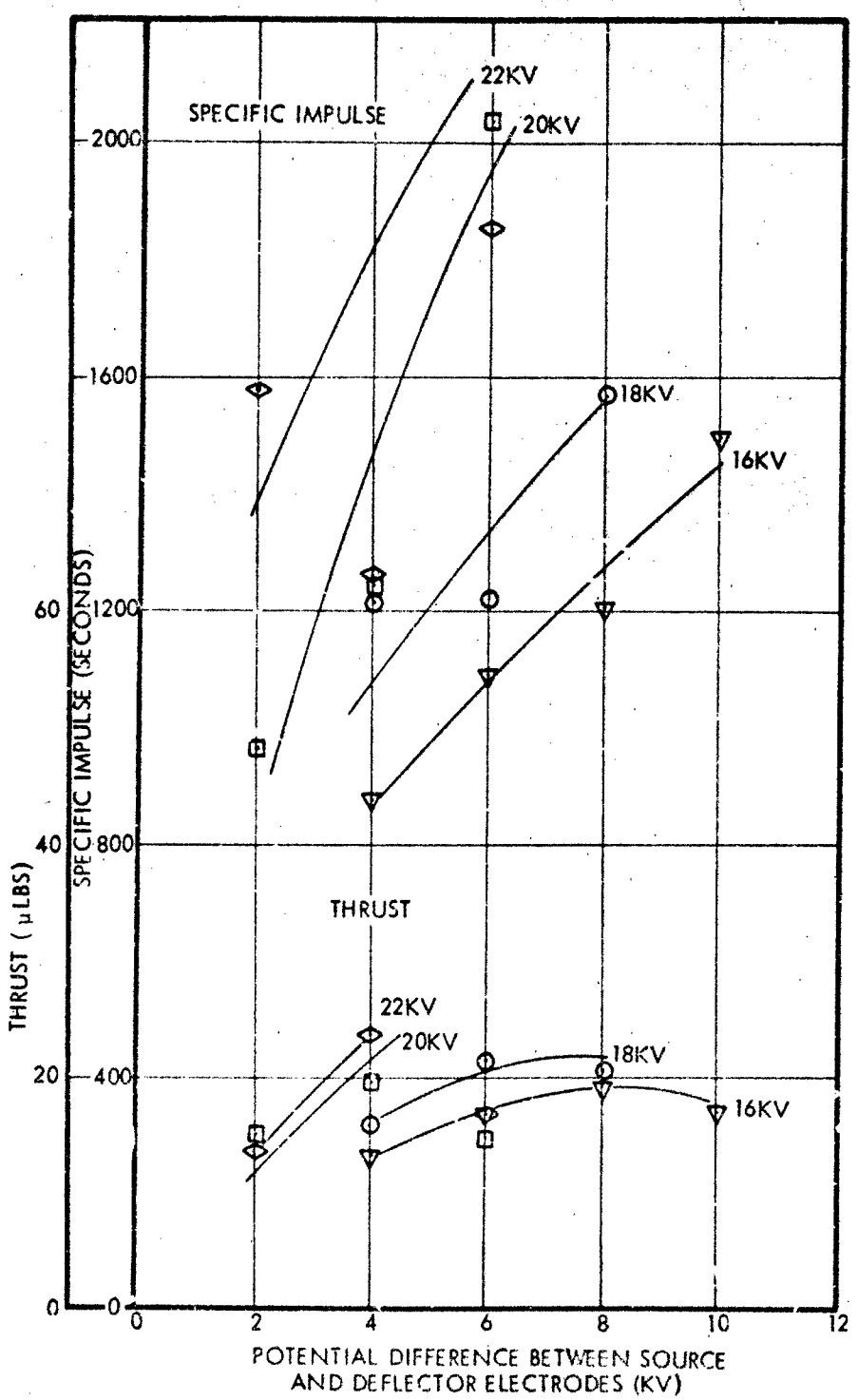


Figure 16. Run 7208-01. Emitter No. TM1, 3/8" Extractor, Horizontal Test, 3.5" Hg Feed Pressure (~ 7 μg/sec mass flow)

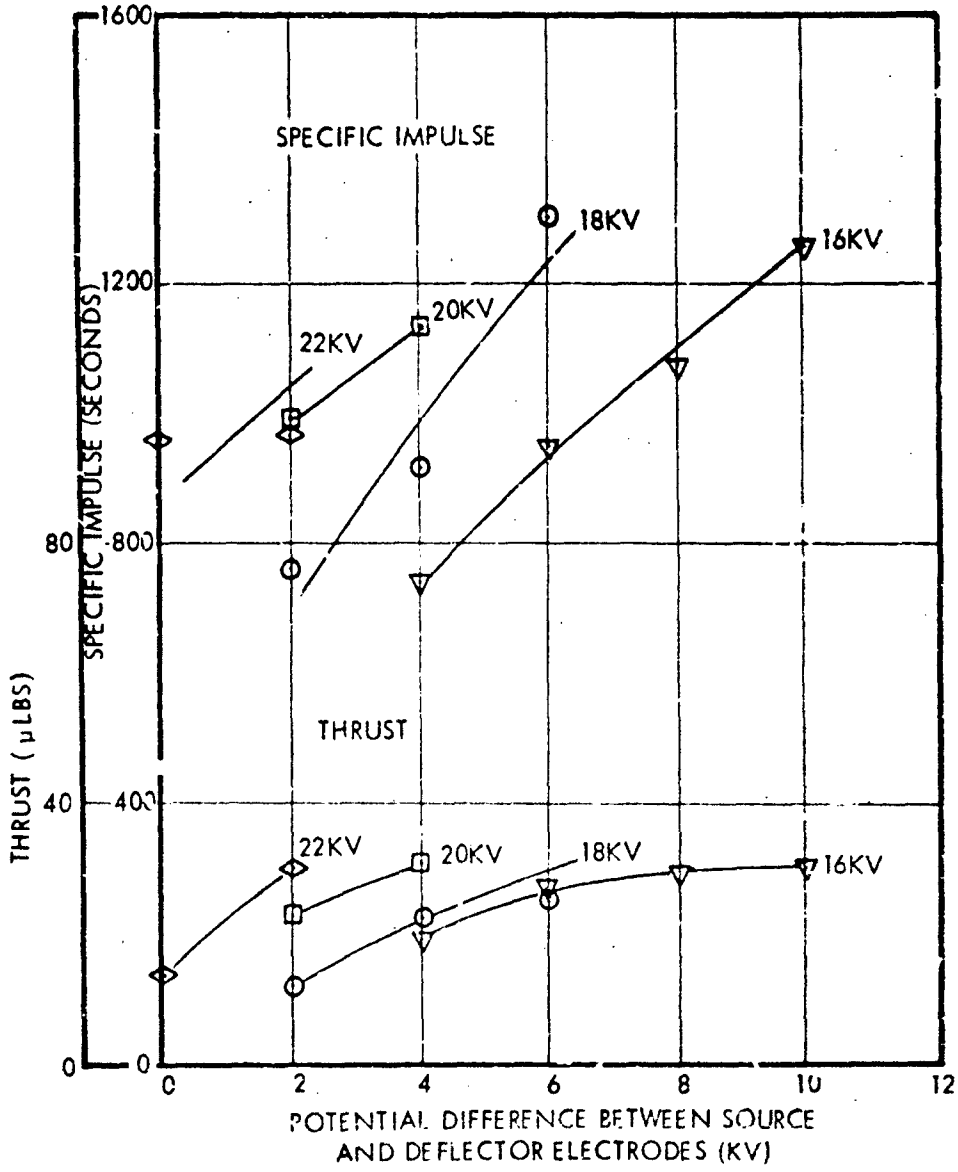


Figure 17. Run 7208-01. Emitter No. TM1, 3/8" Extractor, Horizontal Test, 5.5" Hg Feed Pressure (~ 11 μg/sec mass flow)

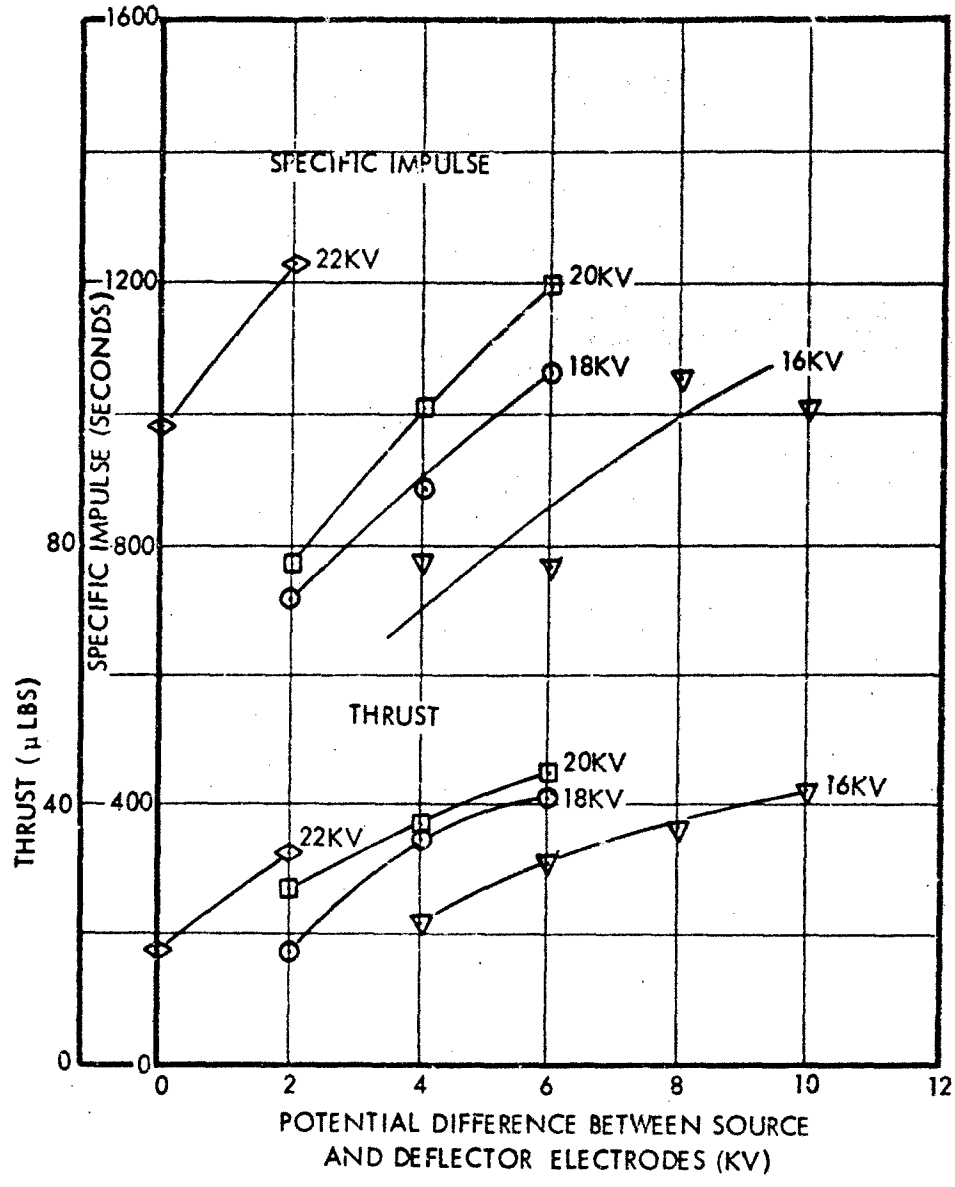


Figure 18. Run 7208-01. Emitter No. TM1, 3/8" Extractor, Horizontal Test, 7.5" Hg Feed Pressure (∿ 16 μg/sec mass flow)

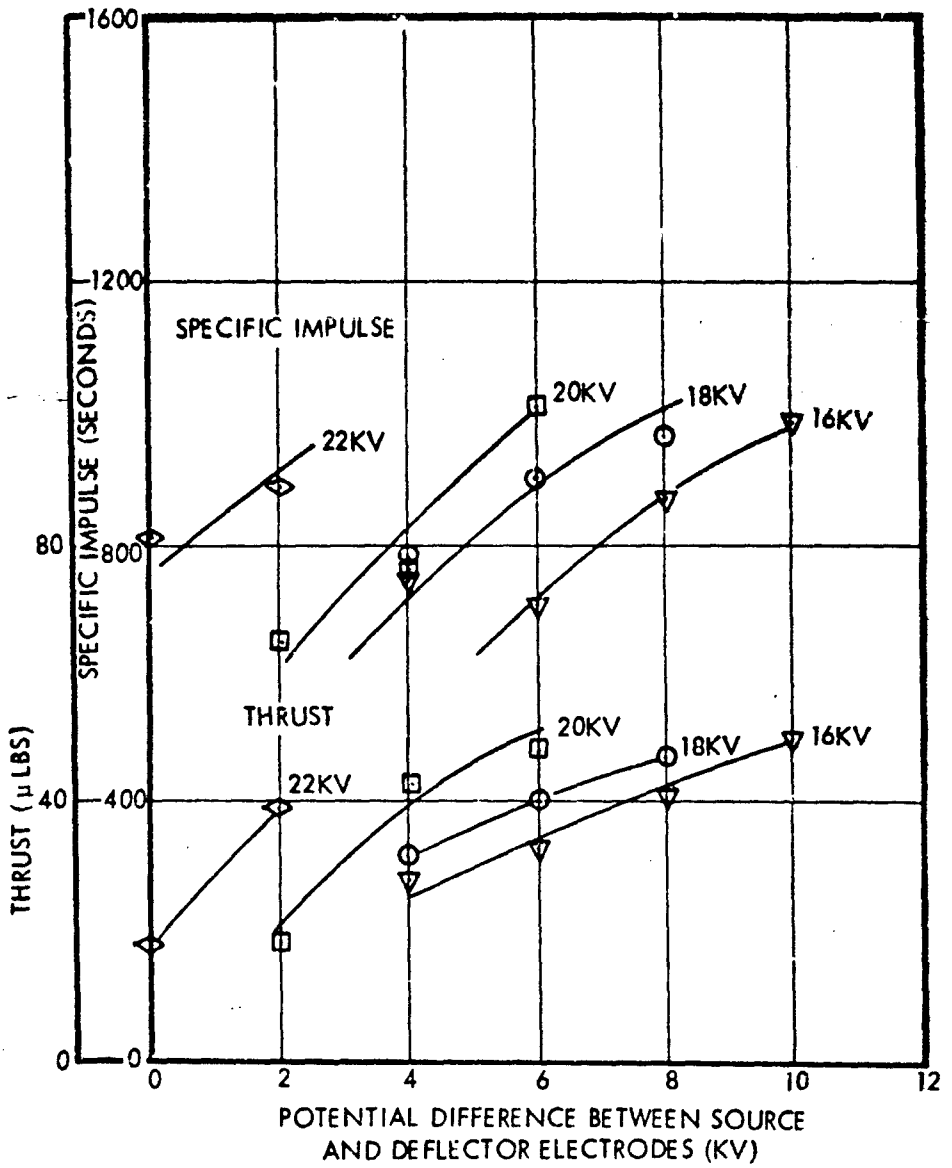


Figure 19. Run 7203-01. Emitter No. TM1, 3/8" Extractor, Horizontal Test, 9.5" Hg Feed Pressure (∿ 21 μg/sec mass flow)

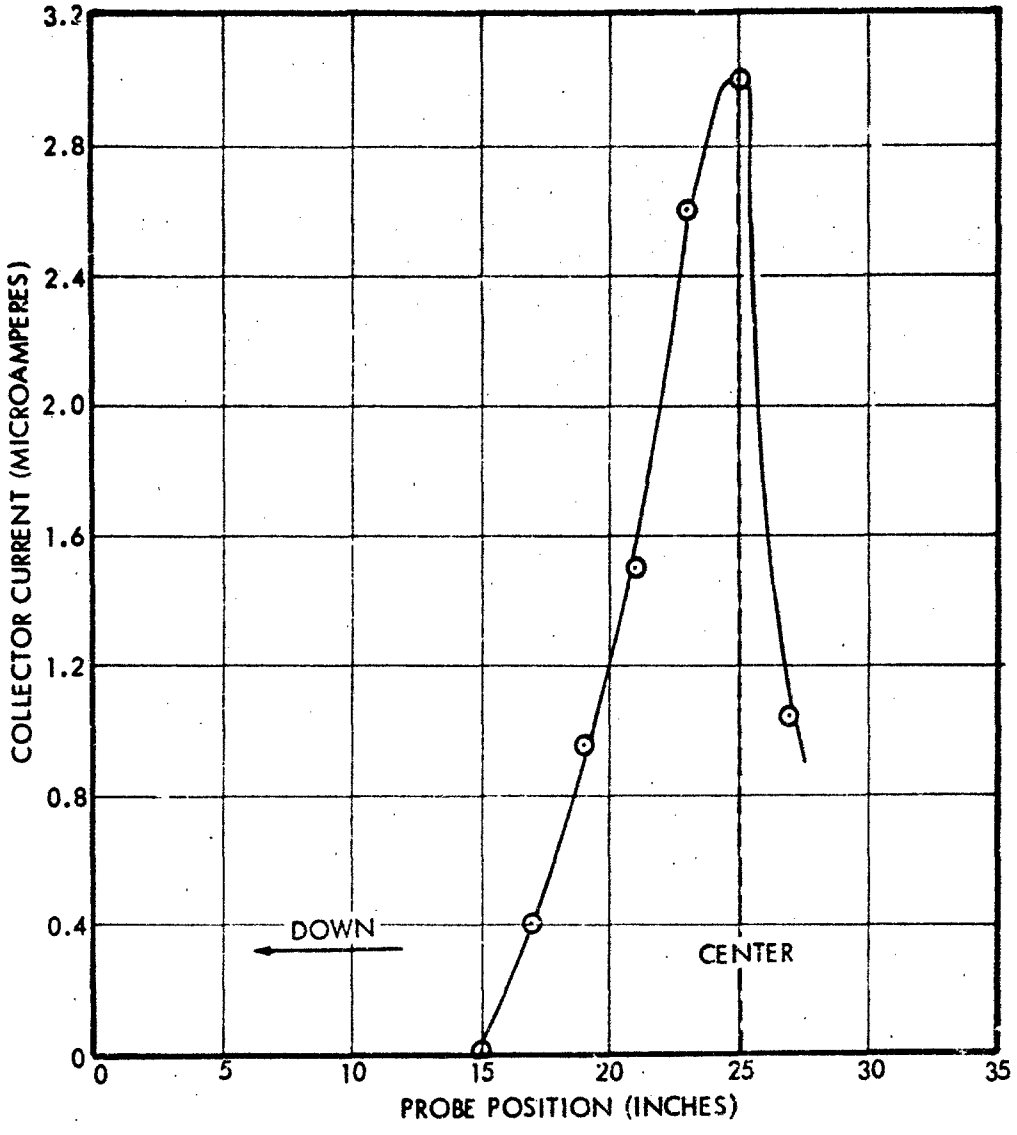


Figure 20. Run 7208-01. Vertical Probe of Current Density

this was, as will be described later in the report, converting the facility to vertical operation. Later results showed that this did indeed greatly improve performance.

RUN 7208-02: EMITTER 1/2" EXTRACTOR, HORIZONTAL OPERATION
EMITTER RECESSED 0.010" BEHIND THE DEFLECTORS AND EXTRACTOR

The purpose of this run was to determine if recessing the emitter could raise the efficiency. The reason for trying this was the fact that the performance of the ADP needles had been found to be sensitive to needle height within the ground shield electrode. We had earlier on this program tried moving the emitter tip 0.005" in and out relative to the deflectors with no noticeable effects. We felt it worthwhile to try once more using the tool-made emitter and this time moving the emitter 0.010" relative to the deflector electrodes and extractor.

The performance was essentially the same as on previous tests except that the $I_{sp}$ was lowered by approximately 50 to 100 seconds for a given voltage and pressure. This was to be expected since pushing the emitter behind the deflectors would lower the extraction field. Some of the results are shown in Figure 21. No efficiency improvements were observed and it was concluded that this geometry change did not help performance.

In addition to operating at the usual 25°C operating temperature, the performance was measured at 16°C and 20°C. Apart from a slight increase in efficiency no significant performance changes were observed.

## 3.2 Vertical Testing

RUN 7208-04: 1/2" EXTRACTOR (EMITTER TM2)

A complete performance map was made as shown in Figures 22-27; the most significant fact was that specific impulses in the 1500 second range could be obtained at thrusts as high as 40 μlbs. This was due to there no longer being a long time of flight tail. This allowed very high efficiency operation. For example at 4.5" Hg, 20 kv source voltage, 16 kv deflector voltage we were now able to get 77 percent efficiency, 1350 seconds specific impulse and 31 μlbs thrust. For the same feed pressure, 22 kv source voltage and 18 kv deflector voltage we were able to get 74 percent, 1450 seconds and 40 μlbs.

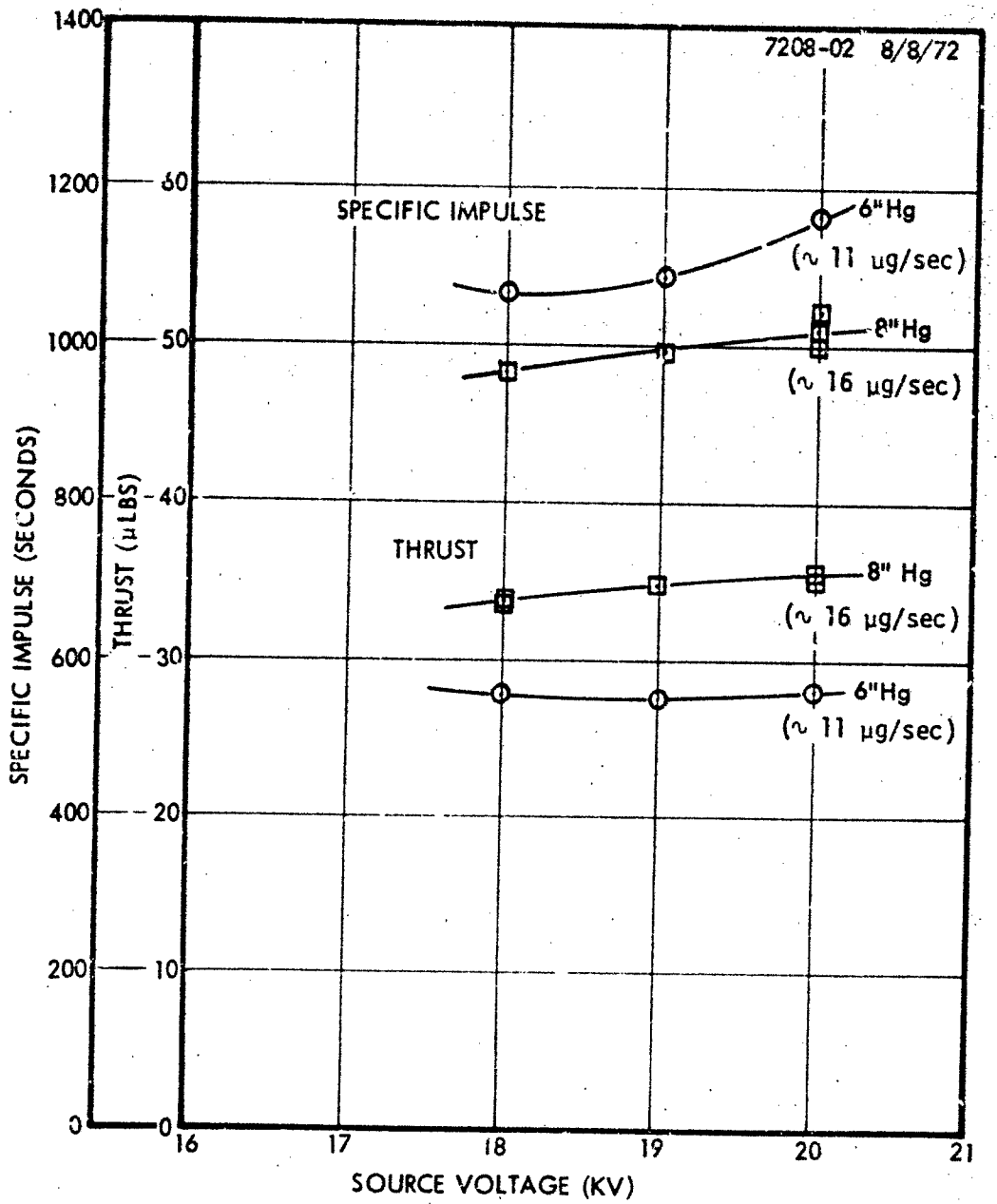


Figure 21. Run 7208-02. Emitter No. TM1, 1/2" Extractor, Vertical Test, Emitter 0.010" Behind Reflectors and Extractor, Thrust and Specific Impulse versus Source Voltage at $V_S - V_D = 6$ kv

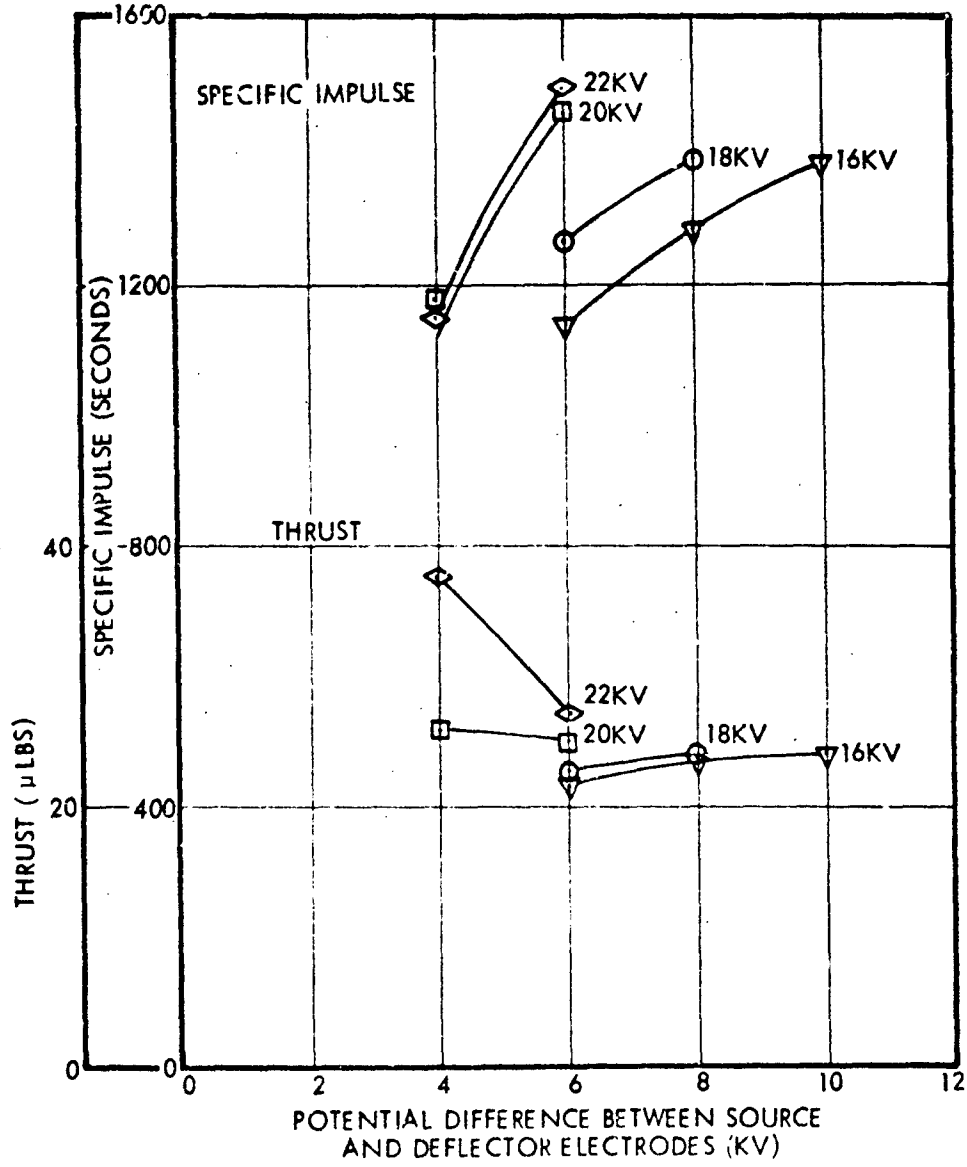


Figure 22. Run 7208-04. Emitter No. TM2, 1/2" Extractor, Vertical Test, 3.5" Hg Feed Pressure (~ 8 μg/sec mass flow)

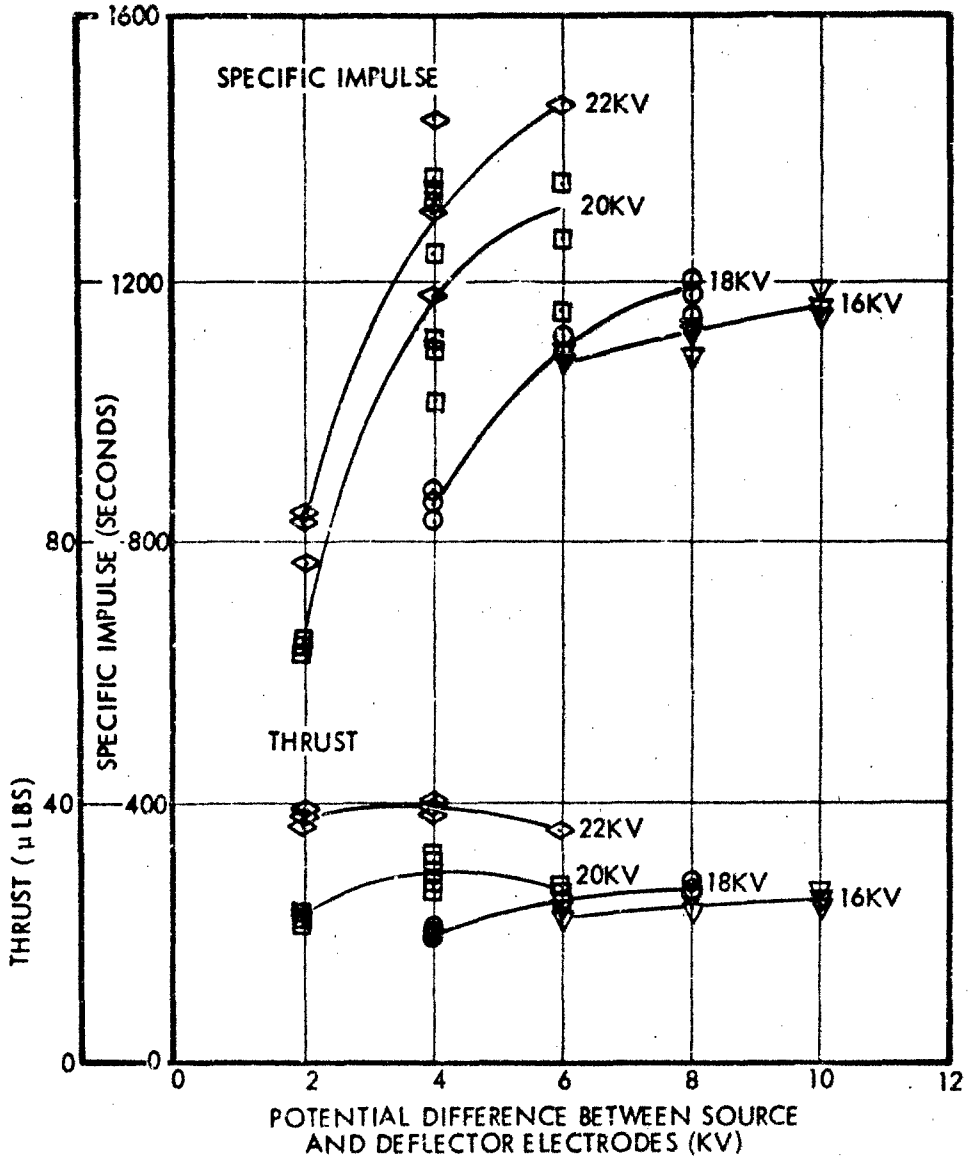


Figure 23. Run 7208-04. Emitter No. TM2, 1/2" Extractor, Vertical Test, 4.5" Hg Feed Pressure (∿ 10 μg/sec mass flow)

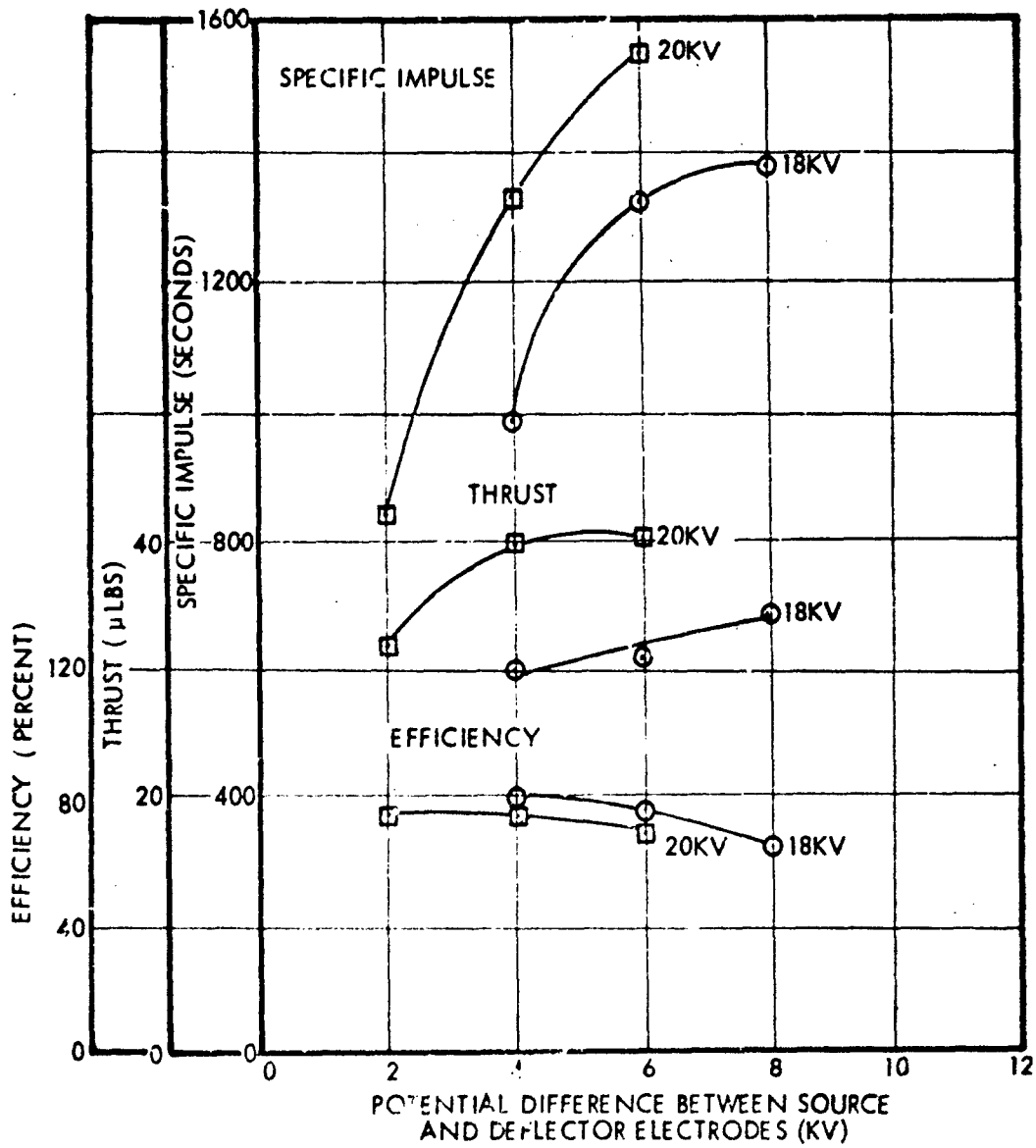


Figure 24. Run 7208-04. Emitter No. TM2, 1/2" Extractor, Vertical Test, 5.5" Hg Feed Pressure (~ 12 μg/sec mass flow)

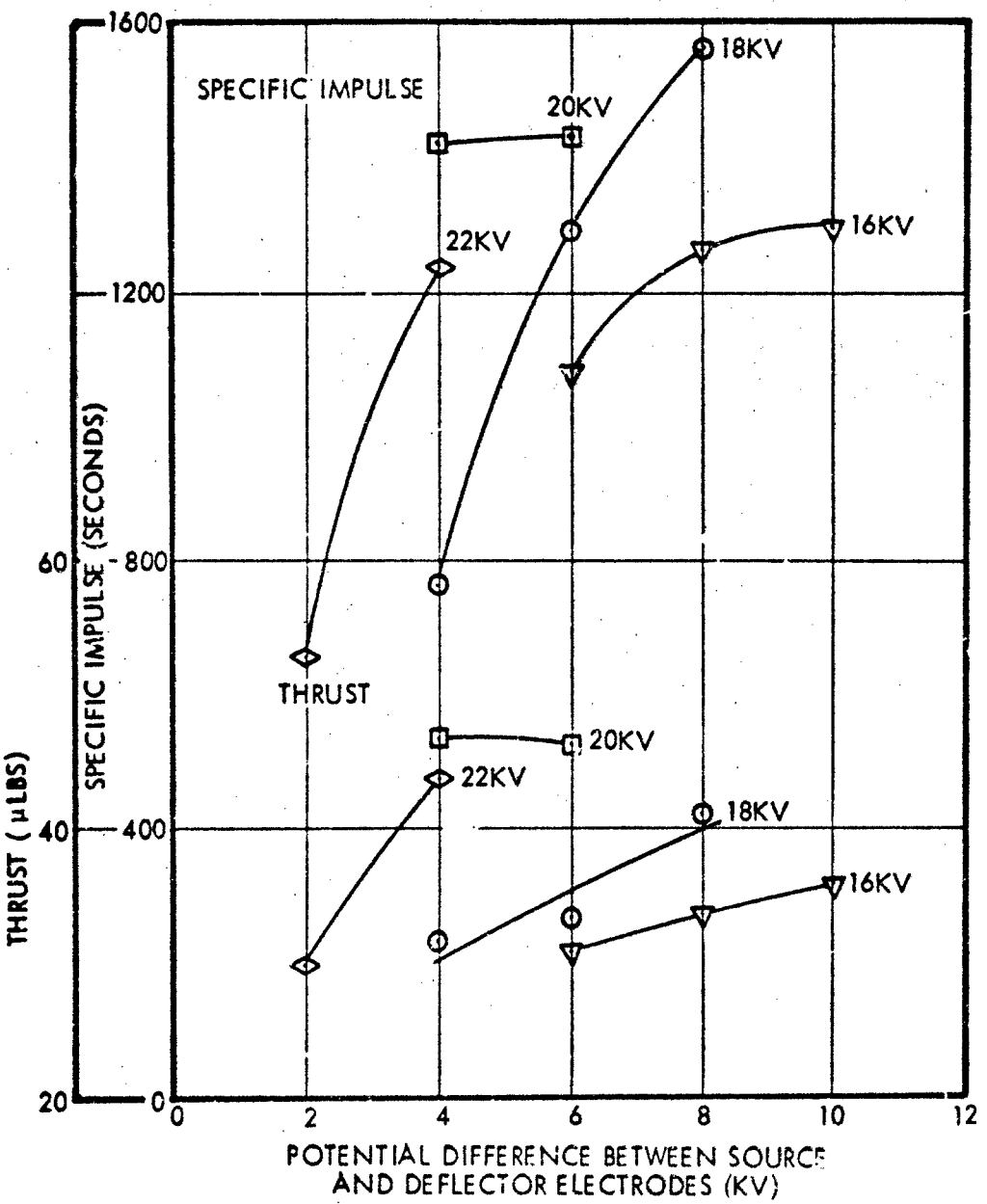


Figure 25. Run 7208-04. Emitter No. TM2, 1/2" Extractor, Vertical Test, 6.5" Hg Feed Pressure (∿ 15 μg/sec mass flow)

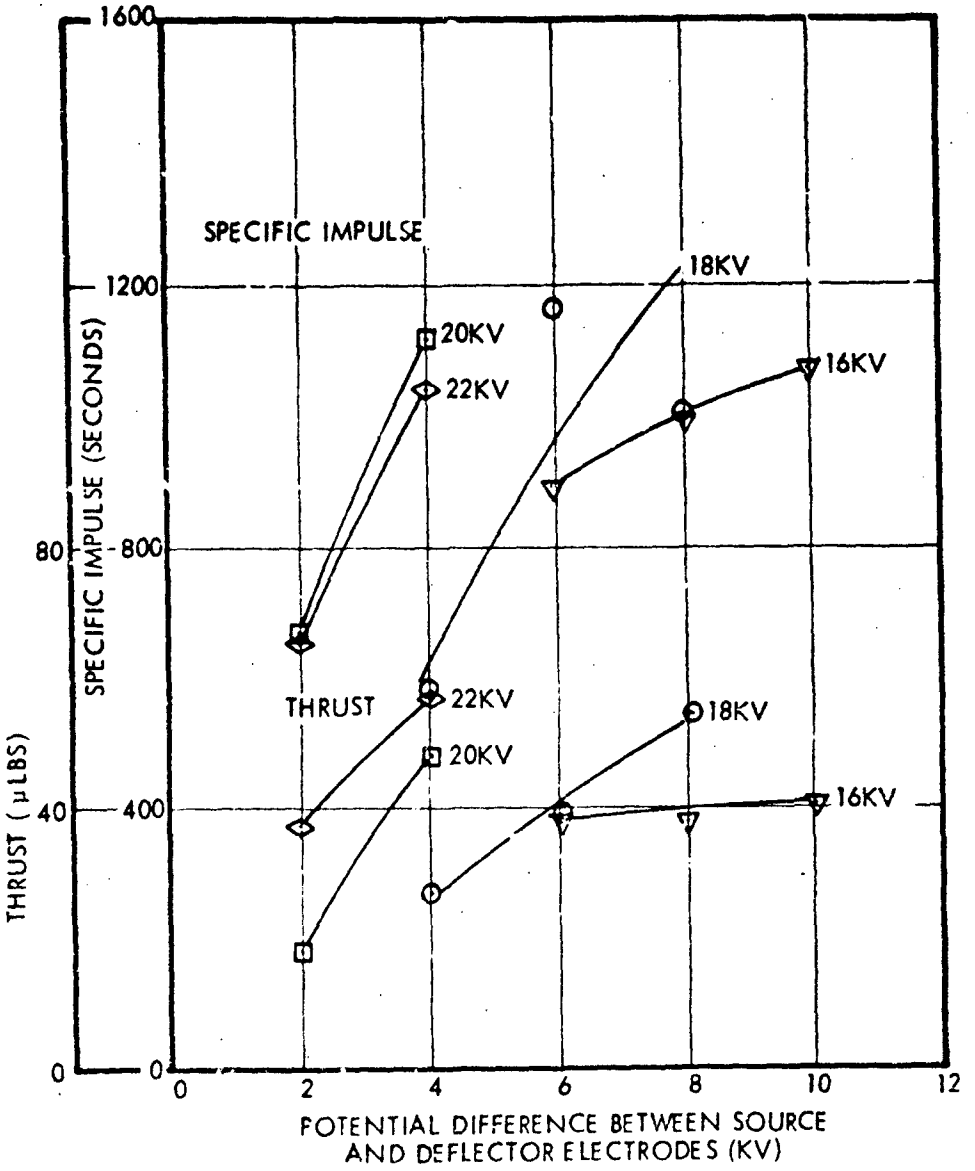


Figure 26. Run 7208-04. Emitter No. TM2, 1/2" Extractor, Vertical Test, 8.5" Hg Feed Pressure (~ 20 μg/sec mass flow)

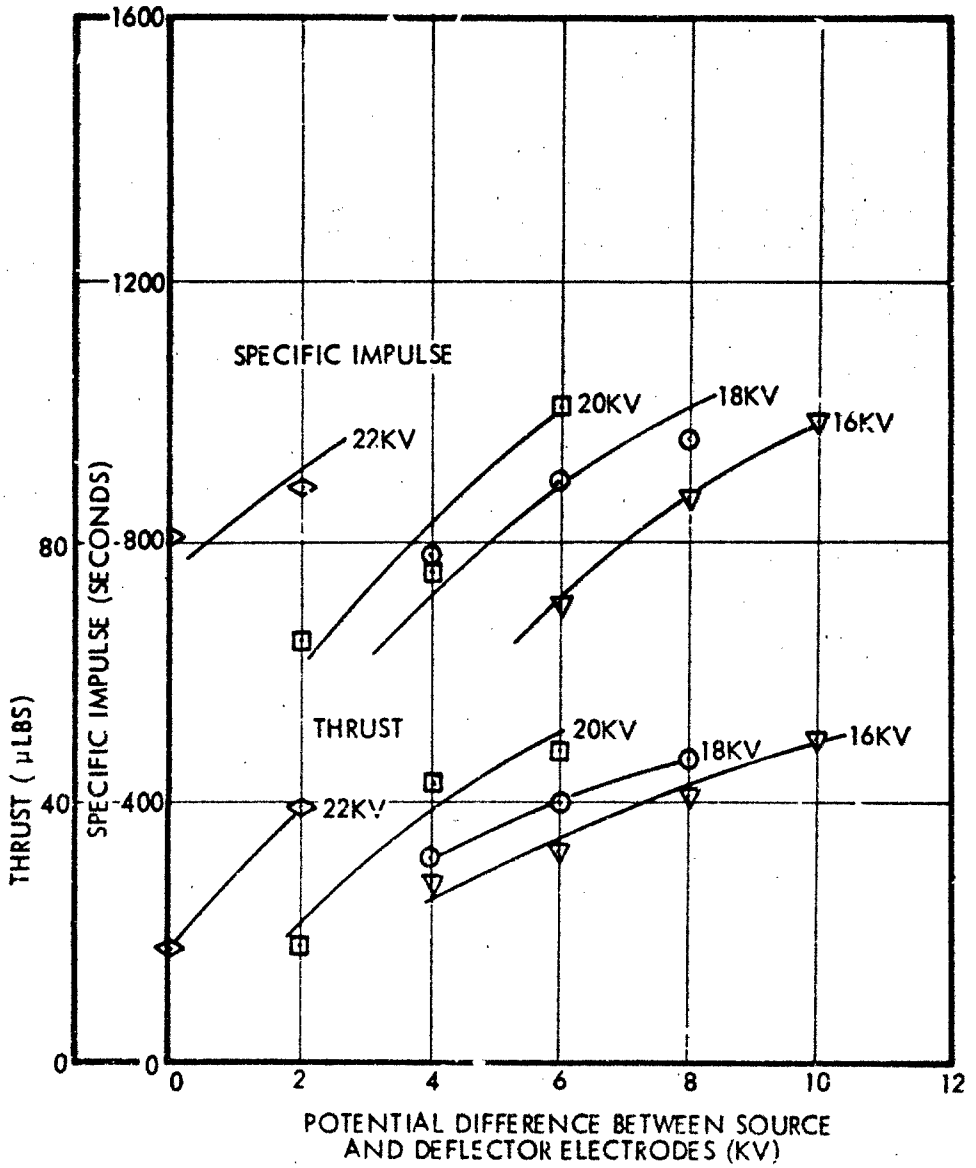


Figure 27. Run 7208-04. Emitter No. TM2, 1/2" Extractor, Vertical Test, 10.5" Hg Feed Pressure (∿ 25 μg/sec mass flow)

This run was very encouraging and tended to verify our belief that the problems with horizontal operation were due to overfeeding at the bottom.

RUN 7208-06: EMITTER TM3, 1/2" EXTRACTOR

The purpose of this run was to see if the previcus good results could be reproduced running emitter TM3 vertically. The results were once again very good. Table VI shows a performance comparison for the two emitters. A 100 hour life test was run. Tables VII and VIII summarize the average performance and control parameters at the end of the test. In order to show the reproducibility of successive time-of-flight measurements, Tables IX and X show successive sets of data taken at the beginning and end of the test. Obviously the values did not change much during the course of the test.

RUNS 7208-07 and 7208-08: VERTICAL OPERATION, DEEPER WELL EMITTER, 1/2" EXTRACTOR HOLE

Past experience with various thrusters had indicated that performance was critically dependent on the shape of the propellant meniscus within the emitter well. One factor affecting the meniscus shape is the depth of the emitter well. We had previously found, when operating horizontally, that a very deep well resulted in practically no emission at all. This indicated that well depth is indeed very important but that we had perhaps gone too far. On these runs, the well of emitter TM1 was deepened just a little — 0.005" more than the usual 0.015". The results were very interesting in that we were able to get high efficiency over a much wider performance range than on the previous tests. We were able to get 80 percent efficiency at 1300 seconds and 26.5 μlbs. Some of the performance data for Run 7208-07 is shown in Figures 28 and 29.

## 3.3 Tool Formed Emitter Results (Both Horizontal and Vertical)

Table XI summarizes the most significant runs with tool formed emitters. It also compares the horizontal and vertical operation. The main conclusions drawn from these tests were that (1) for a given orientation the performance was reproducible from one emitter to the next, (2) tool formed emitters

TABLE VI. EMITTERS TM2 AND TM3 PERFORMANCE COMPARISON AT OPTIMUM

| EMITTER | $P_F$ "Hg | $V_S$ kv | $V_D$ kv | $V_X$ kv | $\eta$ % | $\dot{M}$ µg/sec | $I_{sp}$ secs | F µlbs |
|---|---|---|---|---|---|---|---|---|
| 3 | 4.5 | 20 | 16 | -2 | 75.9 | 9.86 | 1601 | 34.8 |
| 2 | 4.5 | 20 | 16 | -2 | 76.8 | 10.5 | 1350 | 31.3 |
| 3 | 5.0 | 19 | 15 | -2 | 78.2 | 12.1 | 1458 | 38.8 |

TABLE VII. 100-HOUR LIFE TEST SUMMARY (RUN 7208-06) CONTROL PARAMETERS

| | |
|---|---|
| Emitter | #3 |
| Extractor Aperture | 1/2" |
| Orientation | Vertical |
| Source Voltage | 19 kv |
| Deflector Voltage | 15 kv |
| Extractor Voltage | -2 kv |
| Feed Pressure | 5" Hg |

TABLE VIII. 100-HOUR LIFE TEST SUMMARY (RUN 7208-06) PERFORMANCE PARAMETERS

| | |
|---|---|
| Source Current | 74 µA |
| Extractor Current | 0.2 µA |
| Deflector Current | 0 µA |
| Efficiency | 76.6 % |
| Thrust | 35.7 µlbs |
| Specific Impulse | 1382 seconds |
| Mass Flow | 11.72 µg/sec |
| Charge-to-Mass Ratio | 6,370 c/kg |

TABLE IX

TIME-OF-FLIGHT REPRODUCIBILITY AT BEGINNING OF
100-HOUR LIFE TEST - RUN 7208-06

| $\eta$ % | $\dot{M}$ µg/sec | Isp Secs. | F µlbs | $q/m \times 10^{-3}$ coul/kg |
|---|---|---|---|---|
| 76.2 | 12.69 | 1409 | 39.4 | 6.70 |
| 73.5 | 12.46 | 1231 | 33.8 | 5.22 |
| 74.0 | 13.15 | 1355 | 39.3 | 6.39 |
| 74.0 | 12.25 | 1209 | 32.7 | 4.98 |
| 77.9 | 11.30 | 1432 | 35.7 | 6.73 |
| 76.8 | 12.13 | 1357 | 36.3 | 6.10 |

TABLE X

TIME-OF-FLIGHT REPRODUCIBILITY AT END OF
100-HOUR LIFE TEST - RUN 7208-06

| $\eta$ % | $\dot{M}$ µg/sec | Isp Secs. | F µlbs | $q/m \times 10^{-3}$ coul/kg |
|---|---|---|---|---|
| 76.1 | 12.66 | 1397 | 39.0 | 6.56 |
| 77.7 | 12.00 | 1450 | 38.3 | 6.92 |
| 78.2 | 12.09 | 1458 | 38.8 | 6.95 |
| 76.4 | 12.17 | 1302 | 34.9 | 5.59 |
| 71.0 | 11.89 | 1196 | 31.4 | 5.05 |
| 75.3 | 13.09 | 1383 | 39.9 | 6.49 |

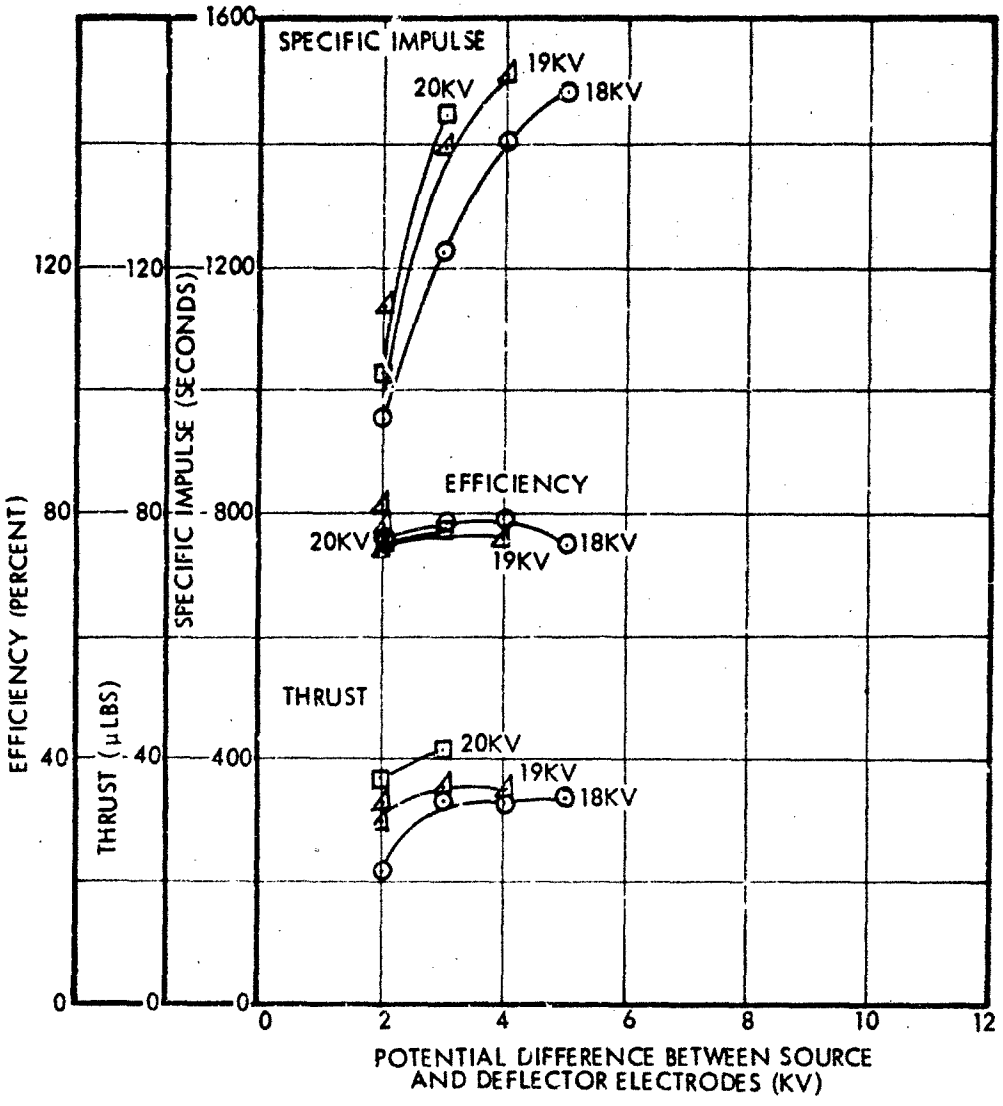


Figure 28. Run 7208-07. Emitter No. 1, 1/2" Extractor Vertical Test, Deeper Well, 5.5" Hg Feed Pressure

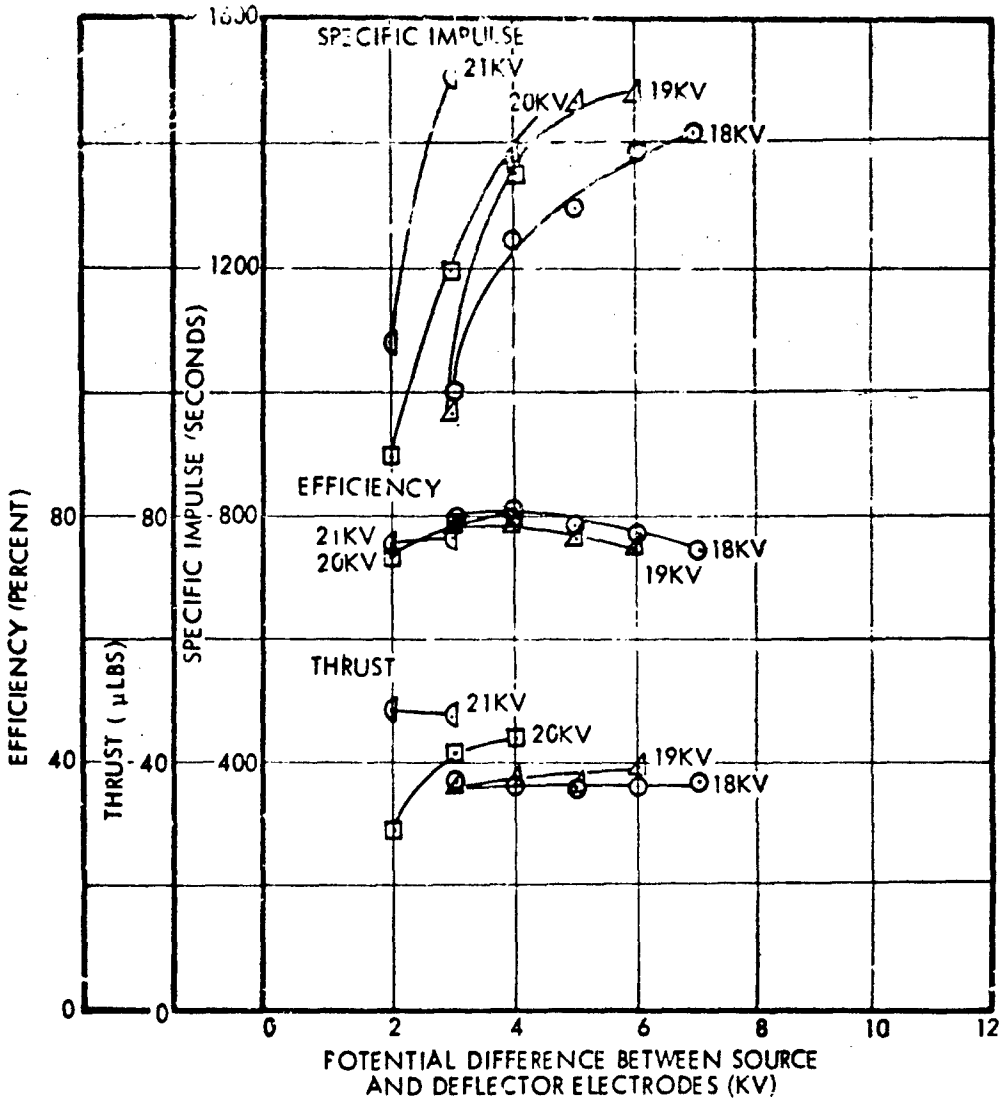


Figure 29. Run 7208-07. Emitter No. 1, 1/2" Extractor, Vertical Test, Deeper Well, 6.5" Hg Feed Pressure

TABLE XI

TOOL FORMED EMITTER RUN SUMMARY (MOST SIGNIFICANT RUNS ONLY)

| RUN # | EMITTER # | EXTRACTOR APERTURE | ORIENTATION | RESULTS |
|---|---|---|---|---|
| 7207-06 | TM1 | 1/2 inch | Horizontal | Thrust 20-50 µlbs<br>$I_{sp}$ < 1200 seconds usually<br>Efficiency 60-65% |
| 7208-01 | TM1 | 3/8 inch | Horizontal | Essentially the same as above<br>Efficiency slightly lower<br>Vertical probe showed off-set to bottom |
| 7208-02 | TM1 | 1/2 inch | Horizontal | Deflector and extractor 0.010 inch forward<br>Essentially same performance<br>Also looked at 16°C and 20°C |
| 7208-04 | TM2 | 1/2 inch | Vertical | 77%, 1350 seconds, 31 µlbs<br>74%, 1450 seconds, 40 µlbs |
| 7208-06 | TM3 | 1/2 inch | Vertical | Same as above<br>100 hour test at 76.6%, 35.7 µlbs, 1382 seconds<br>Best end point value - 78%, 1458 seconds, 38.8 µlbs |
| 7208-07 | TM1 (Deeper well) | 1/2 inch | Vertical | 80%, 1300 seconds, 26.5 µlbs<br>76%, 1500 seconds, 27.8 µlbs<br>Temperature controller failure |
| 7208-08 | TM1 (Deeper well) | 1/2 inch | Vertical | Essentially same as performance above |

operated very smoothly at fairly high performance levels, and (3) vertical operation resulted in greatly improved performance over that obtained with a horizontal orientation.

RUN 7209-01: 100 HOUR LIFE TEST OF DEEP WELL EMITTER

The deep well emitter described under Runs 7208-07 and 7208-08 was operated for 100 hours. The thruster performed stably over a wide range of performance parameters during the 100 hour run. However, it showed a tendency for the current to decrease with time, which could be corrected by turning the thruster off for ten seconds to allow the meniscus to re-establish itself. The efficiencies were usually in the low to mid 70's, thrusts varied from 20 to 40 μlbs and specific impulses as high as 1700 seconds and greater were observed.

The performance was mapped at two separate feed pressures at the end of the test (Figures 30 and 31). The best single point was 74.5 percent, 1523 seconds and 33.6 μlbs at 6" feed pressure, 20 kv source voltage and 17 kv deflector voltage. It is felt that these results did not offer any significant improvement over those obtained with the standard well depth, and for this reason the remainder of the program concentrated on the original standard well depth design.

## 3.4 Thrust Vectoring

The ability to thrust vector a colloid engine increases its applicability for flight applications by allowing it to perform thrust misalignment corrections and center-of-mass shift compensation in addition to allowing a single thruster to perform multiple spacecraft functions such as stationkeeping and attitude control. Electrostatic vectoring is a particularly appealing concept in that it eliminates the moving mechanical parts required by other vectoring techniques.

The ability to electrostatically vector various colloid thrusters has been demonstrated many times in the past,[1-5] but whenever the thruster performance level or design geometry is changed it can be expected that there will be a change in the vectoring response of an electrostatic system. For this reason several runs were made during the program to check the thrust vectoring response of a single source in its present developmental state.

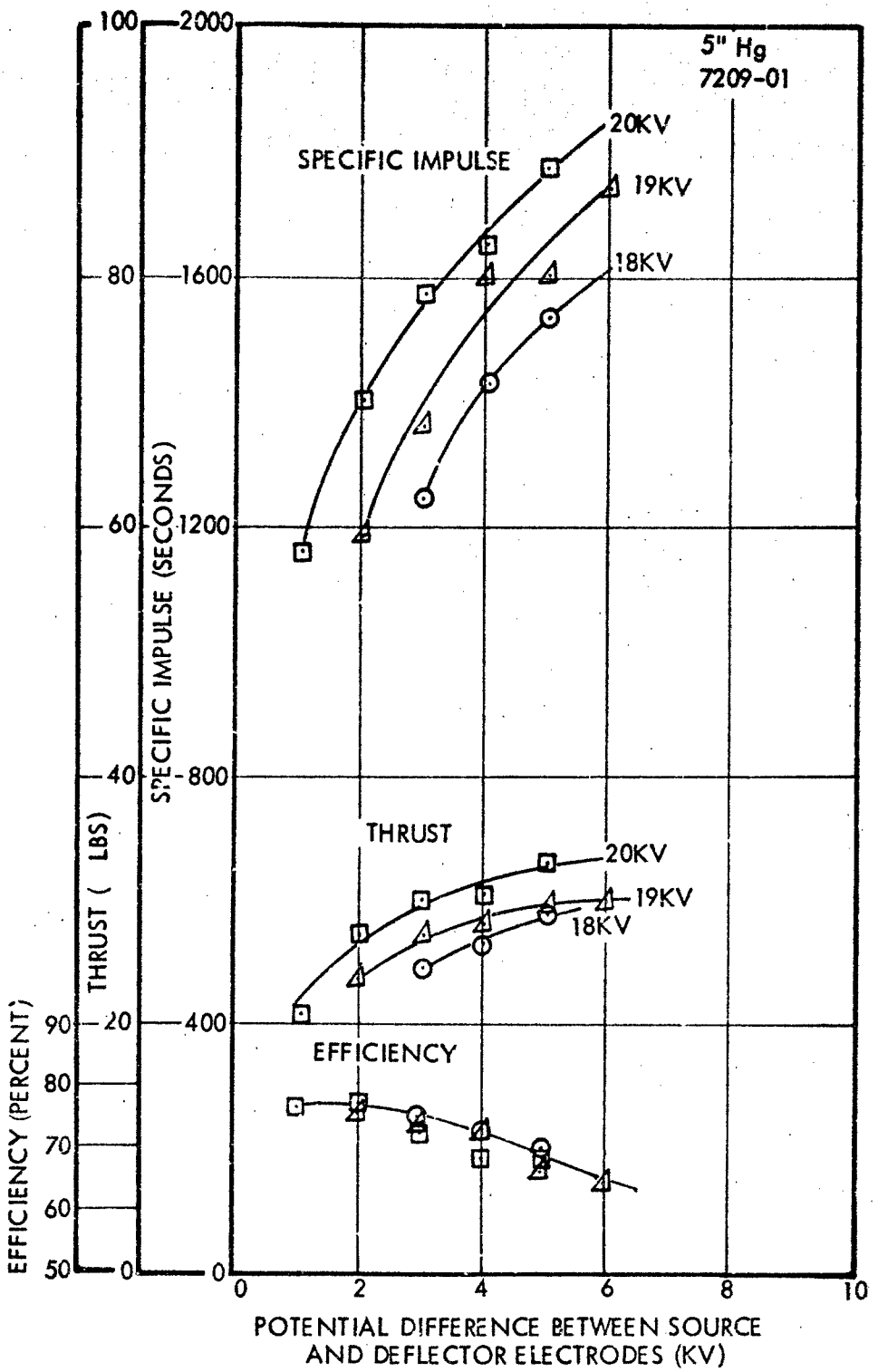


Figure 30. Run 7209-01. Deep Well Emitter, 1/2" Extractor, Vertical Orientation, 5" Hg Feed Pressure, Performance After 100 Hours (∿ 8.5 μg/sec mass flow)

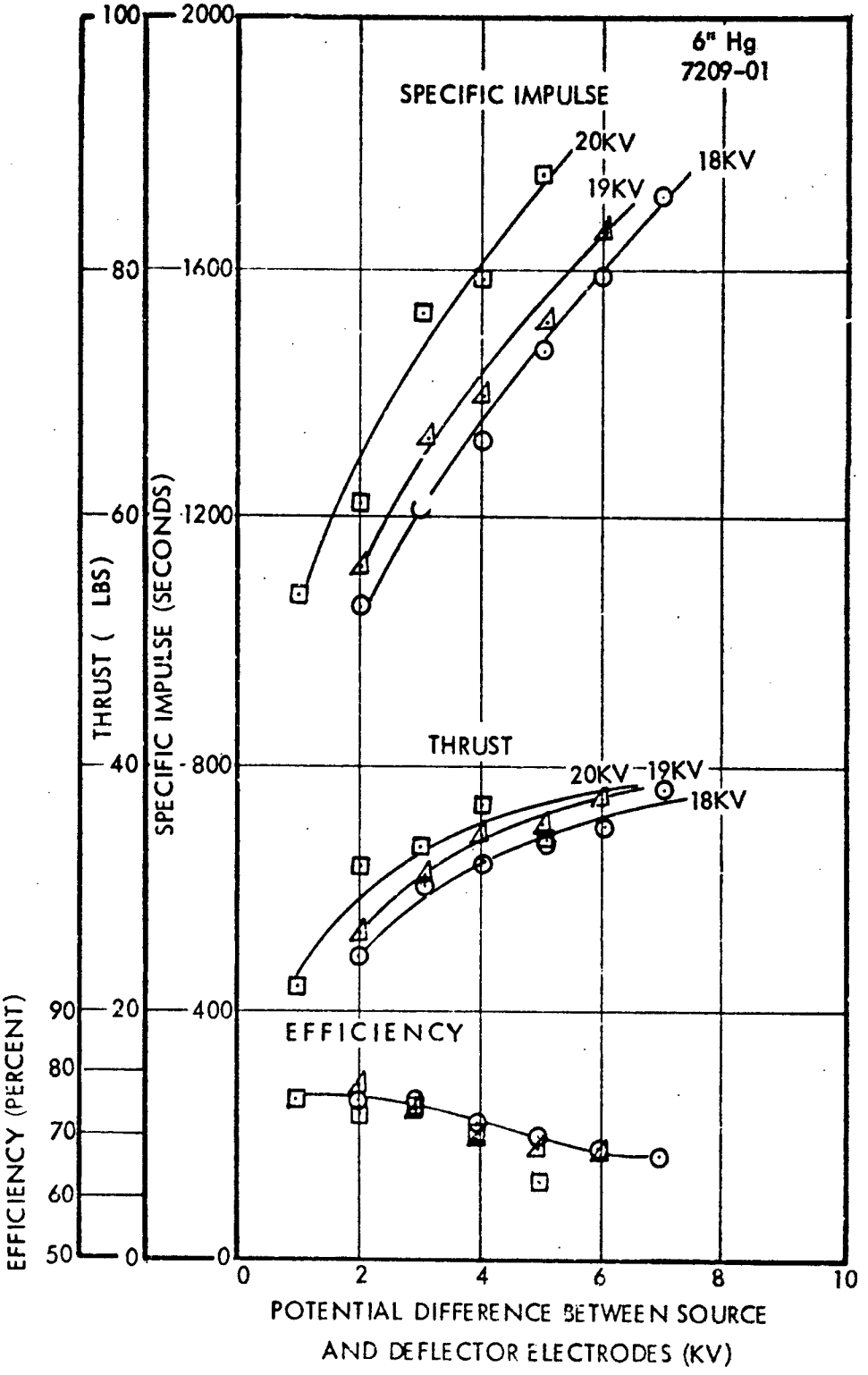


Figure 31. Run 7209-01. Deep Well Emitter, 1/2" Extractor, Vertical Orientation, 6" Hg Feed Pressure, Performance After 100 Hours (~ 10.5 µg/sec mass flow)

Figure 32 shows the orientation of the deflector electrodes. As can be seen from this figure, three deflector electrodes are used to provide x-y vectoring capability. There are several reasons for using three electrodes instead of the more intuitively acceptable four electrode array which is easier to visualize in terms of separate x and y vectoring control. The advantages of having three electrodes include the following: (1) A three-fold vectoring symmetry considerably simplifies the underlying electrode support structure for a hexagonally close packed source array. (2) One less power supply is required than for a four-fold system. (3) Use of a conventional four-fold x-y vectoring system would probably require a square packing geometry for the source which would result in a lower thrust density than for a hexagonal array. A possible advantage of the four-electrode system is that it may be easier to program in a given off-axis vectoring angle.

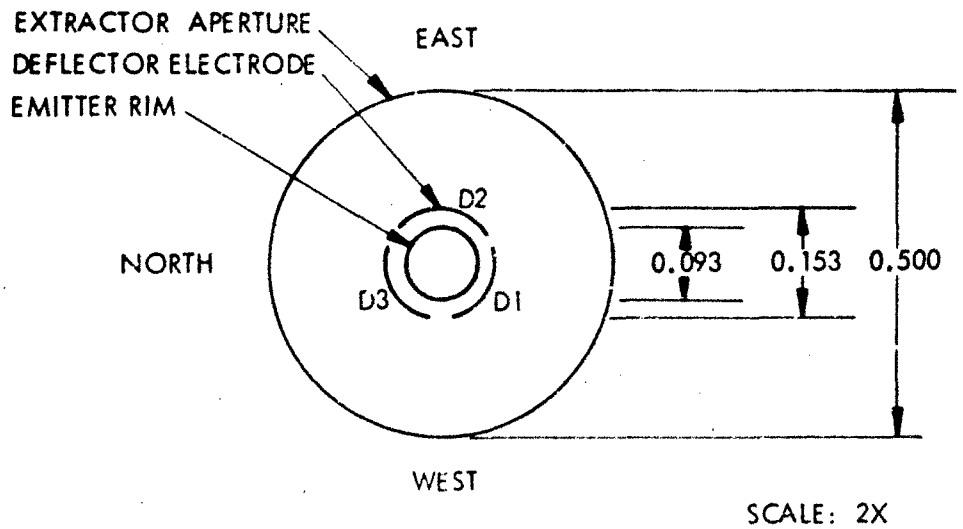


Figure 32. Schematic — Vector Electrode Arrangement

During the vectoring runs, it was easy to demonstrate that the thrust vector direction could be significantly influenced by the application of deflecting voltages. The beam profile could be visually discerned by the florescent pattern on the collector and the motion of

the beam pattern in response to application of deflecting voltages was dramatic corroboration of the thruster vectorability.

The beam profile was scanned across its mid-plane by two 2 x 5 cm probes. The east-west scanning probe was inserted through a feed-through in the front door of a vacuum tank and scanned through a plane 68.6 centimeters in front of the thruster. The north-south probe was inserted through the side of the chamber and scanned through a plane 71.8 centimeters in front of the thruster.

In order to obtain maximum vectoring response, it was necessary to bias some of the deflectors positive with respect to the source. As a consequence, it was no longer possible to use a rectifier between the source and deflectors to allow the deflectors to follow the emitter to ground for a time-of-flight measurement (see Appendix A). Instead, the deflectors were then driven down by the previous technique of running a capacitor between each deflector and the emitter. This produced the risk of increasing the time to zero current during thruster turn-off. A long turn-off can potentially mask the time-of-flight ion peak and increase the low charge-to-mass ratio tail. However, the unvectored results during these runs were sufficiently close to previous performance to indicate that the effect was minimal during straight ahead operation. During vectored operation the capacitors can have a greater impact on time-of-flight turn-off since at least one of the deflectors is biased highly negative relative to the emitter, thus increasing the probability of delayed shut-off at adjacent emitter regions. The observed decreases in efficiency during vectoring could have been due in part to this effect. However, a large part of the observed efficiency changes were due to an increase in the ion peak height and this was undoubtedly a real effect. It should be noted that a decrease in efficiency during vectoring is to be expected since the vectoring process introduces electric field variations around the emitter rim, thus producing corresponding charge-to-mass ratio variations. A potential cure would be to vector after the exhaust leaves the thruster, but this would have to be explored as a separate development program.

Figure 33 and Table XII summarize the results from a north-south vectoring scan. It can be seen from Table XII that the north-south vectoring was obtained by varying the biases on deflectors 1 and 3

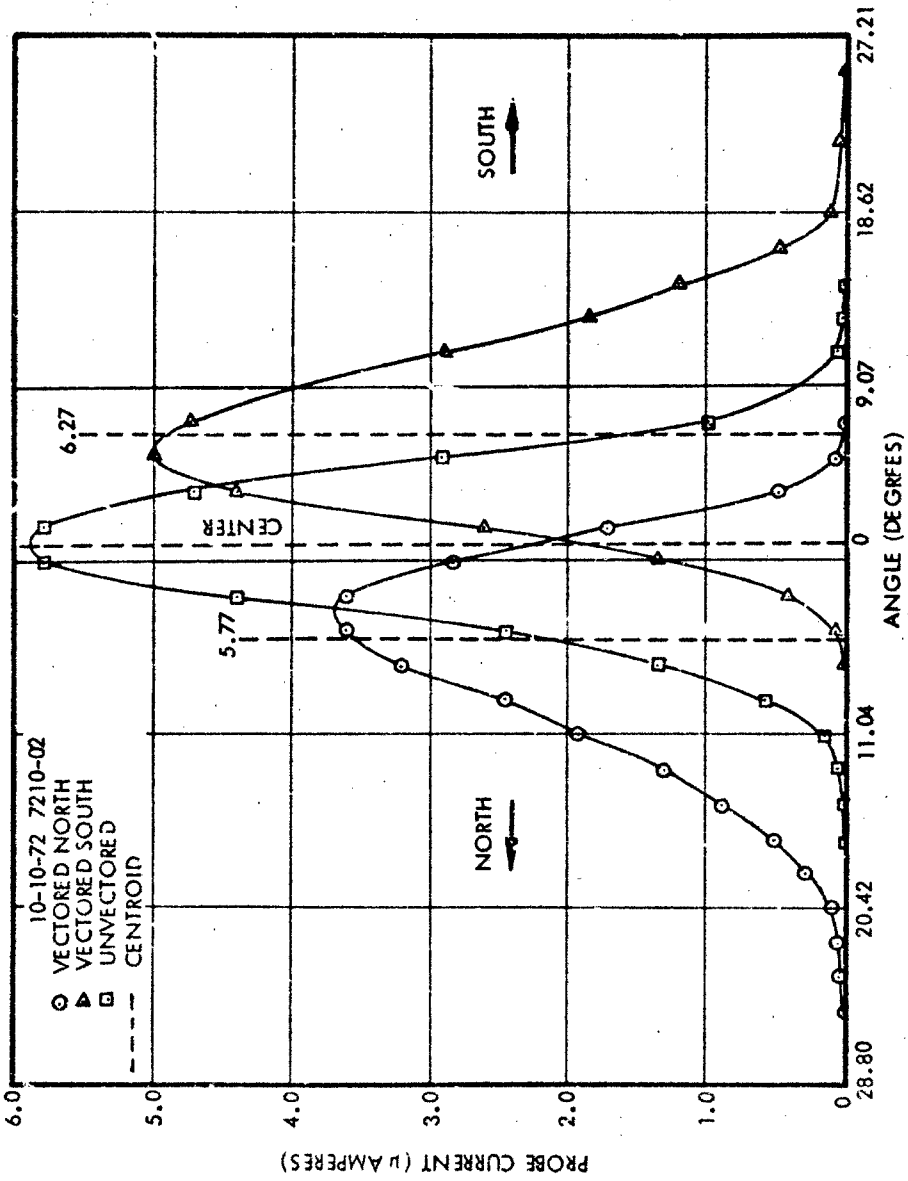


Figure 33. North-South Vectoring Response, Performance Parameters are as Shown in Table XII

relative to each other while holding #2 constant. In this case, deflections of 5.8° and 6.3° were obtained at the cost of some reduction in efficiency and specific impulse as shown in Table XII. An east-west probe of the beam (Figure 34) showed a slight shift to the west during both north and south vectoring. This effect would be less likely to occur with a four-electrode system which would be totally symmetric in the east-west direction during north-south vectoring.

TABLE XII

Performance Data for Figures 33 & 34 ($V_N$ = 18.2 kv, $V_{ex}$ = -2 kv, $P_f$ = 5" $H_g$)

| $V_{D1}$ kv | $V_{D2}$ kv | $V_{D3}$ kv | n % | $I_{sp}$ seconds | Thrust µlbs | Mode | | |
|---|---|---|---|---|---|---|---|---|
| 14 | 14 | 14 | 76.9 | 1405 | 29.1 | Unvectored | | |
| 20 | 14 | 7.5 | 65.8 | 1302 | 25.3 | Centroid Deflected | North | 5.8° |
| 7.4 | 14 | 20 | 65.8 | 1237 | 27.5 | Centroid Deflected | South | 6.3° |

Figure 35 shows the east-west vectoring data obtained by maintaining equal voltages on $D_1$ and $D_3$ and varying the two relative to $D_2$. Thus, the deflector voltages were (1) undeflected $V_{D_1} = V_{D_2} = V_{D_3} = 14$ kv, (2) deflected west $V_{D_1} = V_{D_3} = 8.7$ kv, $V_{D_2} = 22$ kv, (3) deflected east $V_{D_1} = V_{D_1} = V_{D_3} = 22$ kv, $V_{D_2} = 2.5$ kv. The net deflection angles for the centroid was 7° east and 17.5° west.

These measurements have demonstrated that it is possible to electrostatically vector a tubular colloid thruster at the current performance levels. Before this technique can be incorporated into a flight system, the following additional work should be done:

- Comparison of three and four electrode vectoring system control characteristics and a tradeoff study made of the overall system implications of the two designs. The study should include laboratory measurements of the detailed control characteristics for all vectoring angles.

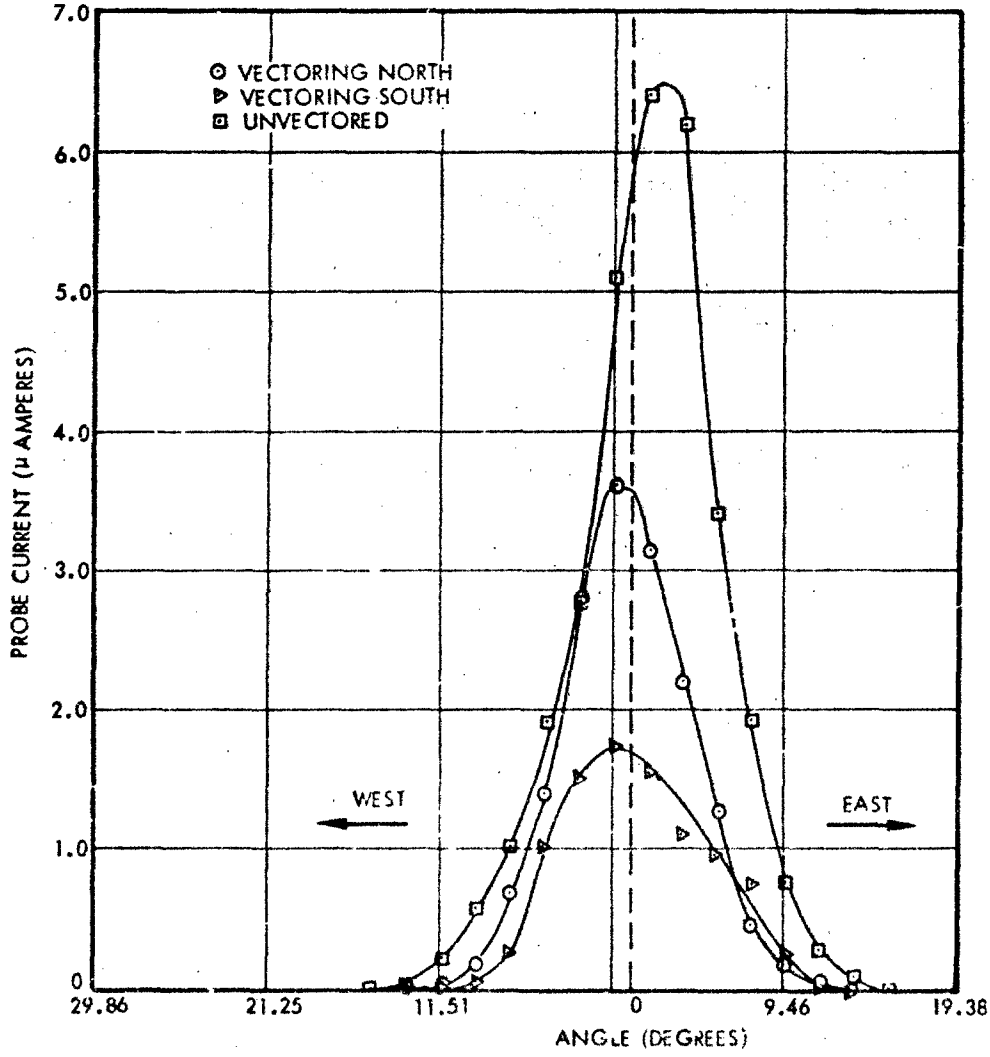


Figure 34. Run 7210-02. East-West Probe of the Beam During the North-South Vectoring Conditions Shown in Table XII

- An experimental design study should be performed to optimize the vectoring performance at the present thruster performance levels.
- The effects of electrostatic vectoring on total long-term performance reliability and lifetime should be determined.
- Tradeoff studies should be made to pinpoint the relative advantages of mechanical and electrostatic vectoring.

The results of the above will then form a basis for evaluating the feasibility of electrostatic vectoring for colloid flight systems.

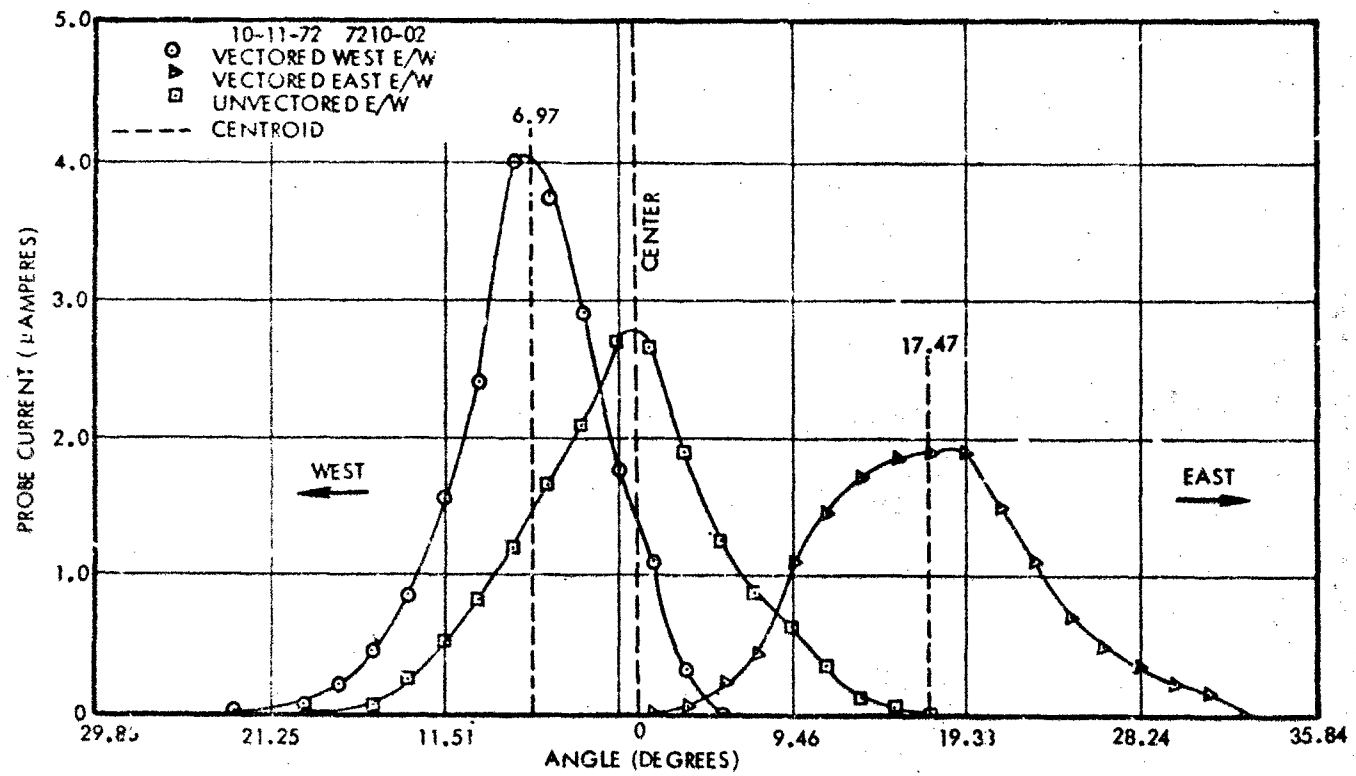


Figure 35. Run 7210-02. East-West Probe of the Beam During East-West Vectoring

# 4. MODULE TESTING

Three-source and four-source modules with frontal areas just under four square inches were fabricated in order to investigate the properties of thruster operation at approximately 100 μlb levels.

## 4.1 Three Source Module

Figures 36 and 37 show the module prior to and after assembly. The emitter impedances from the three emitters had less than ±2% flow variation from the mean impedance value. As can be seen from Figure 37, instead of 3 vector electrodes, each emitter had one continuous shield electrode surrounding its tip. This allowed a considerable reduction in structural complexity over that which would be required for complete sets of vectoring electrodes. To maintain ease of alignment, each shield electrode was mounted on its own individual support structure.

It was possible to obtain thrusts in excess of 100 μlbs, specific impulse in excess of 1500 seconds, and thrust efficiency greater than 75% all with stable, smooth operation. However, it was not possible to achieve all three goals simultaneously. This was due mainly to the fact that the thruster had to be pushed hard to achieve a total of 100 μlbs for three emitters.

Two examples of high performance points at 75% efficiency are: a specific impulse of 1170 seconds at a thrust of 70 μlbs, and a specific impulse of 1340 seconds at a thrust of 93 μlbs. The latter was taken at a higher feed pressure. Figures 38-40 show the performance characteristics of the module for three different feed pressures and three different voltages.

Tests were performed in which two of the emitters were deliberately sealed off with wax plugs in order to evaluate the performance of the remaining emitter. These tests are also shown in Figures 38-40, with thrust scaled up by a factor of three, to provide a comparison. The scaled single emitter results (dashed curves) were usually lower than the total thruster values and indicate that more work is needed to fully understand thruster scaling phenomena.

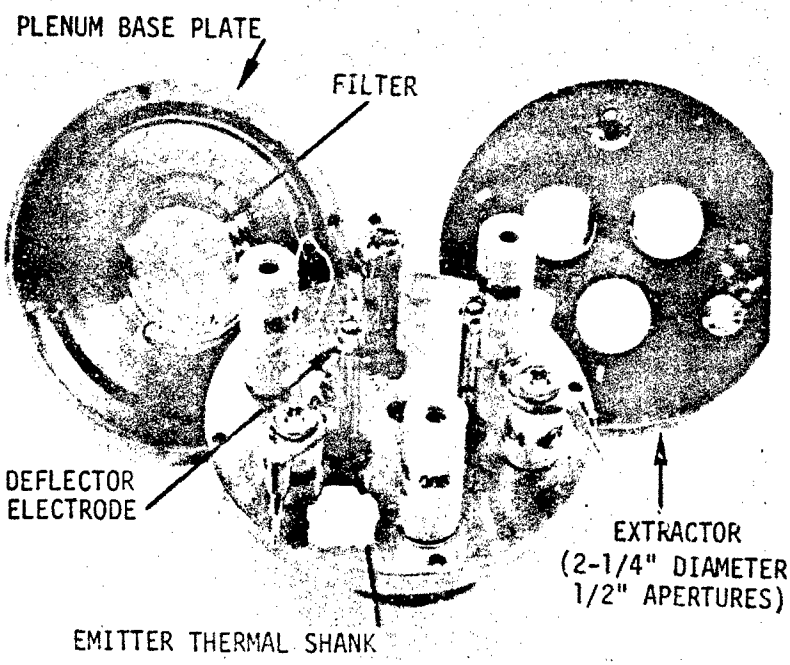


Figure 36. 3 Source Module, Partially Assembled

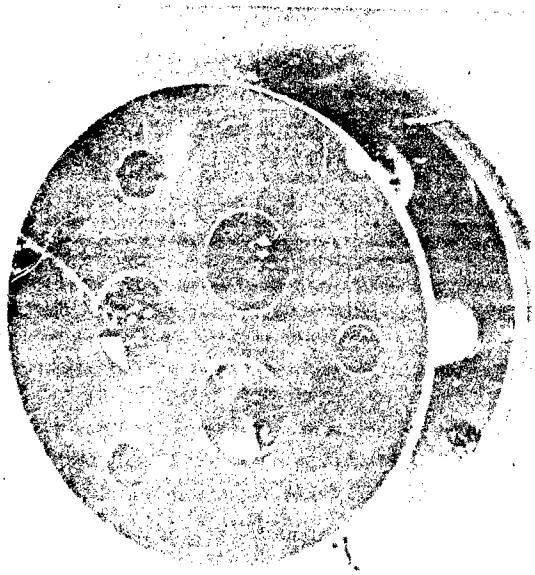

Figure 37. 3 Source Module, Fully Assembled

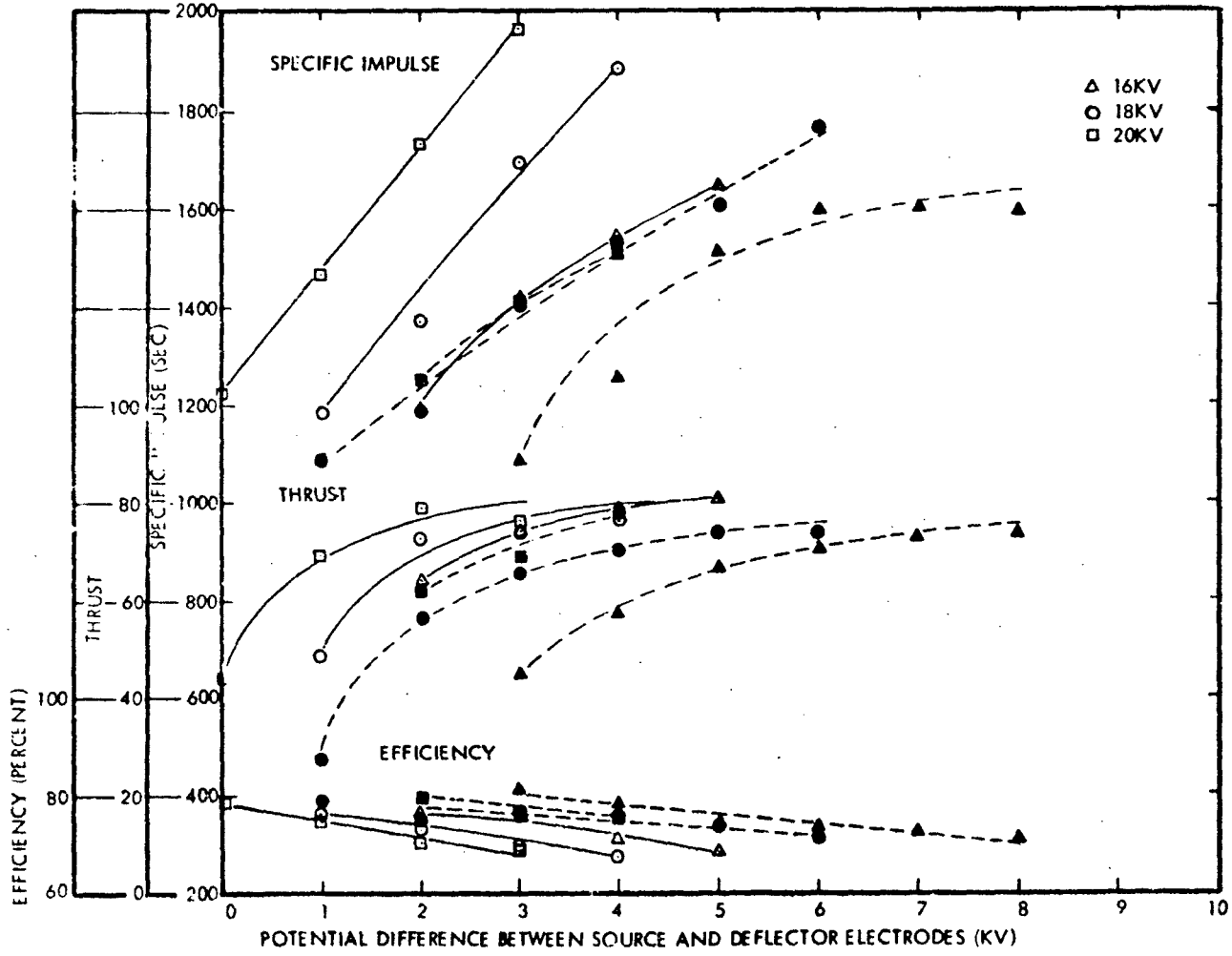


Figure 38. Run 7210-04. Performance Data For Three-Source Module: Feed Pressure, 5.1" Hg: Solid Lines, 3 Sources Operating: Dashed Lines and Solid Points, Scaled Single Source Results (~ 22 µg/sec mass flow)

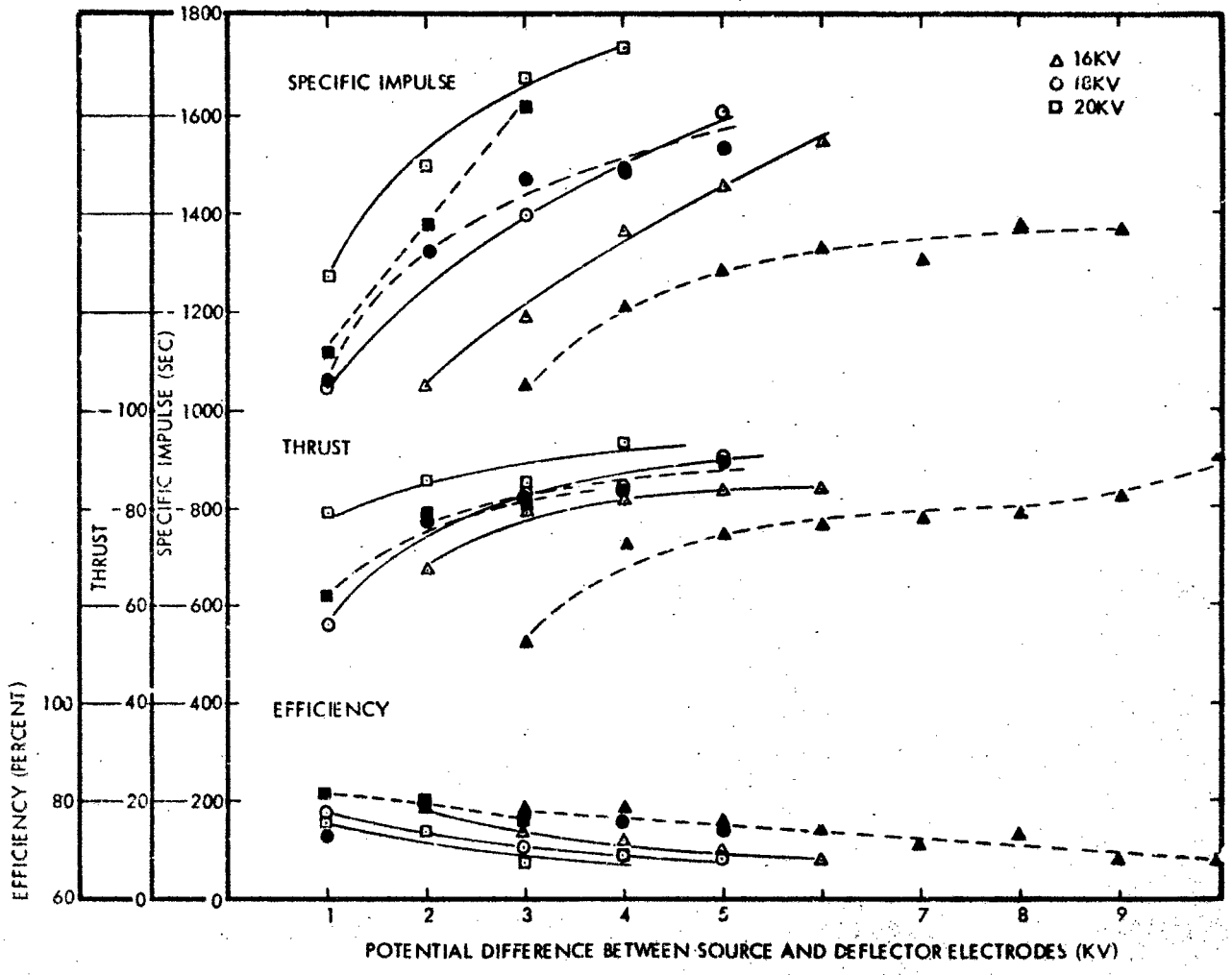


Figure 39. Run 7210-04. Performance Data for Three-Source Module: Feed Pressure, 6.1" Hg: Dashed Lines and Solid Points Indicate Scaled Single Source Results (~ 26 μg/sec mass flow)

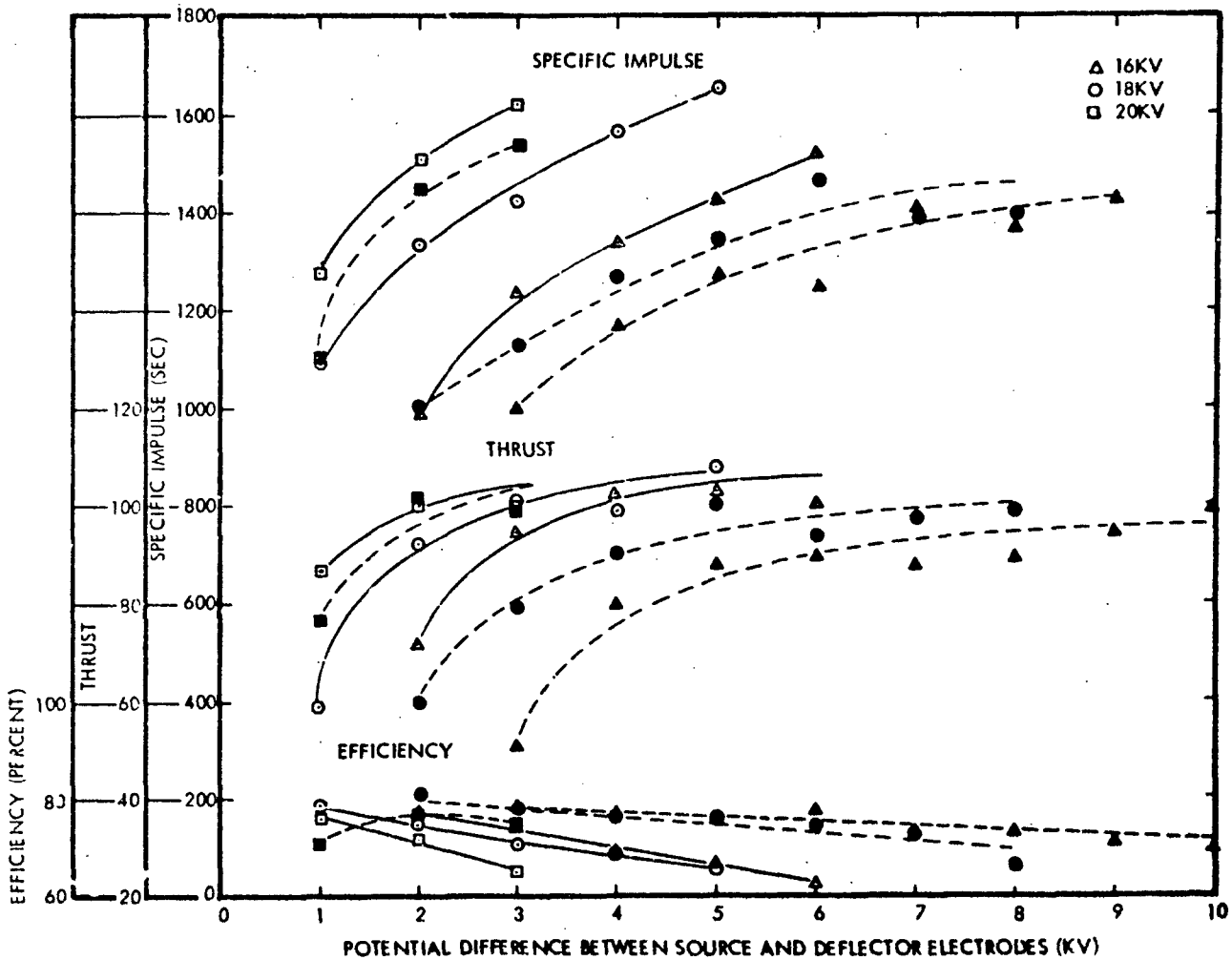


Figure 40. Run 7210-04. Performance Data for Three Source Module: Feed Pressure, 7.1" Hg: Dashed Lines and Solid Points Indicate Scaled Single Source Results (~ 31 μg/sec mass flow)

Two tests were performed with one source in the module capped off; i.e., two sources operating. In order to further understand the influence of cleaning procedures on performance, these tests were conducted after the module had undergone clean room assembly and preparation procedures comparable to those specified for the ADP. These included transmittal to the test site under a sealed, inert atmosphere, and white-glove handling. Prior to test turn-on, the module was subjected to the cleansing action of a negative glow discharge in about 100 microns of nitrogen pressure. Overall performance, including thrust-per-source, was compared with overall performance of the same module with three sources operating, and with only one source operating. The results indicated that "per-source" performance levels with two sources operating were in the same range as the previous tests. Data taken for three separate feed pressures and three source voltages is summarized in Figures 41 and 42, which are parameterized by source voltage and feed pressure. In each figure, thrust is scaled by a factor of 3/2, to normalize to total effective thrust with three sources.

## 4.2 Four Source Module

A four source module (Figure 43) was built and tested extensively during the latter part of the program. For convenience, the four sources were arranged in a square pattern 3/4" on a side with 1/2" diameter extractor apertures. The overall thruster has a 2-1/4" diameter, resulting in a frontal area just under 4 square inches. Thruster temperature is monitored by the usual technique of placing a thermistor probe in the module base plate. Thruster temperature readings are then used to regulate a radiant heater which controls the thruster temperature.

Figures 44-50 show typical performance characteristics obtained during initial short term testing. Smooth performance was obtained at thrusts in excess of 200 μlbs thrust and 1300 seconds specific impulse for control settings of 18 kv source voltage, 14 kv deflector voltage, 15" Hg feed pressure and -5 kv extractor voltage. The highest feed pressure tried was 29.5" Hg. At 19.2 kv source voltage and 16.2 kv deflector voltage, it was possible to get 301 μlbs at 70% efficiency and 1029 seconds specific impulse.

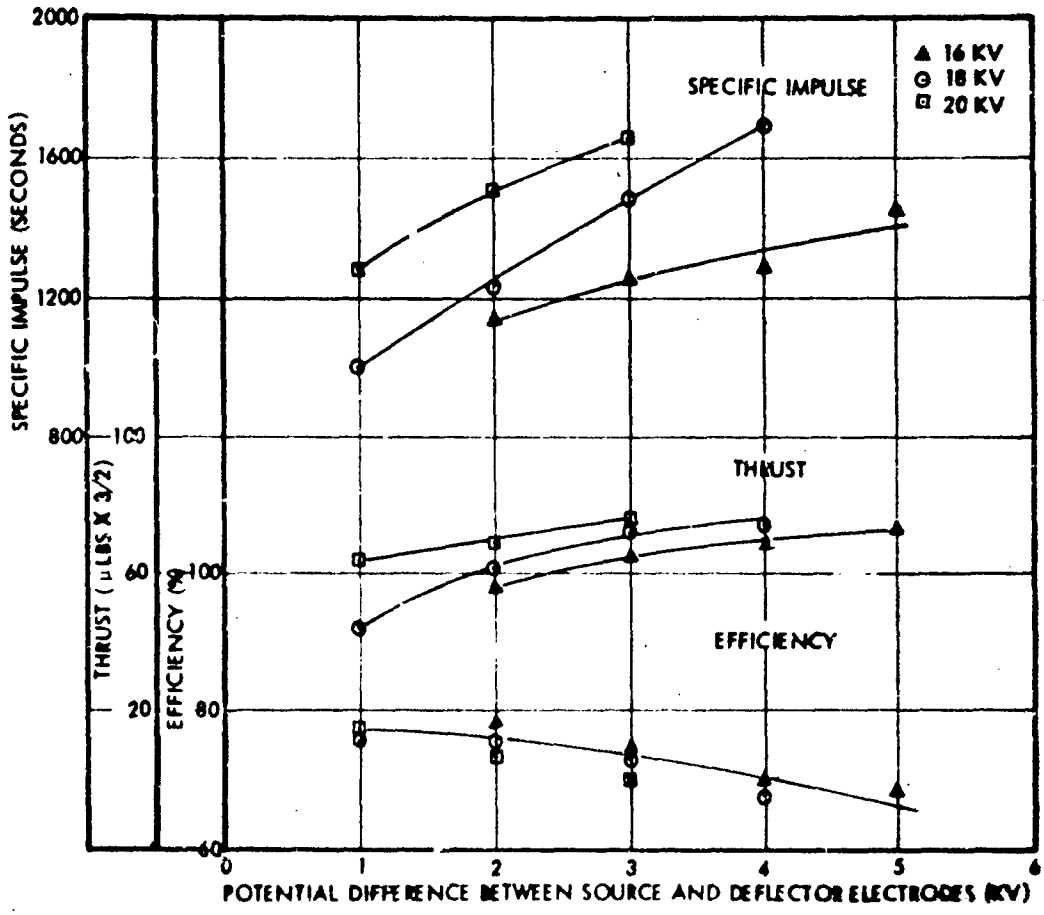


Figure 41. Run 7212-02. Performance Data for the Three-Source Module with Two Sources Operating: Feed Pressure, 5.1 in. Hg: Thrust normalized to effective thrust for three emitters.

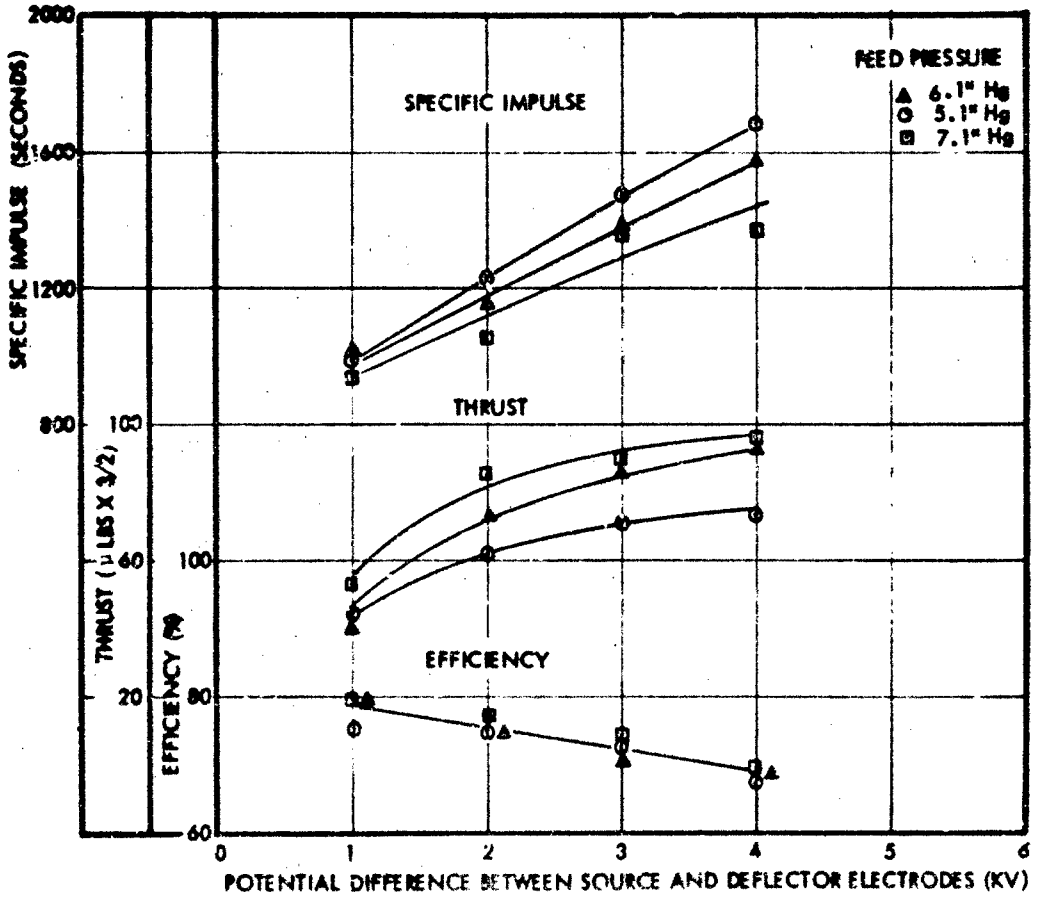


Figure 42. Run 7212-02. Performance Data for the Three-Source Module with Two Sources Operating: Source Voltage, 18 kv: Thrust normalized to effective thrust for three emitters.

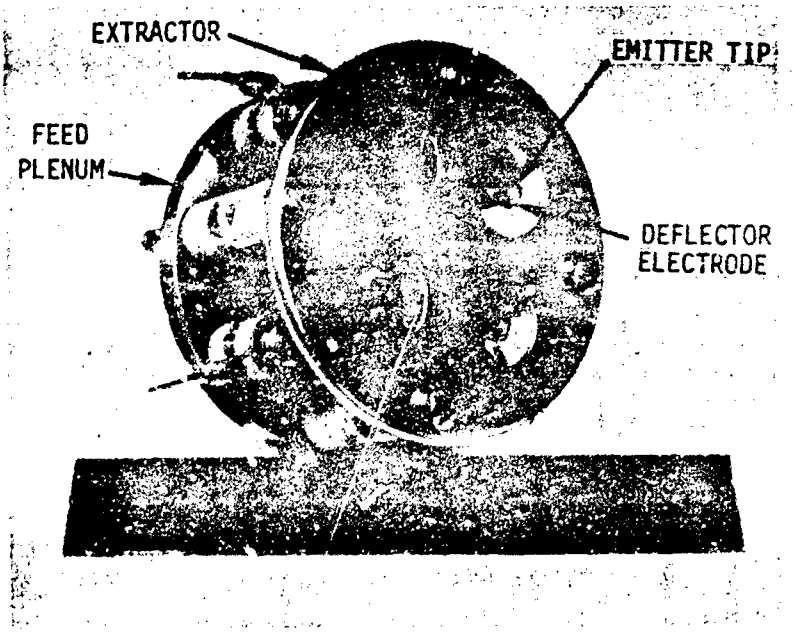


Figure 43. Four Source Module

Run 7301-01: FOUR SOURCE MODULE - SALT COATED EMITTER TIPS

The previous tests performed with the four source module had used the glow discharge to clean the emitters immediately prior to turn on instead of the salting method which had been used in earlier runs. This technique consists of applying a negative bias to the emitters, extractor and deflectors in order to induce a low voltage discharge during the vacuum tank pump-down cycle. When the tank has been roughed down to 600 microns, the negative bias is raised until a discharge current of 4 milliamperes is produced. This usually occurs at approximately 300 volts and the discharge is maintained for five minutes. The positive ion bombardment that occurs during this discharge removes contaminating films that may otherwise have deposited on thruster surfaces. The flow discharge proved to be easier to implement than the salting method and always resulted in an easier start-up and smooth performance.

For the present run, which used the salting technique, start-up was somewhat more difficult. Two emitters wetted immediately; however, the other two emitters required the voltage to be turned off for several minutes before adequate wetting was achieved. Once this was acco plished, the performance was almost as good as previous runs. Figures 51 and 52

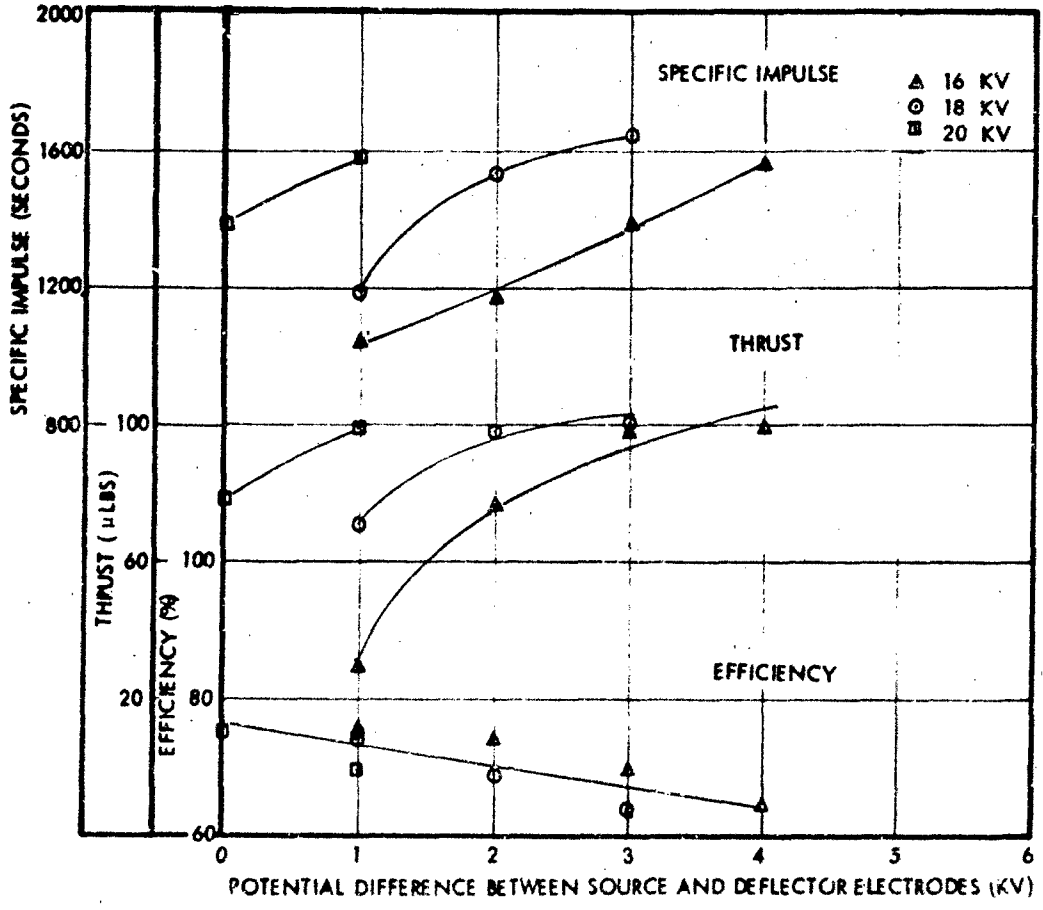


Figure 44. Run 7212-04. Performance Data for the Four-Source Module: Feed Pressure 6.1 in. Hg (∿ 29 μg/sec mass flow)

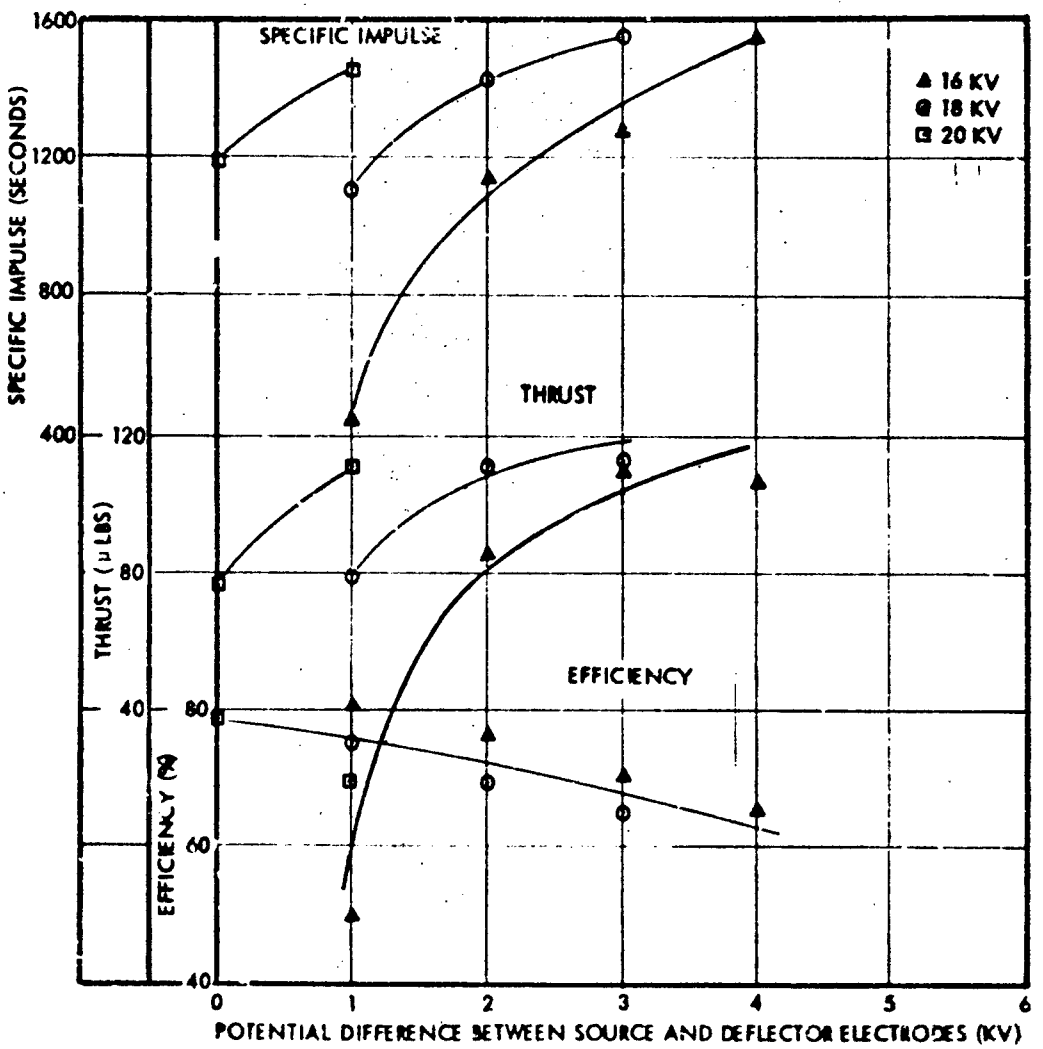


Figure 45. Run 7212-04. Performance Data for the Four-Source Module: Feed Pressure 7.1 in. Hg (~ 34 μg/sec mass flow)

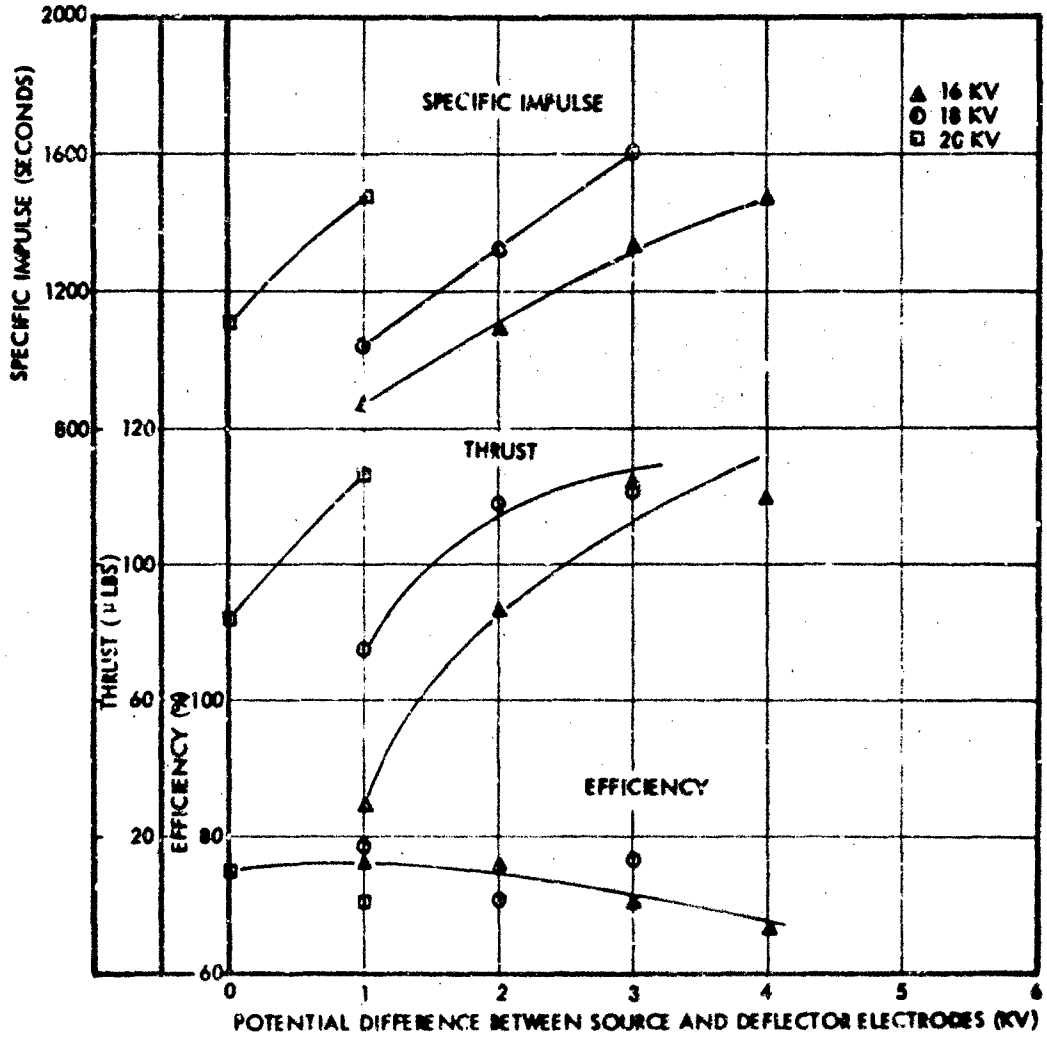


Figure 46. Run 7212-04. Performance Data for the Four-Source Module: Feed Pressure 8.1 in. Hg (∿ 38 μg/sec mass flow)

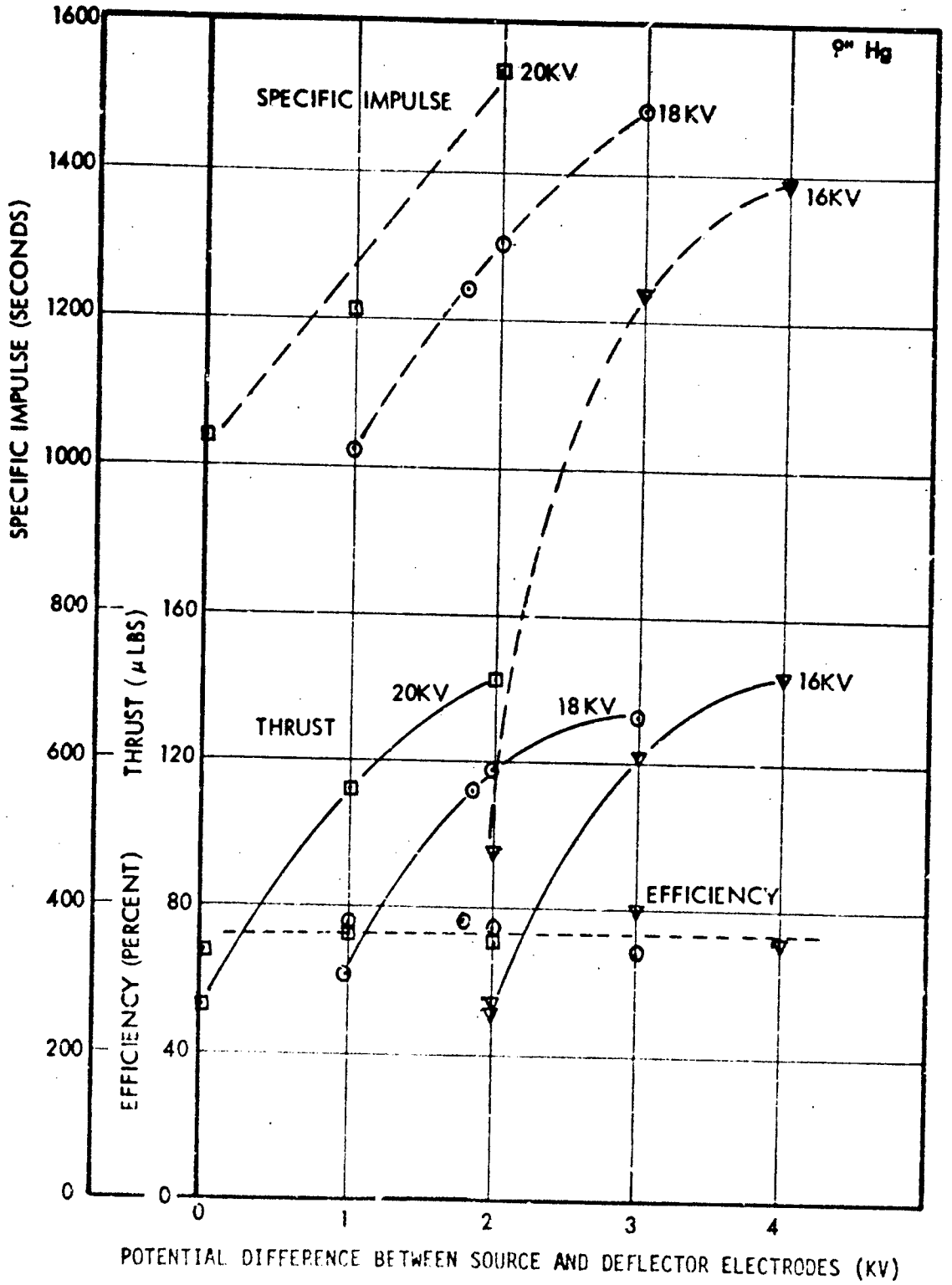


Figure 47. Run 7302-03. Performance Data for the Four-Source Module: Feed Pressure 9" Hg (~ 41 μg/sec mass flow)

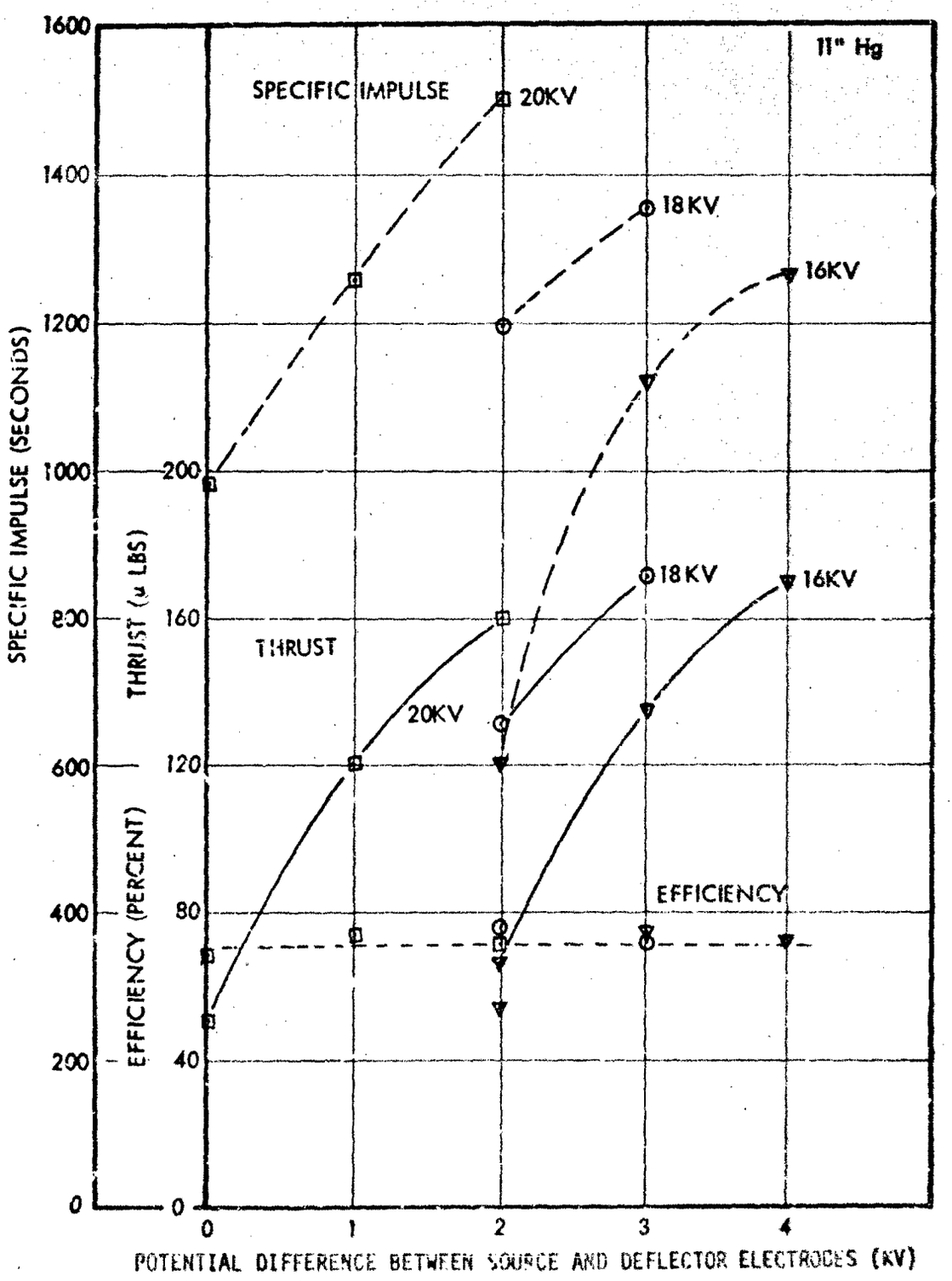


Figure 48. Run 7302-03. Performance Data for the Four-Source Module: Feed Pressure 11" Hg (~ 50 ug/sec mass flow)

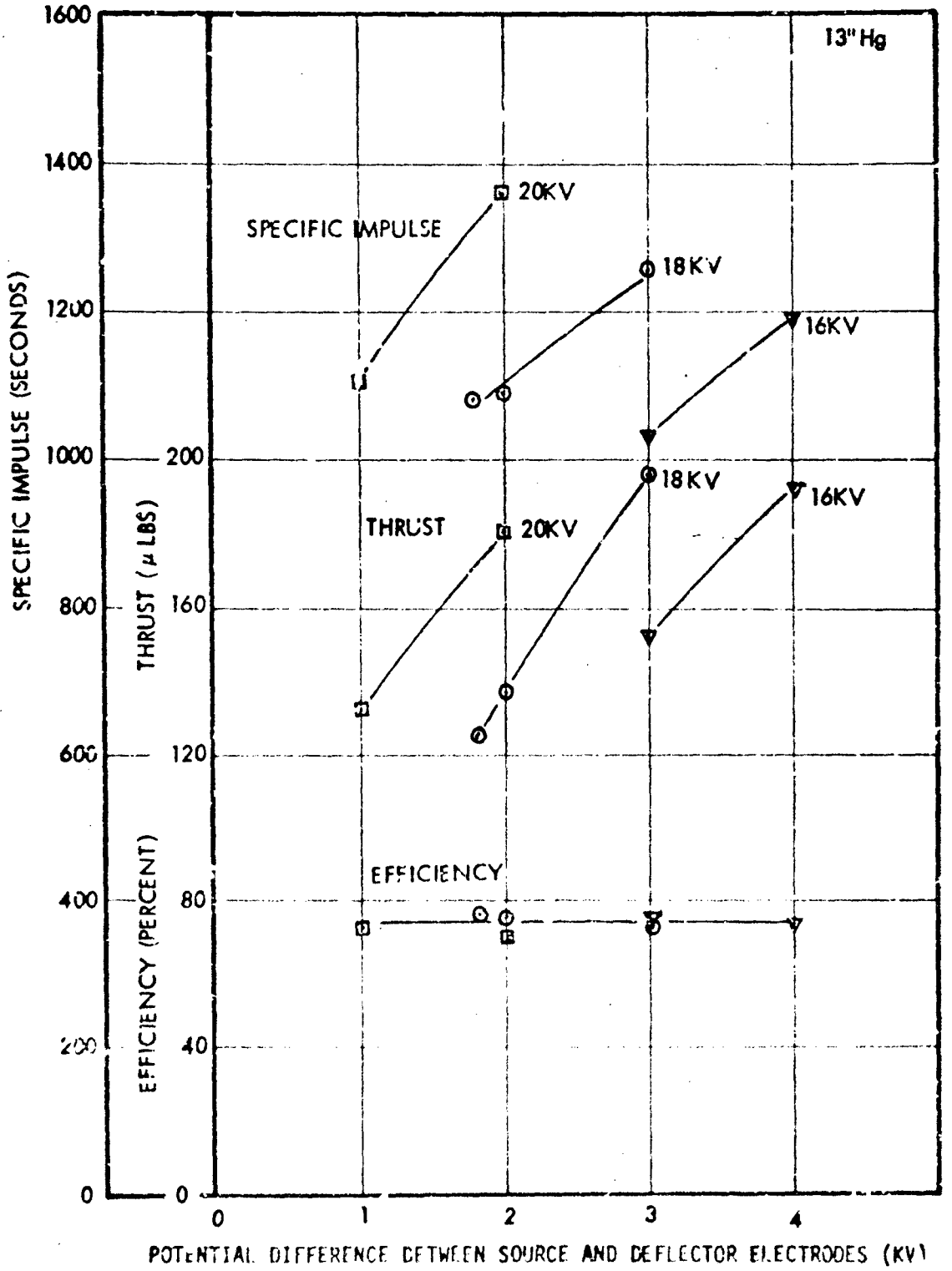


Figure 49. Run 7302-03. Performance Data for the Four-Source Module: Feed Pressure 13" Hg (~ 60 μg/sec mass flow)

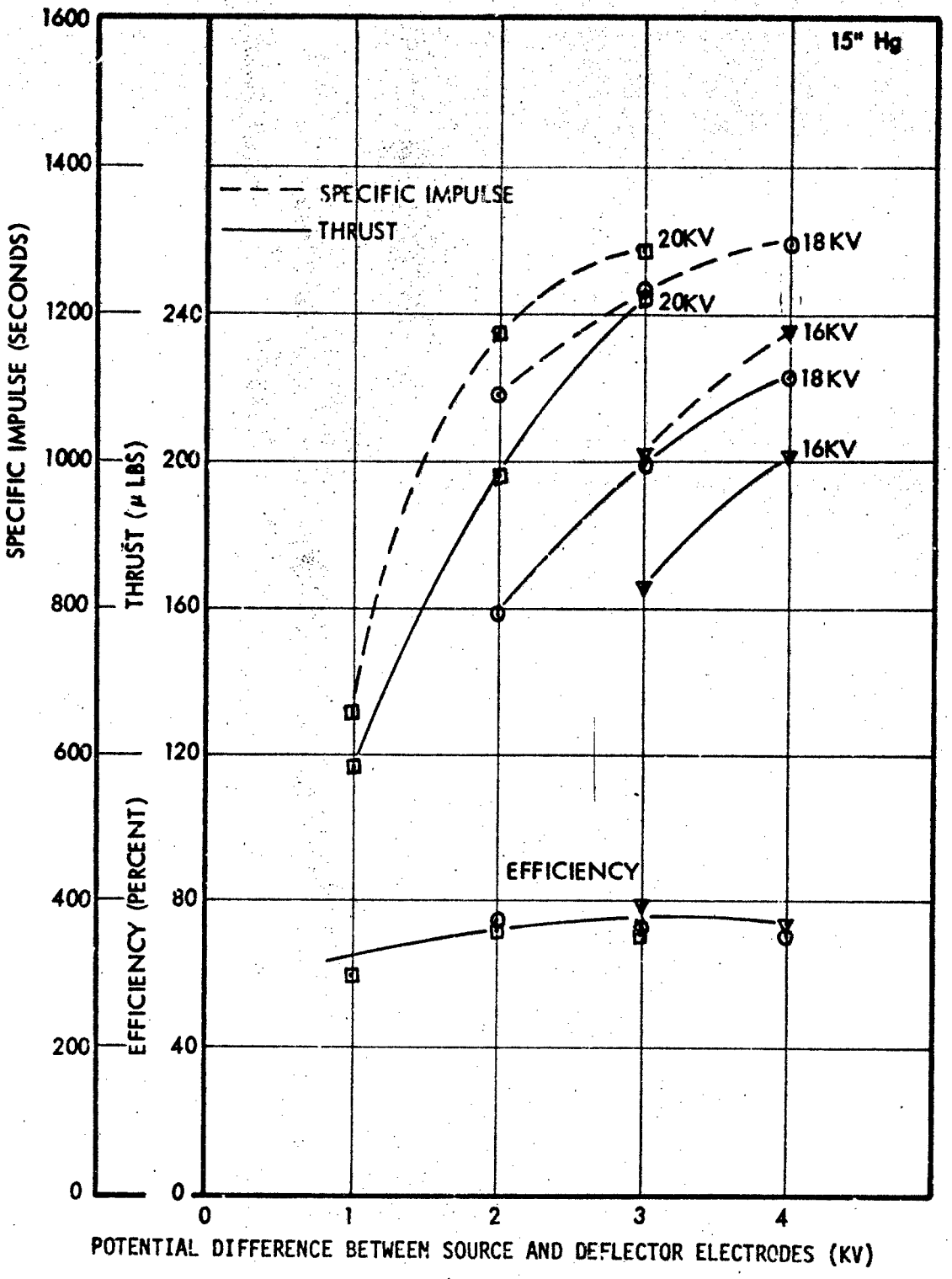


Figure 50. Run 7302-03. Performance Data for the Four-Source Module: Feed Pressure 15" Hg (∿ 62 μg/sec mass flow)

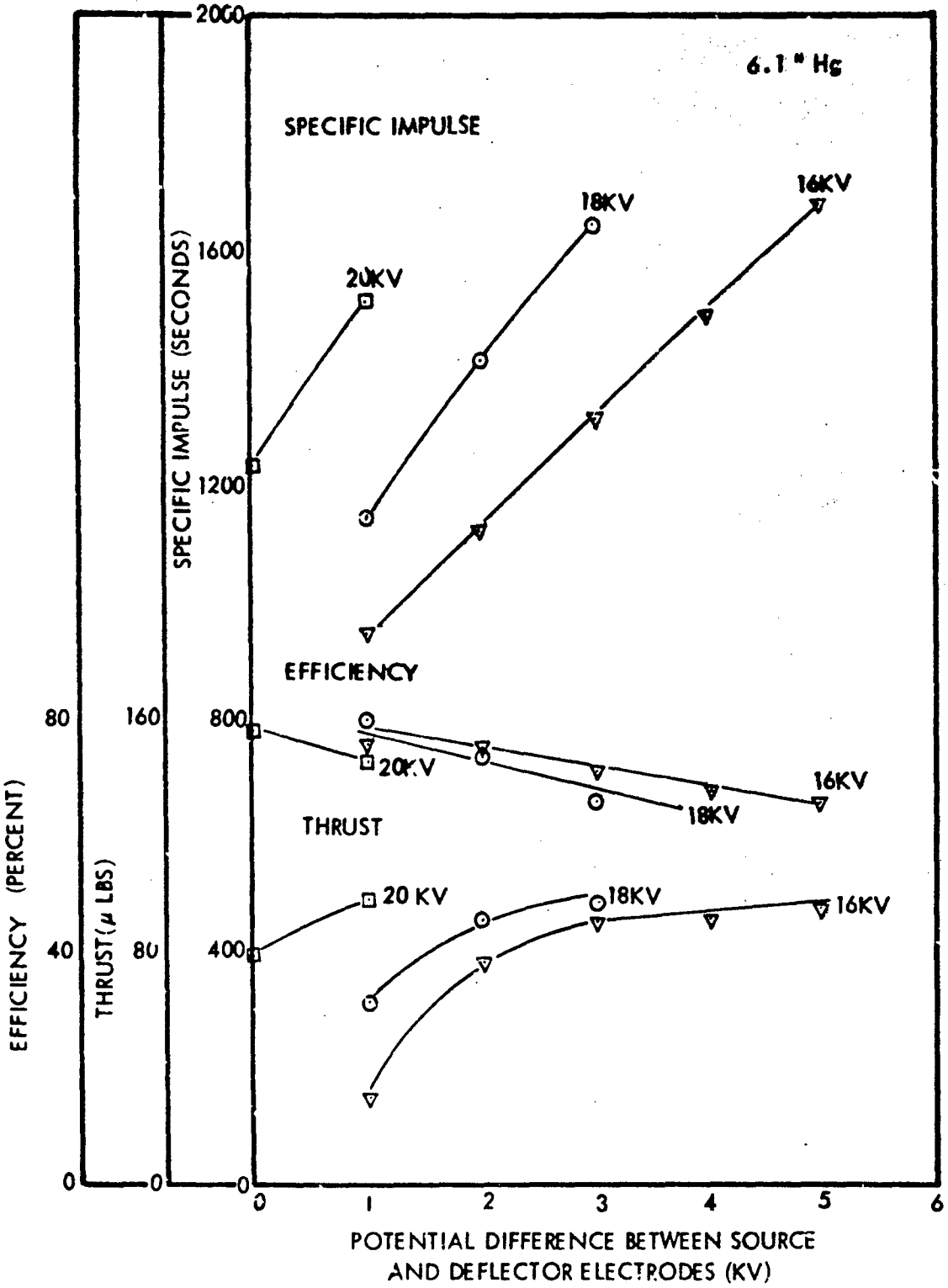


Figure 51. Run 7301-01. Performance at 6.1 in. Hg Feed Pressure (~ 28 μg/sec mass flow)

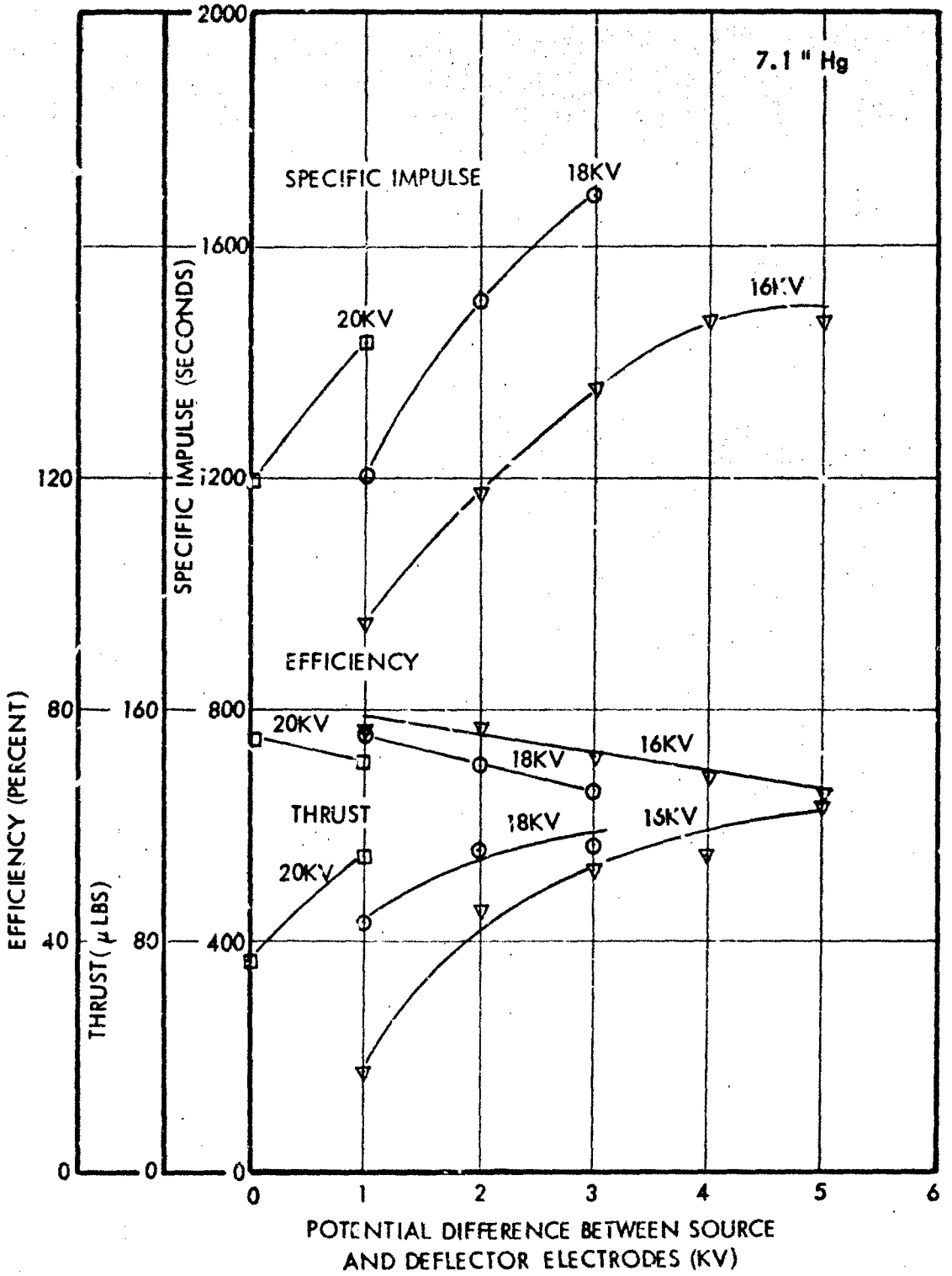


Figure 52. Run 7301-01. Performance at 7.1 in. Hg Feed Pressure (~ 35 μg/sec mass flow)

show the data. As with the previous runs, the performance could be optimized to either 78% efficiency, 1500 seconds specific impulse or as high as 130 µlbs thrust. However, in view of the primary objective of this run, i.e., the comparison of pre-run surface conditioning techniques, only a limited range of operational parameters were employed, and it is believed that higher performance levels would have been attained if a larger operational range had been explored. The major conclusion from this run was that glow discharge cleaning appeared to be the better technique for achieving the desired emitter surface state.

RUN 7301-02: FOUR SOURCE MODULE 360 HOUR ENDURANCE TEST

The main purpose of this run was to perform a preliminary test of the thruster's ability to perform over durations of 100 hours at various performance levels. The total test duration was 360 hours which included, in addition to long runs at various performance levels, demonstration of neutralized performance and profile mapping of the angular beam spread. The last 100 hours were run at average performance values of 75.4% efficiency, 1265 seconds specific impulse and 110 µlbs thrust. The thruster was in excellent operating condition at the end of the run and the test was terminated voluntarily in order to allow other experiments to proceed.

Figure 53 shows the total performance time history. It can be seen that there are three main segments to the test, each of the order of 100 hours or greater duration. The efficiency was greater than 75% for all three periods. For the first period the thrust averaged slightly over 100 µlbs and the average specific impulse was approximately 1025 seconds. This was achieved at 18 kv source voltage, 16.6 kv deflector voltage, -5 kv extractor voltage and 13" Hg feed pressure. Thruster temperature was held constant at 25°C throughout the entire test. After 115 hours small variations in deflector voltage were explored to determine if the specific impulse and efficiency could be raised at constant feed pressure. Table XIII summarizes the results obtained. Based on these data, the maximum efficiency point (16.2 kv) was selected for the next long duration segment (~135 hours). For this period the specific impulse averaged 1100 seconds and the efficiency 77%. There was a decrease in mass flow and thrust during this period which may have

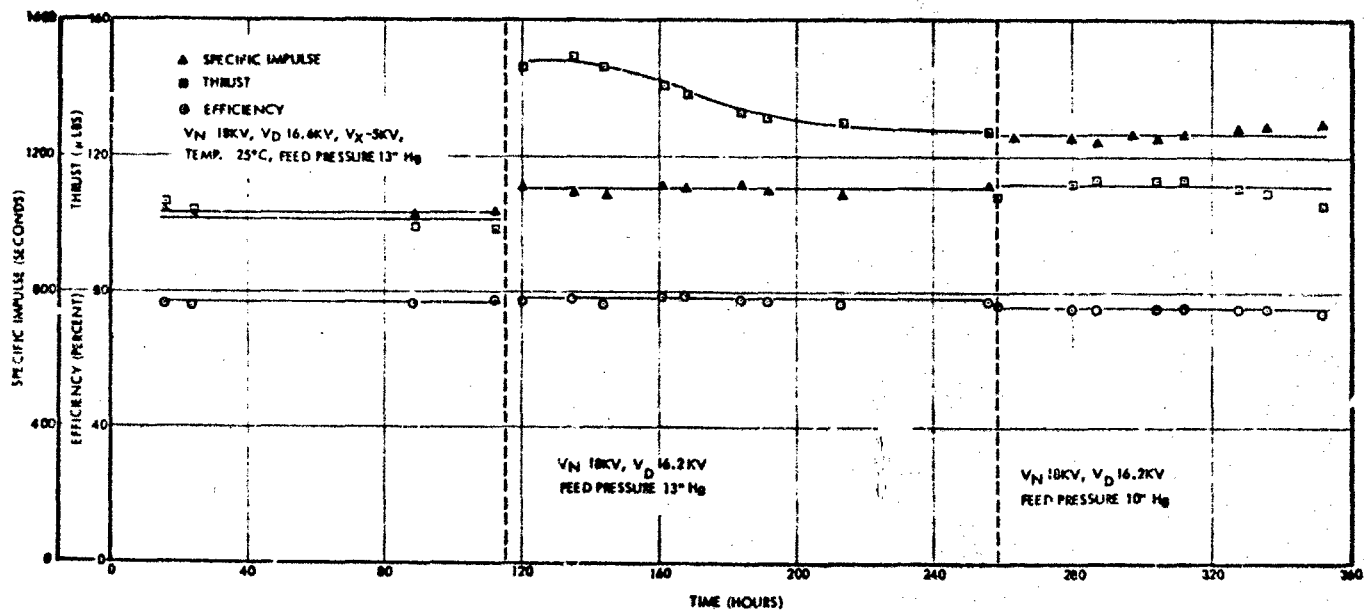


Figure 53. Performance Time History - Run 7301-02, 360 Hour Test

been due to the appearance of a partial blockage in either the feed line or filter. At the end of this period the thrust was 127 μlbs after being initially in the 150 μlb range. Since the thrust was still well above 100 μlbs, the feed pressure was then lowered to 10" Hg in order to increase the specific impulse. This succeeded in raising the specific impulse to an average value of 1265 seconds for the remaining 100 hours of the run. This was accomplished while still maintaining 75.4% efficiency and 110 μlbs thrust. A neutralizer was used for the first 122 hours of the run. At this time the neutralizer filament (0.002 inches diameter x 1.5 inches long non-sag tungsten) broke. This was believed due to a combination of a small kink that was initially in the wire and the fact that the neutralizer was rapidly switched completely off and on again for each time-of-flight experiment. To avoid this problem in later runs, for time-of-flight measurements the neutralizer heater current was slowly reduced below the emission threshold and the filament was kept warm to minimize thermal cycling.

TABLE XIII. RUN 7301-02 PERFORMANCE DEPENDENCE ON DEFLECTOR VOLTAGE AFTER 115 HOURS. (SOURCE VOLTAGE = 18 kv, EXTRACTOR VOLTAGE = -5 kv, FEED PRESSURE = 13" Hg, TEMPERATURE = 25°C)

| Deflection Voltage (kv) | Efficiency % | Specific Impulse (Seconds) | Thrust (μlbs) |
|---|---|---|---|
| 16.6 | 76.7 | 1025 | 98.5 |
| 16.4 | 76.0 | 1043 | 113.7 |
| 16.2 | 77.2 | 1084 | 135.7 |
| 16.0 | 76.6 | 1123 | 149.4 |
| 15.8 | 76.6 | 1155 | 158.3 |
| 15.6 | 75.9 | 1184 | 169.5 |
| 15.4 | 75.4 | 1226 | 178.0 |
| 15.2 | 73.4 | 1216 | 190.0 |

The neutralizer was placed 1-1/4" in front of the extractor and 1-1/2" from the side of the beam. An aluminum box partial enclosure shielded the emitters from a direct line of sight view of the wire. This box, which was maintained at the neutralizer bias potential, also shielded the neutralizer from adjacent grounded surfaces in order to assure that all the emission was directed towards the thruster exhaust.

When all collecting surfaces and walls in the tank were grounded, a neutralizer bias of -40 volts was required for the emission current to equal the beam current ($\sim$ 175 microamperes during the first 100 hours). At the beginning of the test, before the propellant flow was turned on, it was impossible to draw any neutralizer current, even at -200 volts negative bias, when all the thruster voltages were turned on. This demonstrated that during normal operation the neutralizer was strongly coupled to the thruster exhaust plasma potential and depended upon it to control the emission current. Similarly, when the beam plasma potential was driven more positive, the emission current would increase, even when the neutralizer bias was dropped to zero. The method of driving the plasma potential positive was to apply a positive potential to the time-of-flight collector screen, since the potential of a neutralized plasma will follow the most positive boundary that it is in intimate contact with[7]. For 300 volts screen bias, and zero bias on the neutralizer, the neutralizer ran emission limited at 330 microamperes, which was the setting used throughout the neutralized portion of the test, thus insuring that a more than adequate supply of electrons entered the beam. The neutralizer heater power was 4 watts. Turning the neutralizer on and off had no effect on the measured source current, thus proving that neutralizer electrons were not going to the emitter. Decreasing the extractor bias from -5 to -2 kv resulted in increased neutralizer current even though the beam current decreased due to the decreased total extraction field strength. This indicated that although, as previously discussed, the beam plasma did provide sufficiently positive potential to counteract the negative extractor field, in this experiment the negative extractor field still had some retarding effect on the emission.

The thruster beam profile was mapped during the last 100 hours and the results are shown in Figures 54 and 55. The results indicate that 90 percent of the beam is contained within a cone of less than 15° half angle. However, due to an initial thruster misalignment, the beam was centered approximately 6° off the nominal symmetry axis. The post inspection test of the thruster and tank interior were especially interesting. A major portion of the tank interior was coated with dense black substance due to backscattering from the beam. Figure 56 is a photograph of the tank door. The lower silvery portion is where the door was shielded by the time-of-flight collector.

The thruster also received considerable backscattering due to the short collector distance (1 meter) and this was quite evident from the resulting deposition pattern on the extractor (Figure 57). The clean areas are where the extractor was kept clean by ion bombardment. The extremely black areas immediately surrounding the extractor holes are evidence that energetic bombardment in this region was minimized by the deflecting fields due to the high positive potential in the vicinity of the emitter and deflector electrodes. Although these pictures show that obviously there was considerable backscattering to the entire thruster, the emitters themselves remained completely clean. Figure 58 is a closeup of one of the emitters. The cleanliness of the emitters was probably due to a combination of the cleansing action of the propellant and the tendency of the thruster exhaust to molecularly pump backscattered vapor away from the thruster. Post inspection of the thruster also indicated no signs of erosion or other thruster deterioration. Thus indicating that the test could have been continued for a considerably longer duration.

100 HOUR LIFE TEST (RUN 7302-01)

A new neutralizer was installed in the tank and an additional 100 hour life test was performed to further demonstrate that the thruster could operate satisfactorily at high performance levels while being neutralized. The results are shown in Figure 59. The final control parameters; 9" Hg feed pressure (∿ 43 μg/sec mass flow), 18 kv emitter voltage, 16.2 kv deflector voltage, -5 kv extractor voltage, -50 volts

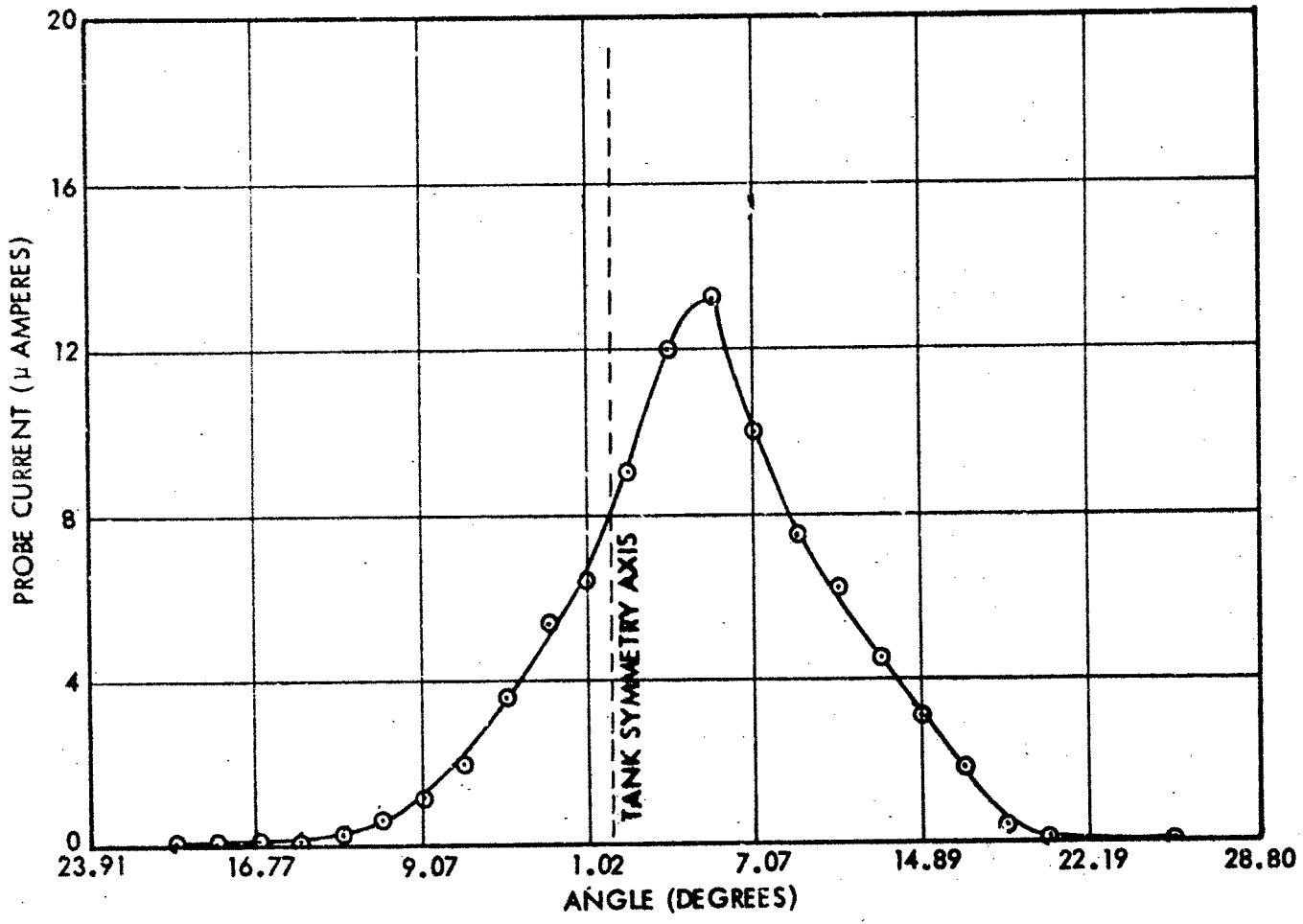


Figure 54. Run 7301-02. North-South Beam Profile During Last Third of Test

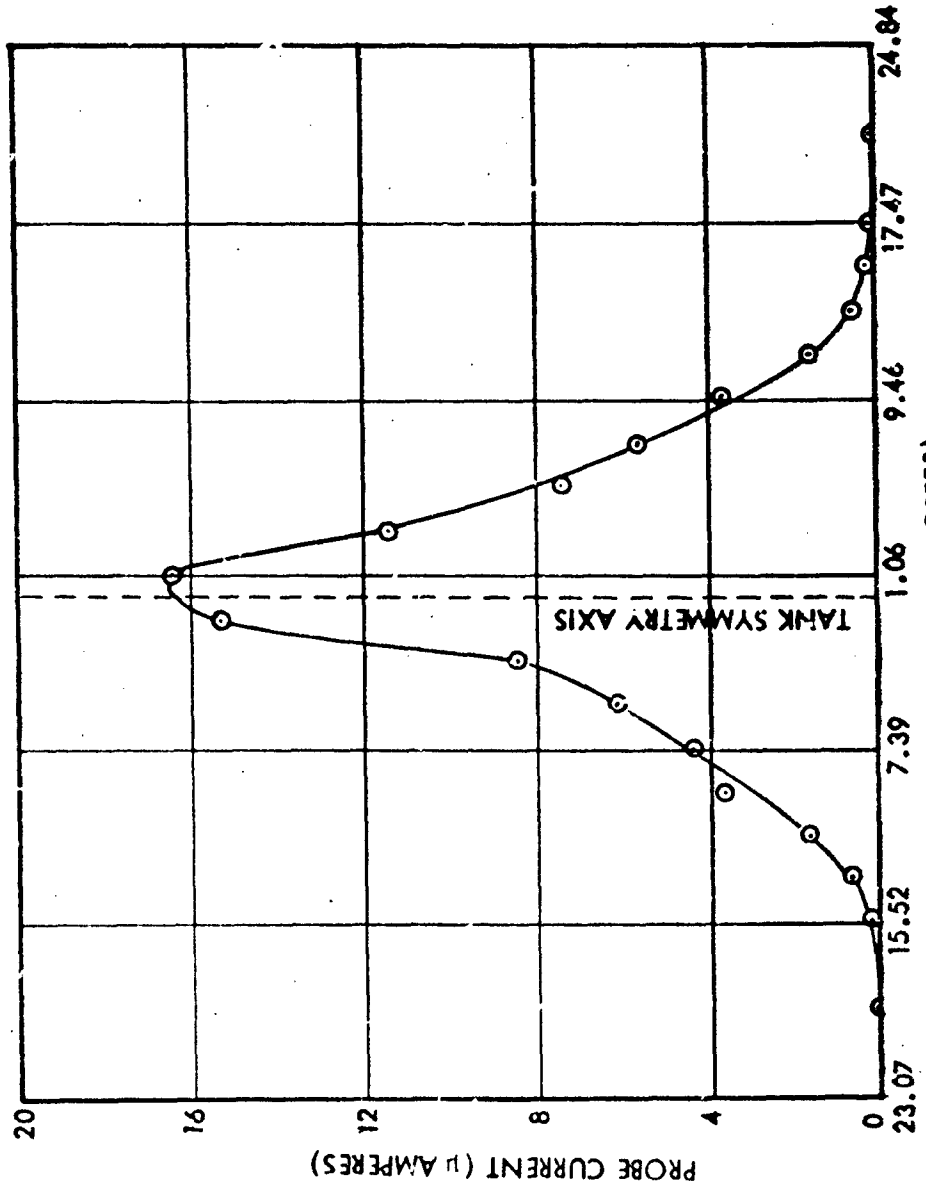


Figure 55. Run 7301-02. East-West Beam Profile During Last Third of Test

Figure 56. Vacuum Tank [illegible] After 360 Hour Run (Lower Silvery Portion was Shielded by Collector)

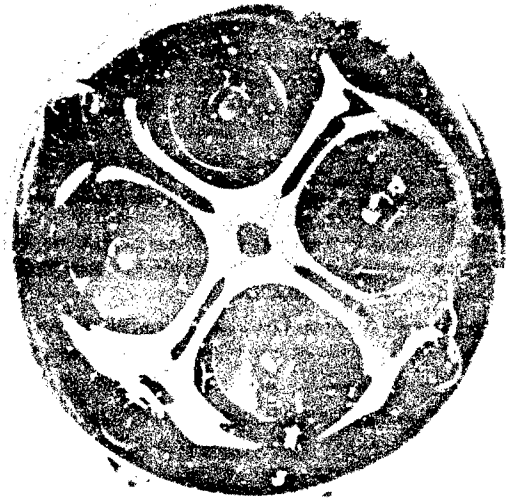

Figure 57. Four Source Module After 360 Hour Run

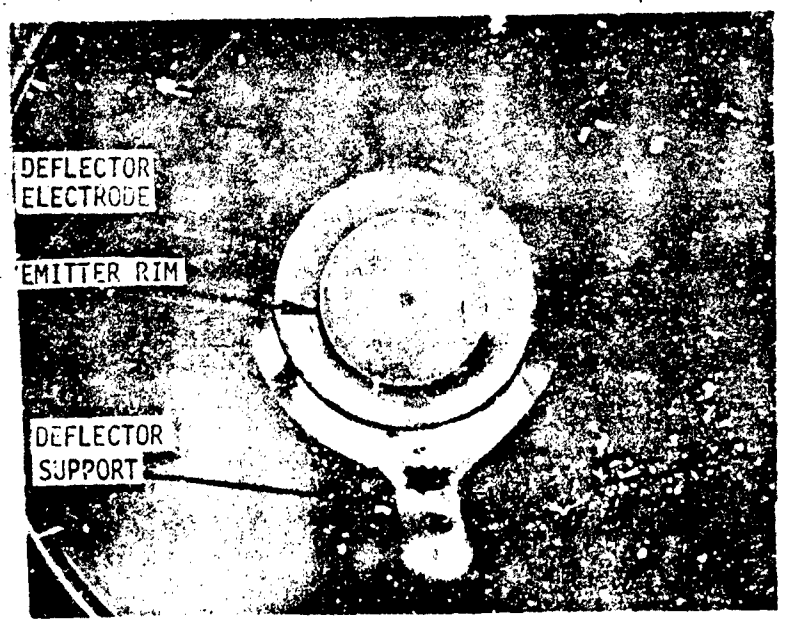


Figure 58. Close-up of Emitter and Deflector Electrode Assembly after 360 Hour Test. The shaded area is due to lighting shadows when the picture was taken.

neutralizer bias, were set in the second day of the test and the thruster was kept at these values for the remainder of the test (78 hours). The average performance over this period was 75% efficiency, 1325 second specific impulse, 265 microamperes beam current, and 123 μlbs thrust (hence an average of 31 μlbs/unit). All the performance parameters remained constant to within ±3% through this period. Post inspection showed the needles to be completely clean and with no traces of wear.

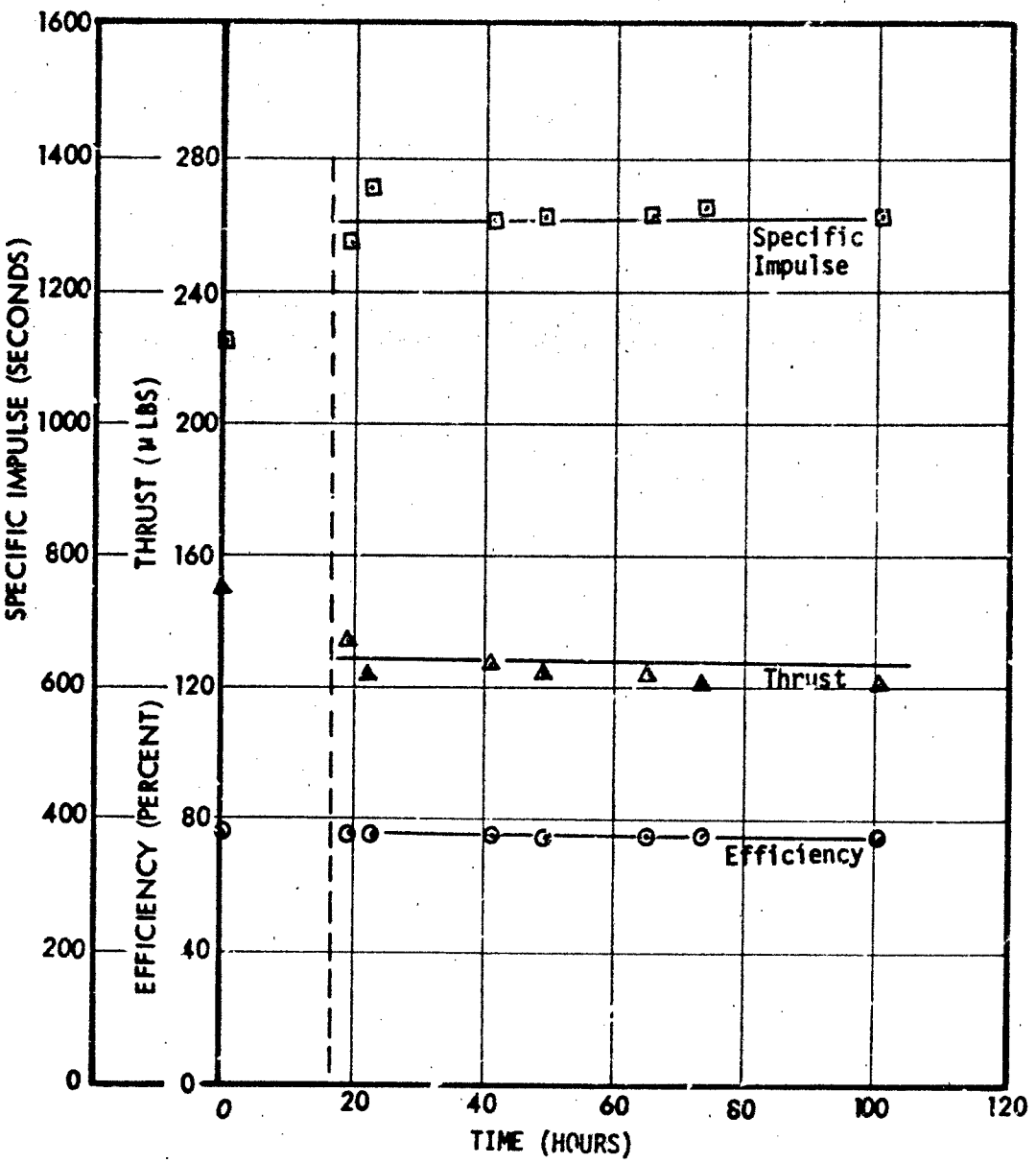


Figure 59. Run 7302-01. Four Source Module 100 Hour Test Performance History

# 5. SUPPORTING RESEARCH

## 5.1 Collisions Within the Thruster Exhaust

An approximate theoretical model has been developed for predicting the number of ion-droplet collisions per second within the thruster exhaust, and equations have been derived which provide an order-of-magnitude estimate of the collision rate. The model assumes a two-component beam, one component consisting of heavy droplets of uniform size and charge-to-mass ratio and the other component consisting of ions having a mass of approximately 100 amu (glycerol molecular weight is 92 amu). The theory further assumes that both the ions and heavy particles are emitted uniformly over the entire emitting surface, with negligible subsequent angular divergence and that the collisions are due solely to the ions overtaking the slower heavy particles. This is the most tenuous part of the argument since if, for example, ions and heavy droplets originate at separate spray sites, one could argue that they never collide. On the other hand, if they originate at the same, highly localized spray sites, the collision probability would be greatly enhanced. What little evidence there is in this regard, tends to support the latter assumption. However, in the absence of specific quantitative data, it seems reasonable to use the uniform emission density picture.

Using this model and assuming a thruster exhaust composed of 75 microamperes of $1.5 \times 10^6$ cm/second velocity heavy particles and 25 microamperes of ions, 15 kv accelerating voltage, and 0.1 inch diameter emission area; a value of $5.8 \times 10^9$ collisions per second in the first centimeter of flight path was calculated. Liberation of one electronic charge pair per collision could then lead to extractor and back bombardment currents of the order of $10^{-9}$ amperes. It is difficult to assess the effects of a back bombardment of this magnitude. However, at this point we can say that these collisions do take place and their rate and energy will increase as the thrust density and voltage are increased.

The rest of this section will now be devoted to outlining, in greater detail, the way in which the collision rate was estimated.

The collision cross section of a single large droplet of radius R is approximately $\pi R^2$. If there are $N_T$ target droplets per centimeter length of exhaust plume, the total target area in one centimeter length of exhaust plane is $N_T \pi R^2$. The probability of an ion colliding with one of these particles while traversing one centimeter of path length is given by $P = N_T \pi R^2 / A$ (where A = beam cross sectional area) provided that (1) $P << 1$ (negligible target overlap) and (2) the ion cross sectional area is much smaller than the target droplet cross-section. Since P is the probability of one ion having a collision, the total number of collisions per second is $n_i P$ where $n_i$ is the number of ions per second traversing a one-centimeter long cloud of target particles ($n_i$ is lower case to emphasize that it is a particle flux as differentiated from $N_T$ which is a particle density).

Summing up what has been said so far, the collision rate $\nu$ is given by:

$$\nu = \frac{n_i N_T \pi R^2}{A} \text{ collisions/second/cm of path length}$$

The ion flux is easily calculated since

$$n_i = \frac{J_i v_{ir}}{e v_i} \text{ ions/second}$$

where $e = 1.6 \times 10^{-19}$ coulombs (assuming only singly charged ions)

$v_i$ = absolute ion velocity

$v_{ir}$ = ion velocity relative to heavy particle motion

$J_i$ = ion current contained within thruster exhaust

Thus, $$\nu = \frac{J_i N_T \pi R^2}{e v_i A} v_{ir}$$

The heavy particle density is given by

$$N_T = \frac{J_T}{Q V_T}$$

where $J_T$ = heavy particle current contained within thruster exhaust

$Q$ = charge per particle

$v_T$ = particle velocity = $1.5 \times 10^6$ cm/second (initial assumption)

The expression for the collision frequency now becomes:

$$\nu = \frac{J_i J_t \pi R^2}{e v_i A Q v_T} v_{ir}$$

and $v_T$ is related to the particle charge-to-mass ratio since:

$$1/2\ M v_T^2 = QV_S$$

where $V_S$ = source voltage = 15 kv

Thus $\frac{Q}{M} = \frac{v_T^2}{2V_S}$ ( ≈7500 coulombs/kilogram heavy particle charge-to-mass ratio)

$R^2$ and Q are approximately related to each other by the Rayleigh stability criterion:

$$\frac{Q^2}{R^3} \geq 16\pi\gamma$$

where $\gamma$ is the surface tension = 68 dyne-cm$^{-1}$.

Assuming the droplet is just at the stability limit we get:

$$\frac{R^2}{Q} = \left[\frac{R}{16\pi\gamma}\right]^{1/2}$$

The Rayleigh expression can be further rearranged in order to obtain R as a function of Q/M:

$$R = \left[\frac{9\gamma}{\pi\rho^2}\left(\frac{Q}{M}\right)^{-2}\right]^{1/3}$$

where $\rho$= propellant density ≈1.45 gm/cm$^3$

Using the previous expression for Q/M, the expression for R becomes

$$R = \left[\frac{9\gamma}{\pi\rho^2}\ \frac{4V_s^2}{V_T^4}\right]^{1/3}$$

$$\text{and } \frac{R^2}{Q} = \frac{1}{4}\left[\frac{6V_S}{\pi^2\rho\gamma V_T^2}\right]^{1/3}$$

Inserting this in the previous collision rate expression results in:

$$\nu = \frac{J_i J_T v_{ir}}{4eAv_i v_t}\left[\frac{6\pi V_S}{\rho\gamma v_T^2}\right]^{1/3} \text{ collisions/second/cm}$$

which is a general expression for the collision rate in a two-component colloid beam when one of the components consists of ions.

The conditions specified for the present problem are:

$J_i$ = 25 microamperes

$J_t$ = 75 microamperes

$v_i$ = $1.7 \times 10^7$ cm/sec

$v_T$ = $1.5 \times 10^6$ cm/sec

$v_{ir} = v_i - v_T \approx 1.55 \times 10^7$ cm/sec

$V_S$ = 15 kv

A = $5.06 \times 10^{-2} cm^2$

$\rho$ = 1.45 $gm/cm^3$

$\gamma$ = 68 dyne/cm

e = $1.6 \times 10^{-19}$ coulombs

Substituting these values (in cgs units) in the collision rate equation leads to a collision frequency value of

$\nu$ = $5.8 \times 10^9$ collisions/second

within the first centimeter of path length.

## 5.2 Other Propellants

### RUN 7204-01: LITHIUM IODIDE DOPED PROPELLANT (STANDARD EMITTER)

This test was performed relatively early in the program, using a 3/8" extractor aperture and horizontal orientation. The propellant was a mixture of 30 grams of lithium iodide in 100 cc of glycerol. The resistivity of this solution was 9330 ohm cm and the viscosity was 2200 centistokes at 25°C. For the normal TRW sodium iodide doped propellant, the corresponding resistivity and viscosity are 4700 ohm-cm and 1280 centistokes, respectively. Performance-wise, the thruster tended to run at around 1000 seconds specific impulse, 25 micropounds thrust and 73 percent efficiency. Since the specific impulse was lower than was being obtained with conventional sodium iodide doped propellant, no further work was done with lithium iodide.

## RUN 7206-03: POTASSIUM IODIDE DOPED PROPELLANT

The purpose of this run was to try potassium iodide doped propellant. Experiments performed several years ago with potassium iodide doping had shown a tendency for higher efficiencies and lower charge-to-mass ratios. The performance was fairly good. Figures 60 and 61 plot some of the performance attained during these tests. Good thrust (20-40 μlbs) and specific impulse (1400-1600 seconds) could be obtained at a number of operating points. However, there was an ion peak which kept the efficiency below 70 percent.

## SHELL ASA-3 ANTI-STATIC ADDITIVE

The Shell Chemical Company has developed a proprietary product called Shell ASA-3 which can produce a small degree of electrical conductivity in conventional hydrocarbon fuels. This compound was developed to prevent fire hazards due to the buildup of electrostatic charge during fuel handling operations.

A brief experimental check was made to see if ASA-3 could produce sufficient electrical conductivity for colloid applications in Santovac 5, a very low vapor pressure hydrocarbon diffusion pump oil. No detectable conductivity was produced as measured by a resistivity bridge which could measure as high as $11.990 \times 10^6$ ohm-cm, as compared with the 4500 ohm-cm resistivity of the standard TRW NaI/glycerol propellant. However, even if sufficient conductivity had been induced, the high vapor pressure of ASA-3 would still have been a deterrent to its use, and therefore, no further investigations of ASA-3 were made.

## Registered Grid Time-of-Flight Collector

Prior to initiating the tool made emitter performance test program, the experimental test facility was checked out and a new registered grid time-of flight collector was installed. The main feature of the collector is the "registering" of the grids, as shown in Figure 62, so as to ensure that there is no direct beam impingement on the suppressor. Therefore, all particles passing through the screen will end up on the honeycomb collector. The negative bias on the suppressor prevents

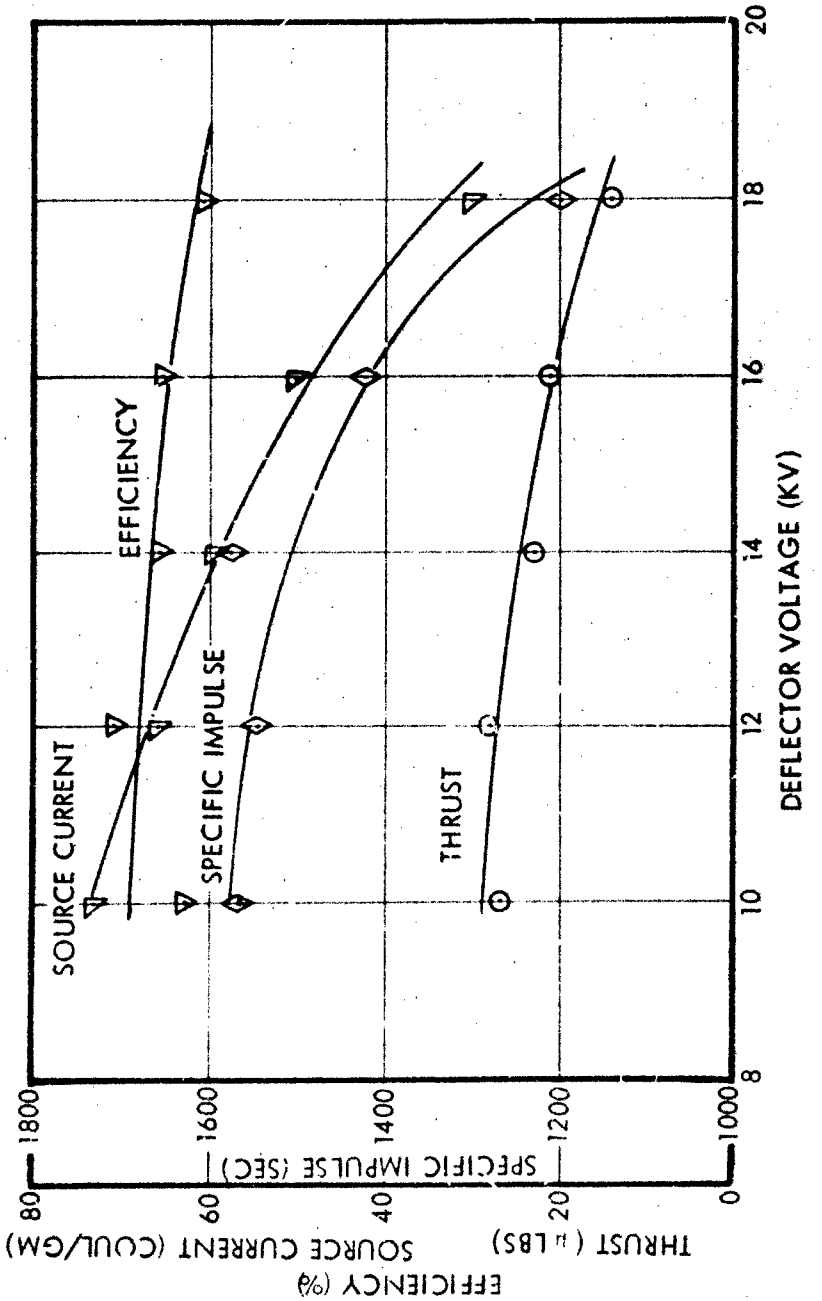


Figure 60. Run 7206-03 Performance versus Deflector Voltage at 20 kv Source Voltage and 2 Inches Hg Feed Pressure (Potassium Iodide Dopant)

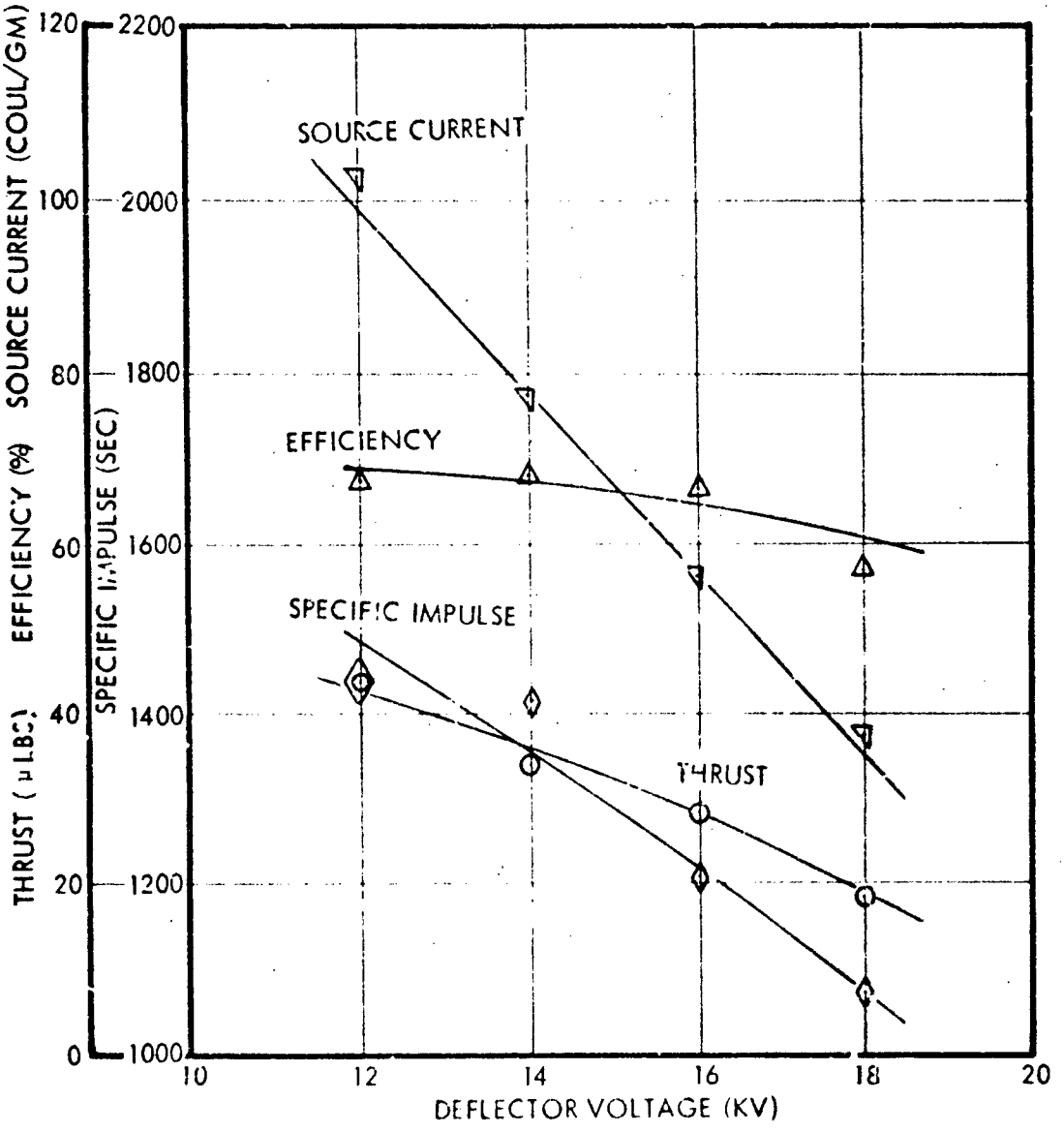


Figure 51. Run 7206-03 Performance versus Deflector Voltage at 20 kv Source Voltage and 3 Inches Hg Feed Pressure (Potassium Iodide Dopant)

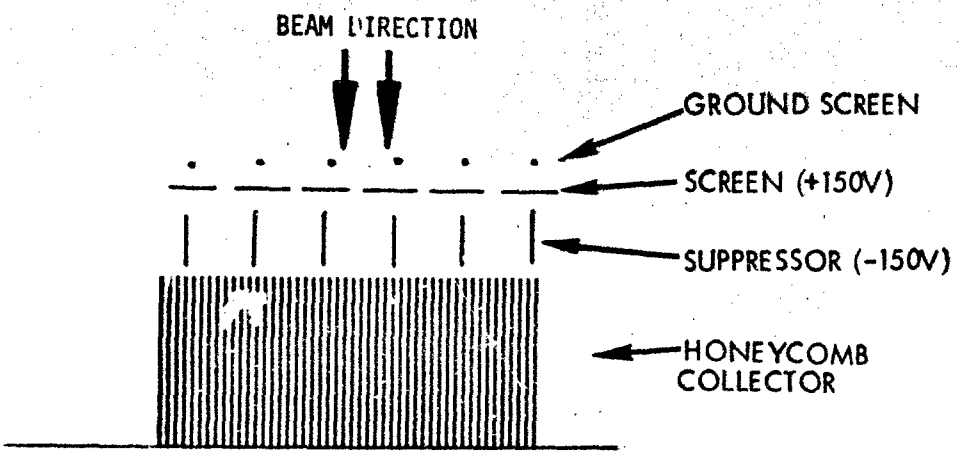


Figure 62. Registered Time-of-Flight Collector Geometry

secondary electrons from leaving the collector. Secondary positive particles can still leave the honeycomb but they are energetically incapable of penetrating back out through the positively biased screen. Most of these positive secondaries will then end up being pulled into the suppressor. For this reason, it is necessary to read the total of the collector and suppressor currents, which will be equal to the total beam current entering the collector. In order to read the total current while still maintaining a negative suppressor bias, the suppressor is connected to the collector through a battery. A 1 mfd capacitor shunt is placed across the battery to ensure adequate response speed. As an added precaution, a thin ground screen wire is positioned in front of each screen grid strip to collect secondary positives created at the front surface of the screen strip.

The screen grid consists of an array of 1/2-inch wide by 0.003-inch thick vertical stainless steel ribbon strips positioned with their flat sides parallel to the collecting plane. A 1/2-inch spacing is maintained between the strips in order to provide 50 percent transparency. The suppressor consists of an array of similar strips oriented end on with respect to the screen strips in order to allow them to be completely shielded and also to ensure that a negative field can be

created in the region between the supporessor strips. The overall collection area is a 30-inch square at a distance of 1.86 meters from the thruster. Thus, the collector intercepts a 12° half-angle at its mid-plane. For vertical operation the distance is 1.06 meters and the half-angle is 20°. Test runs made with the collector have shown the time-of-flight trace to be constant over wide ranges of suppressor and screen biases and indicate that well-defined, unambiguous time-of-flight traces can be obtained. The collector current is always approximately 50 percent of the beam current, as would be expected from the geometric screen transmission. This also confirms that the thruster beam spread is minimal, which is in good agreement with visual observation of the beam profile.

## 5.4 Propellant Evaporation Rates

### Experimental Method

In order to estimate the thruster exhaust neutral fraction due to evaporation, experiments were performed to measure the evaporation rates, in vacuum, of glycerol and NaI/glycerol propellant. The experiments basically consisted of measuring the rate of weight loss due to evaporation from the surface of a shallow dish of liquid. To do this, we designed and built the simple flotation-type balance shown in Figures 63 and 64. The dish of evaporating liquid was supported on a float which would steadily rise as evaporation reduced the total buoyancy required to support the dish. Relatively non-evaporative DC 704 pump oil ($\sim 3\times10^{-8}$ torr vapor pressure) was used to provide flotation. The flotation device consisted of a large glass bulb from which a relatively heavy metal weight was suspended to provide vertical stabilization. A narrow graduated glass support column extended upward to the dish of evaporant. The support column cross section was made relatively small to provide a large vertical displacement for a small weight loss. The system dimensions were chosen so that an approximately full-scale deflection would be obtained during an eight-hour day.

The support rod cross-sectional area was 0.354 $cm^2$ and the published specific gravity of DC 704 is 1.066. From this we calculate a theoretical vertical sensitivity of $[(1.066)(0.354)]^{-1}$ = 2.65 cm rise per gram of

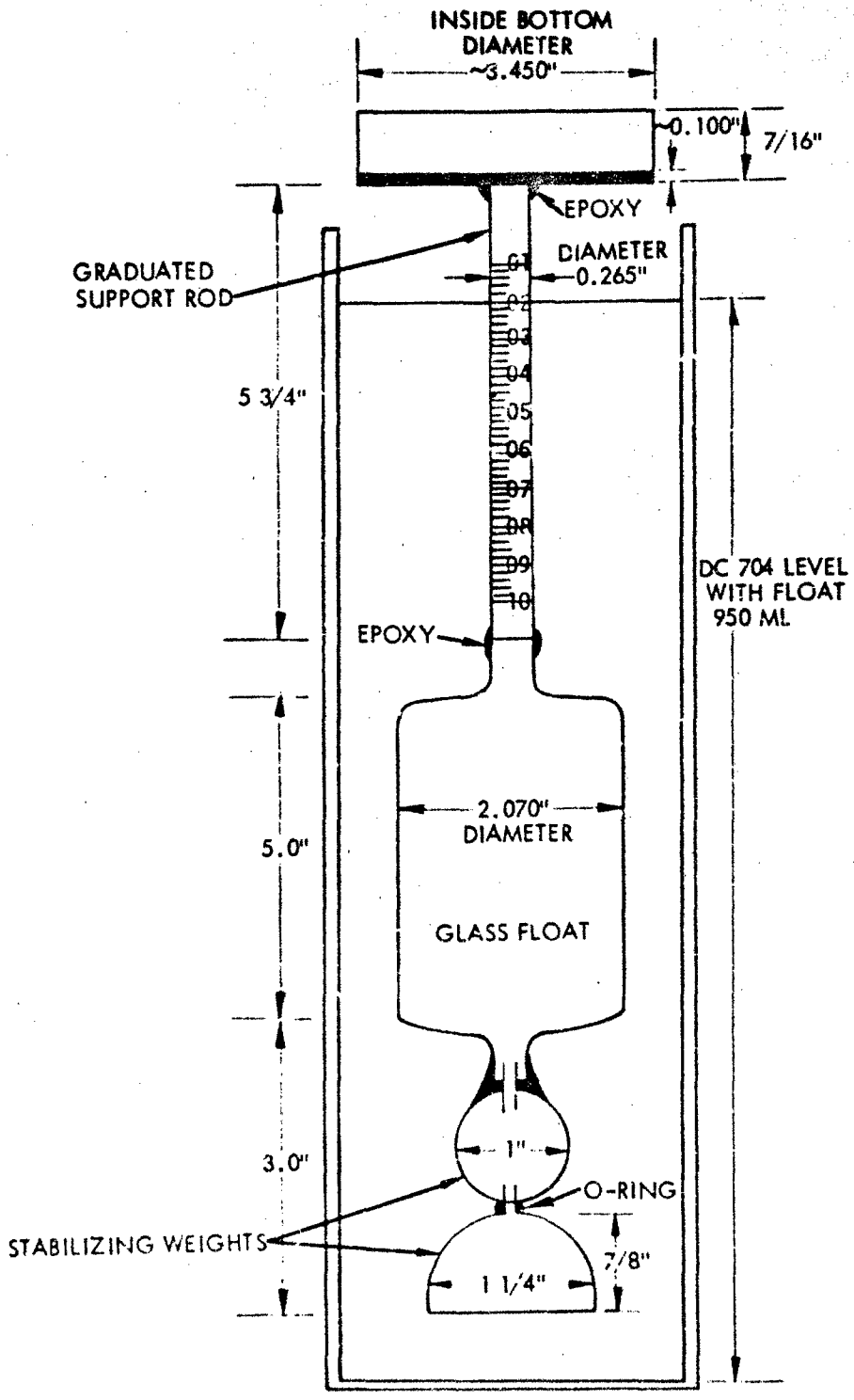


Figure 63. Evaporation Experiment Schematic

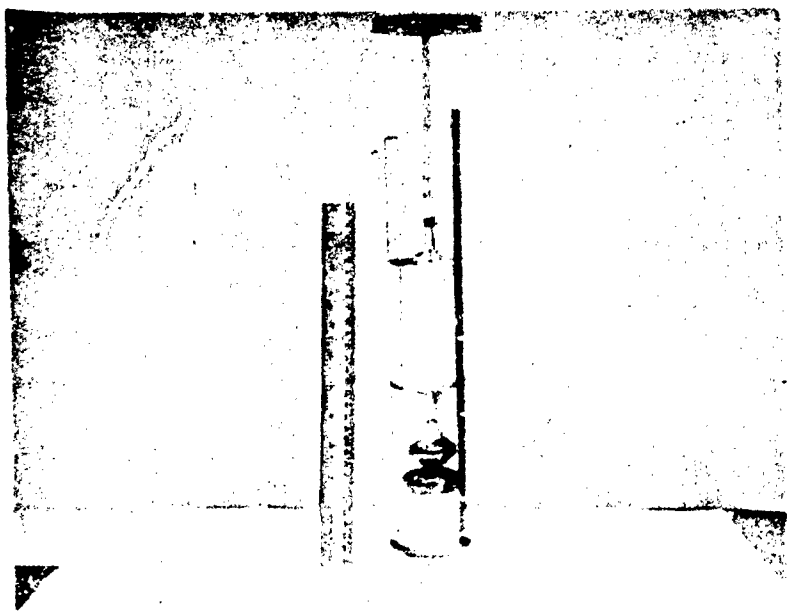

Figure 64. Photograph of Evaporation Experiment

weight loss. The division spacing on the graduated support was equal to 0.1394 cm. Thus the calculated scale sensitivity was 19.0 divisions per gram using the published density of DC 704. The system was then experimentally calibrated using small weights. These measurements yielded a sensitivity of 18 div/gm $\pm$ 1%. For the purposes of the experiment, the measured value of 18 div/gm was used.

Results

Figure 65 shows a typical time history of weight loss versus time for glycerol and propellant. All evaporation runs were performed in a 4 x 8 foot vacuum chamber at a background pressure of approximately $4 \times 10^{-5}$ torr. A mercury bulb thermometer positioned near the experiment measured the interior equilibrium temperature which was approximately 20°. The temperature usually remained constant to within 0.1°C throughout the test. The following table summarizes the results.

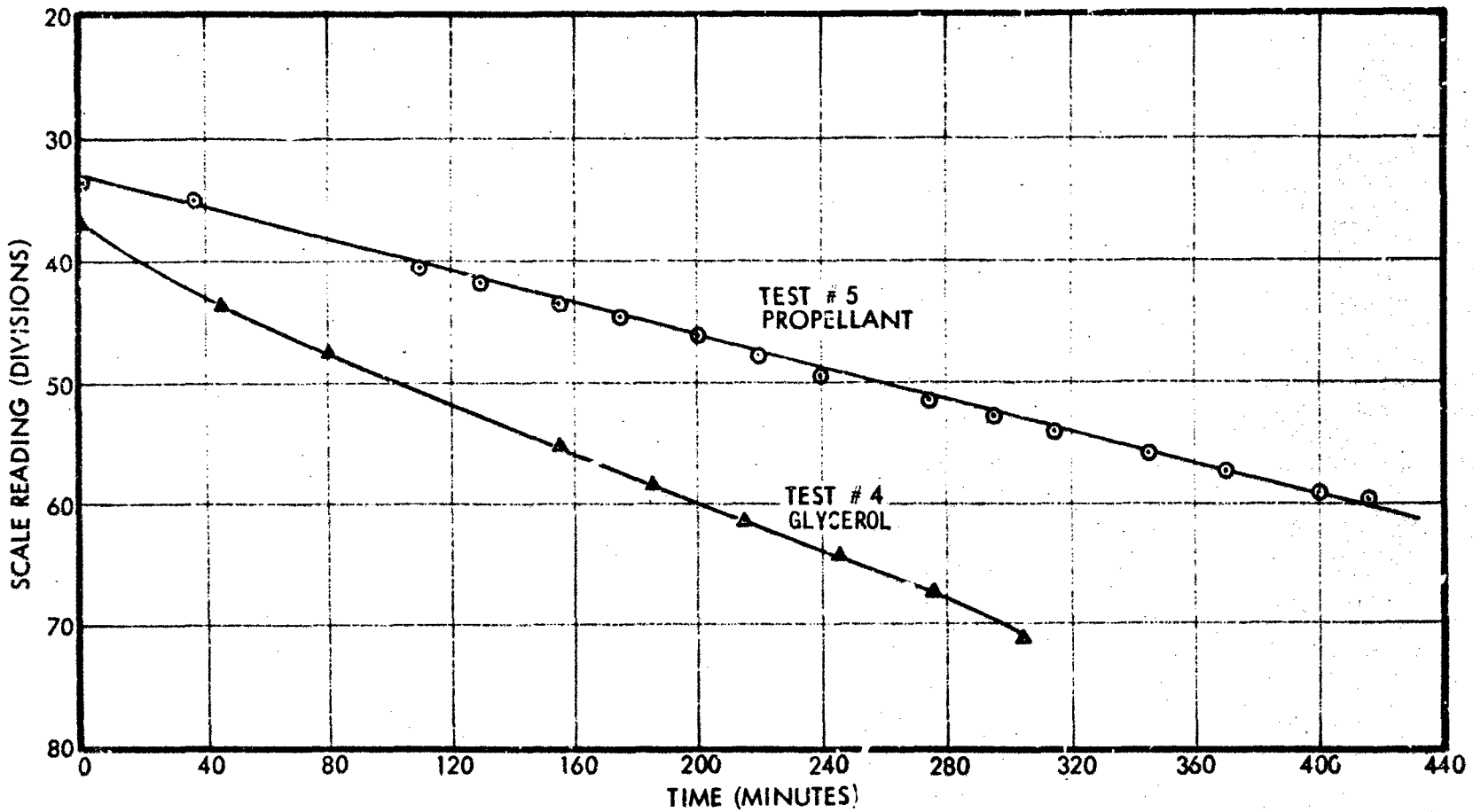


Figure 65. Evaporation Experiment, Runs #4 and #5

| Evaporant | Temperature (°C) | Evaporation Rate ($\mu g/sec/cm^2$) |
|---|---|---|
| Glycerol | 20.0 | 1.69 |
| Glycerol | 20.3 | 1.61 |
| Propellant | 20.3 | 0.975 |
| Propellant | 19.9 | 0.911 |

Discussion

Kinetic theory predicts that the number ($\epsilon$) of molecules per second per square centimeter leaving a surface of vapor pressure P dynes/$cm^2$ is given by:

$$\epsilon = \frac{P}{\sqrt{2\pi mkT}}$$

where m is the molecular mass in grams, $k = 1.38 \times 10^{-16}$ ergs/°K, and T is the absolute temperature, °K.

At 20°C, for glycerol (92 amu), using the appropriate conversion factors, this equation reduces to the following expression:

$$P = 30.4\ \dot{m}$$

where $\dot{m}$ is the evaporation rate in grams/sec/$cm^2$ and P is the kinetically predicted vapor pressure in torr. The two glycerol runs yielded a P of approximately $5 \times 10^{-5}$ torr at 20°C. The published[6] vapor pressure of glycerol is $1.7 \times 10^{-4}$ torr at 20°C. Thus, our measurements indicate that glycerol evaporates at 0.3 times the rate predicted by kinetic theory. This disagrees with the published evaporation coefficient of 0.05 by a factor of six. We have no explanation for this disagreement and can only say that it would be desirable to perform further measurements.

We note that the addition of the sodium iodide reduced the evaporation by 40 percent.

Finally, we can predict the evaporation from a colloid emitter. The vapor pressure of glycerol increases by a factor of approximately 1.9 for every 5°C temperature rise in the temperature range of 20 to 30°.[6] The effective cross-sectional area for evaporation for a large (0.090-inch) diameter thruster is ≈ 0.0428 $cm^2$. The corresponding evaporation rates would be

| Temperature (°C) | Evaporation (μg/sec) | Percentage Mass Loss |
|---|---|---|
| 20 | 0.04 | 0.4 |
| 25 | 0.07 | 0.7 |
| 30 | 0.14 | 1.4 |

where the last column is the percentage mass loss based on an estimated 10 μg/second steady-state mass flow.

## 6. CONCLUSIONS AND RECOMMENDATIONS FOR FUTURE WORK

The major accomplishment of this program has been the experimental development and feasibility demonstration of the ability of tubular colloid thrusters to operate at 75 percent efficiency, 1300 seconds specific impulse and greater than 25 micropounds thrust per source as measured by time-of-flight techniques. A four-source module has been built and tested to demonstrate the tubular source's adaptability to parallel staging up to the 100 micropound thrust range at a thrust density greater than 25 micropounds per square inch. The ability to perform smoothly, with a neutralizer, for periods of the order of 100 hours has been demonstrated. Beam probe measurements indicated that 90 percent of the propellant exhaust was contained within a 15° half-angle. The ability to electrostatically deflect the beam was also demonstrated.

The impetus of future work should be directed towards proving the ability of the thruster, operating at its presently demonstrated performance levels, to meet spacecraft flight system requirements. Specifically, this means demonstrating the required reliability, life time and performance reproducibility and regulation at specific mission oriented thrust levels. Specific tasks required to accomplish this goal would include the following:

1. Establish a practical ultimate flight demonstration thrust level to be factored into the exploratory development work.
2. Perform direct thrust and mass flow measurements to provide accurate performance data.
3. Define and implement experimental procedures for establishing acceptable reliability, lifetime and performance statistics.
4. Perform preliminary flight-type thruster hardware development.
5. Establish and meet requirements for thrust vector alignment accuracy.
6. Map thruster effluents and relate to potential spacecraft contamination problems.

7. Measure electromagnetic noise spectrum radiated by the thruster.

8. Perform tradeoff study to establish the desirability of electrostatic vectoring. If it is determined that the potential benefits of electrostatic vectoring warrant extensive continued development, the following tasks should be performed.

   a) Comparison of three and four electrode vectoring system control characteristics and a tradeoff study made of the overall system implications of the two designs. The study should include laboratory measurements of the detailed response characteristics for all vectoring angles.

   b) An experimental design study should be performed to optimize the vectoring performance at the present thruster performance levels and to achieve the degree of control required for spacecraft applications.

   c) The effects of electrostatic vectoring on total long-term performance reliability and lifetime should be determined.

## APPENDIX A

## EXPERIMENTAL FACILITY

The experiments were performed in a four-foot diameter by eight-foot long vacuum test chamber (Figure 66). The chamber was oriented horizontally. High vacuum was maintained by an Edwards Model F2404 24-inch water-cooled oil (Santovac 5) diffusion pump pumping through an Edwards Model P24R24 24-inch water-cooled right-angle baffle valve. The half of the chamber farthest away from the thruster was lined with a liquid nitrogen shroud. The pump is rated at 12,000 liters/second (International Vacuum Society Standards). However, the baffle valve reduces the effective speed to approximately 6700 liters/second. An Edwards Model ISC3000 mechanical pump provides a 100 cfm roughing capability through a 4-inch roughing line. The system also includes an Edwards Model FS150 mechanical holding pump.

The time-of-flight collector has been described in Section 5.3. For vertical operation the thruster was mounted directly over a port on the top of the chamber (Figure 67) with the time-of-flight collector positioned at the bottom. In this case, since the flight path was directly across the chamber, the time-of-flight distance was limited to 1.05 meters as opposed to 1.86 meters when operating horizontally.

Figure 68 shows the basic source and deflector voltage control circuitry. The component values are listed in Table XIV. The thruster is turned off during time-of-flight measurements by a solenoid controlled spark gap. In the diagram, the deflectors are capacitively coupled to the source voltage so that they are simultaneously lowered in voltage during time-of-flight initiation. This creates a potential problem when the operating deflector voltages are considerably below the source voltage since the capacitors will maintain the voltage differential during turn-off, thus possibly allowing for an above threshold extraction field to exist even though the source is brought down to practically zero voltage. For this reason, in some runs, blocking diode rectifiers were substituted for capacitors $C_1$, $C_2$, and $C_3$. During a time-of-flight shut-off, the diodes would be non-conducting until the source voltage dropped to the deflector level. As the source voltage continued to drop,

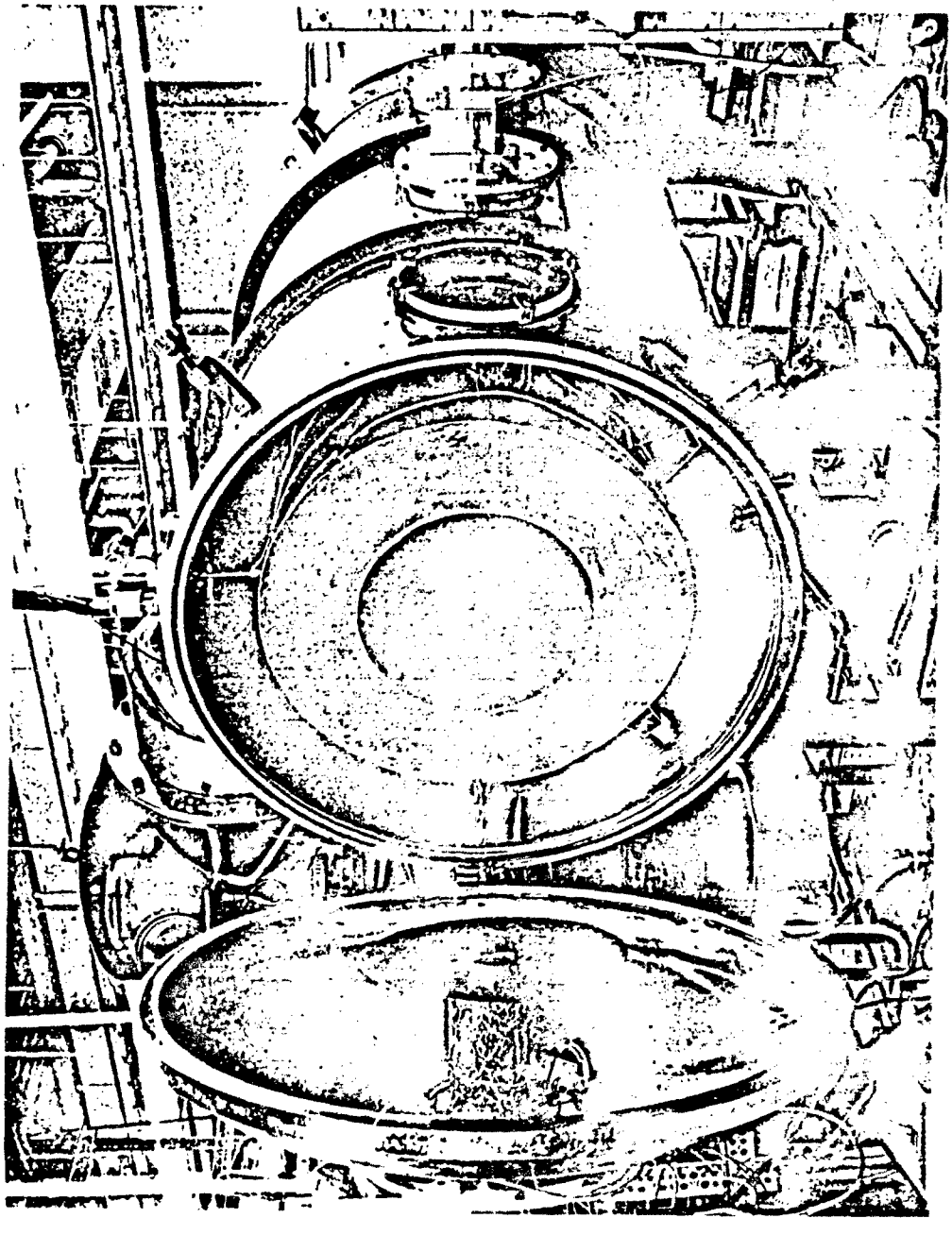

Figure 66. Colloid Test Chamber

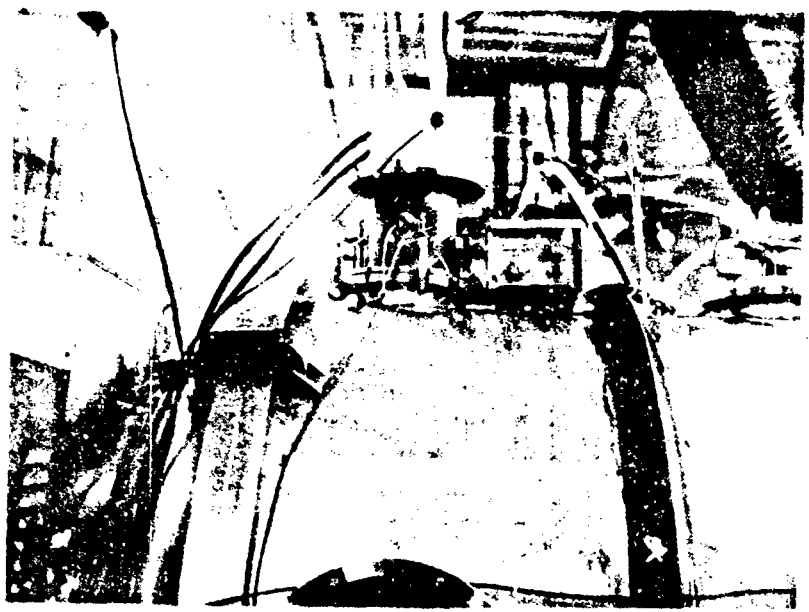

Figure 67. Thruster Mounting Arrangement for Vertical Operation

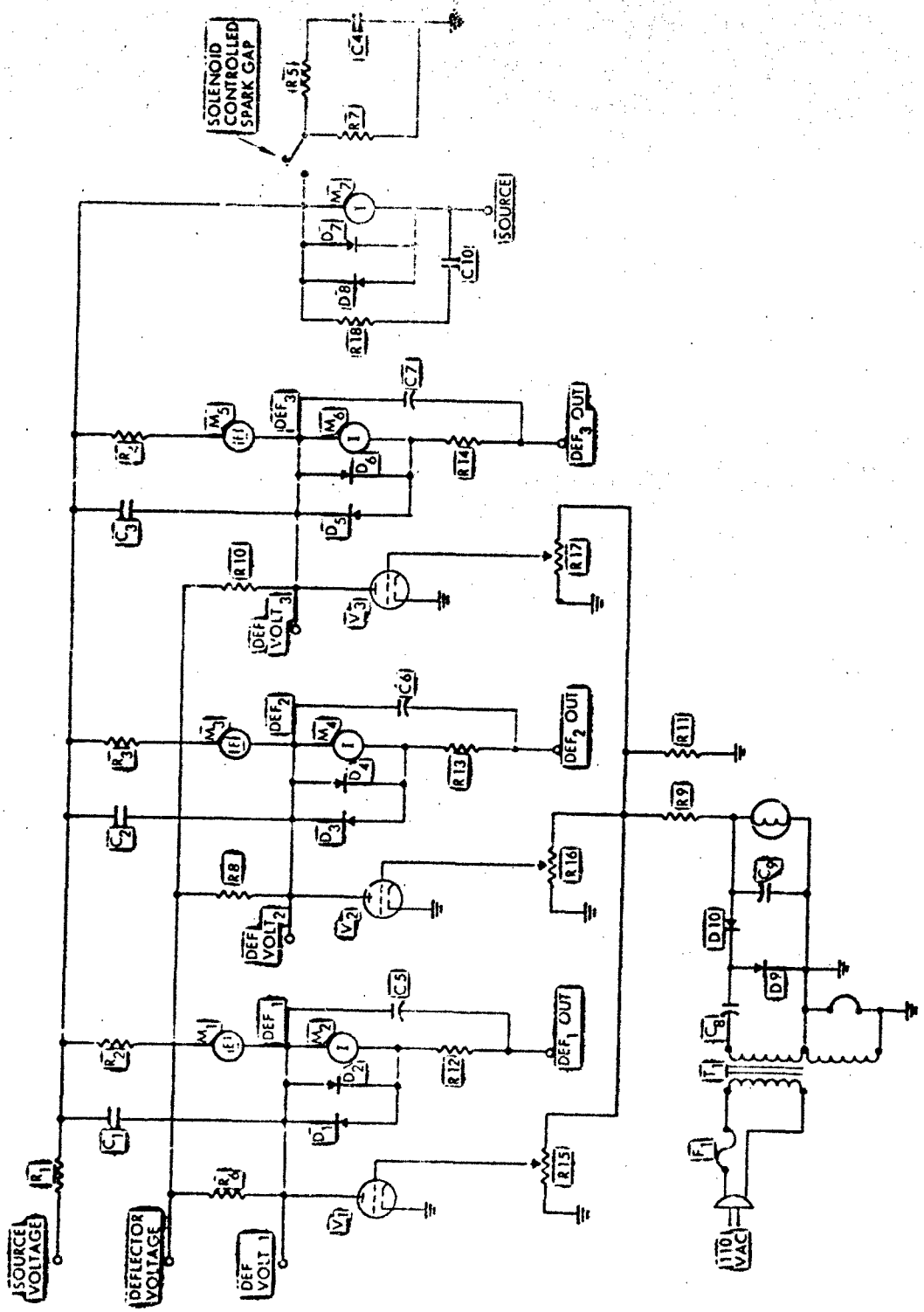


Figure 68. Source and Deflector Voltage Control Circuitry

TABLE XIV. COLLOID THRUSTER CONTROL AND MONITOR UNIT COMPONENT LIST

| Resistors | | Capacitors | |
|---|---|---|---|
| $R_1$ | 3 x 3.92Ω, 2W, 5% | $C_1$, $C_2$, $C_3$ | 0.005 mfd, 10 kv |
| $R_2$, $R_3$, $R_4$ | 1000mΩ | $C_4$ | 0.005 mfd, 30 kv |
| $R_5$ | 6.8K | $C_5$ thru $C_{10}$ | 100 mfd, 50V, electrolytic |
| $R_6$, $R_8$, $R_{10}$ | 100MΩ | | |
| $R_7$ | 20 meg | | Meters |
| $R_9$ | 300KΩ, 2W, 5% | $M_1$ thru $M_6$ | ±25 μa dc, zero center |
| $R_{11}$ | 100KΩ, 2W, 5% | $M_7$ | 500 μa dc |
| $R_{12}$, $R_{13}$, $R_{14}$, $R_{18}$ | 10KΩ, 1/2W, 5% | | |
| $R_{15}$, $R_{16}$, $R_{17}$ | 1MΩ, 2W, potentiometer | | Miscellaneous |
| | | $D_1$ thru $D_{10}$ | 1N647 |
| | | $F_1$ | 0.5A, slow blow |
| | | $I_1$ | 28V lamp |
| | | $V_1$, $V_2$, $V_3$ | 6BK4 |
| | | $T_1$ | 110 to 12.6V secondary |

the diodes would then turn on, allowing the deflectors to follow the source, thus maintaining zero voltage differential. This technique had the disadvantage of not allowing the deflectors to be biased positively with respect to the source during vectoring operation. For the latter part of the program the capacitive method was used since the deflectors were usually only a few kv below the source and no evidence of turn-off problems was observed in this mode.

Another purpose of the circuit is to allow the deflector voltages to be individually controlled while using a single high-voltage supply. This is done by connecting individual deflectors to the mid-points of resistor-triode voltage dividers. The triode grid biases are individually controlled by potentiometers. The net result is essentially a set of three high gain, high voltage, dc amplifiers which individually determine the deflector voltages.

The propellant feed system is shown in Figure 69. Prior to beginning a test the propellant flask is maintained in a lowered position so that the vertical feed tube is completely above the surface of the liquid. A magnetically stirred hot plate is placed below the flask and a vacuum is pulled on the pressurizing line. This allows a final outgassing immediately before start-up. When the experimental run is to begin, the flask is raised, submerging the feed tube, and a dry pressurant gas (nitrogen or argon) applied. Due to the extremely low diffusion velocity of dissolved gas in glycerol, this does not affect thruster performance during runs of the order of hundreds of hours. It is of course necessary to correct for the negative pressure head in the tube when measuring the feed pressure.

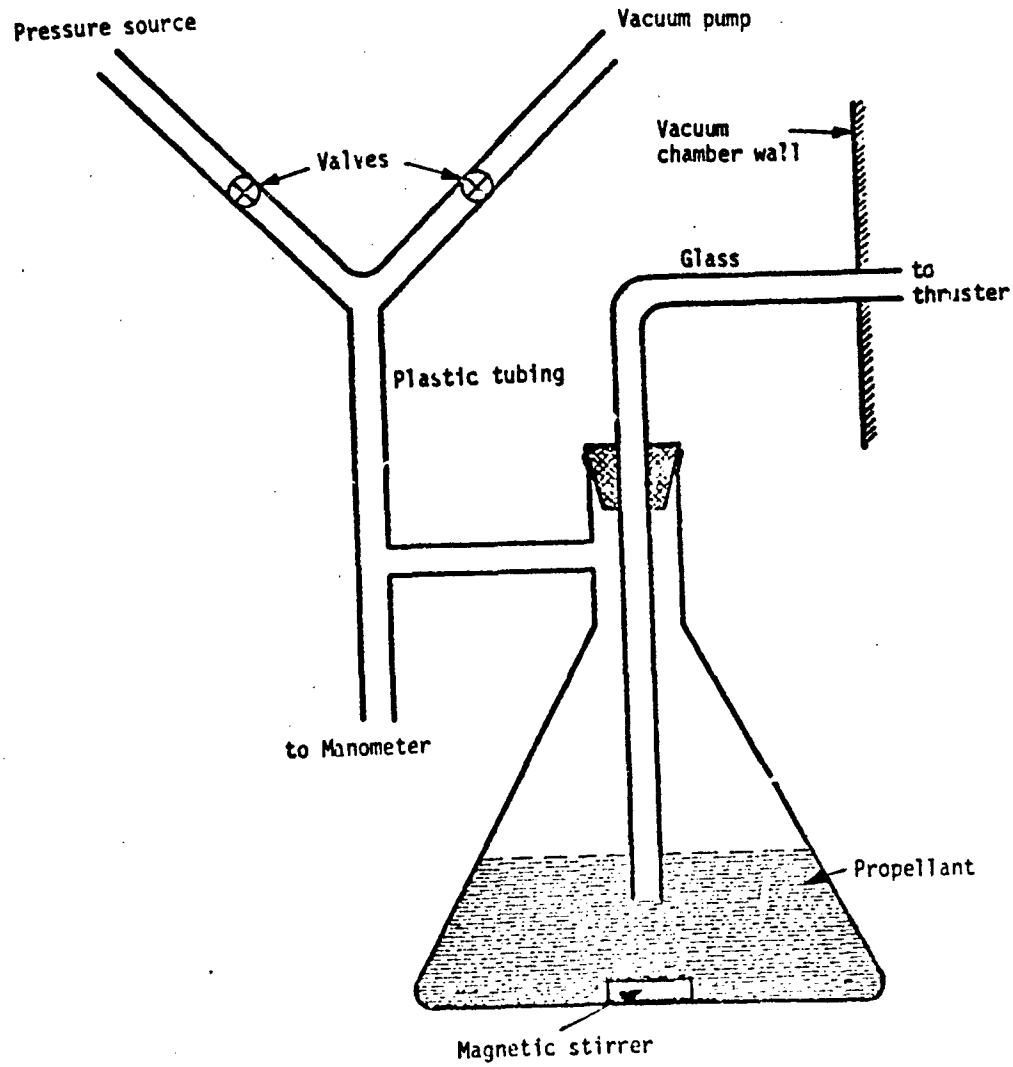


Figure 69. Propellant Feed System

## APPENDIX B

## RIM FORMING TOOL

The rim forming tool was developed to insure that uniform, reproducible emitter rims could be formed using standard jeweler's lathe techniques. The tool had a cutting edge which was essentially the negative of the cross section of the emitter rim at one point. Thus, as a rough cut emitter was rotating on a jeweler's lathe, the tool would be slowly moved forward to cut out the desired rim shape (Figure 70).

Figure 71 is a schematic of the tool. It was formed from a length of 1/8 inch diameter tungsten carbide rod. The tool was formed after first grinding off a portion of the rod's tip to leave a thin flat working section as shown in Figure 70. The cutting groove was then formed by filing with successively thinner sheets of tungsten loaded with diamond grit. The final radius at the bottom of the groove was formed using 0.001 inch tungsten wire loaded with one micron diamond grit. Finally additional material was removed from the tip of the rod as required to provide cutting clearance.

Two tools were used on the program, the first having been broken before fabrication on the four source module. High efficiency results were obtained with the products of both tools, thus lending a fair degree of confidence to the utility of these tools.

Figure 70. Microphotograph of Lead Imprint of Tool Formed Emitter Rim Scale is as shown in Figure 70.

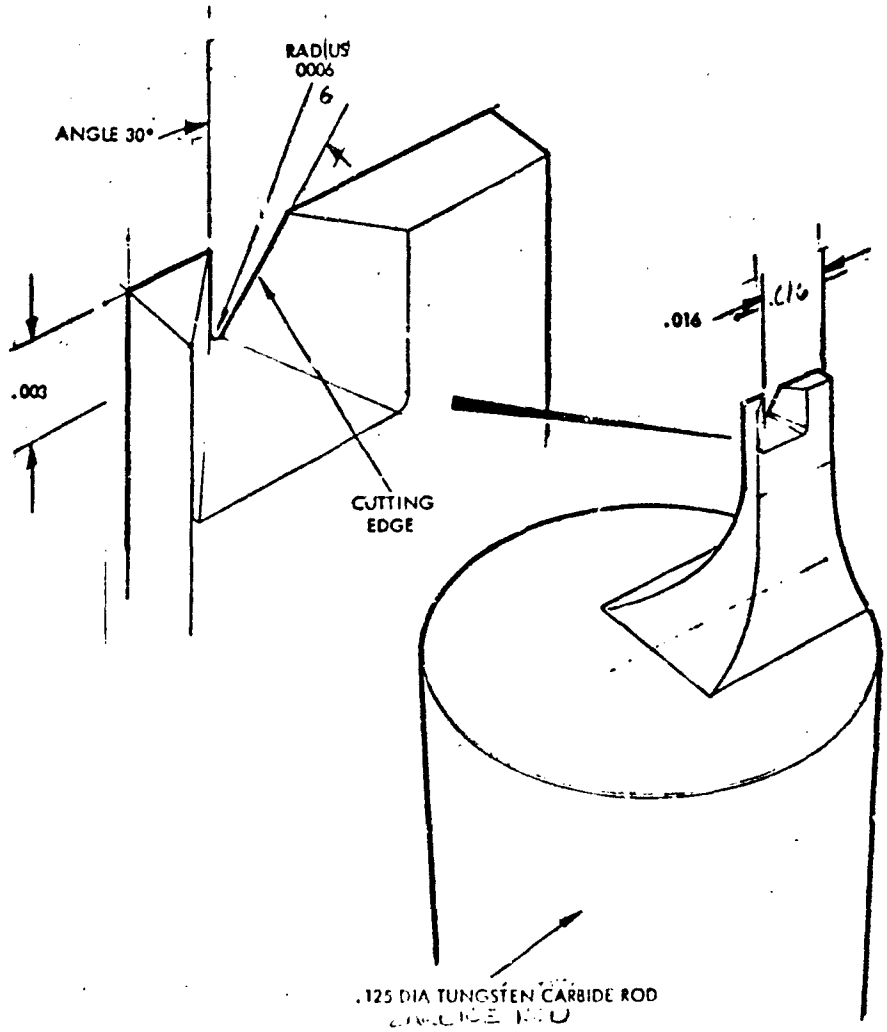


Figure 71. Rim Forming Tool Schematic

## REFERENCES


1. M. N. Huberman, C. W. Lear, H. Shelton, W. F. Krieve and R. F. Kemp, "Exploratory Development of Advanced Colloid Thrusters," AFRPL-TR-71-128, November 1971.

2. J. Perel, et al, "Electro-Optical Systems, Final Report for Colloid Thruster Technology," August 1970 - September 1971.

3. H. Shelton, et al, "Charged Droplet Electrostatic Thruster Systems," AFAPL-TR-70-31, June 1970.

4. M. N. Huberman and P. W. Kidd, "Charged Particle Electrostatic Thrusters," AFAPL-TR-69-14, March 1969.

5. M. N. Huberman and E. Cohen, "Research on Charged Particle Electrostatic Thrusters," AFAPL-TR-67-115, September 1967.

6. "Physical Properties of Glycerine and Its Solutions," Glycerine Producer's Association, New York, New York.

7. David Bohm, "Minimum Ion Kinetic Energy for a Stable Sheath" in "The Characteristics of Electrical Discharges in Magnetic Fields" edited by A. Guthrie and R. K. Wakerling, 1st Ed. pp 77-86, McGraw-Hill Book Co., New York 1949.